UNIVERSITY OF CLIFORNIA, SAN DIEGO

N-linked glycosylation regulates protease-activated receptor-1 trafficking and signaling

A dissertation submitted in partial satisfaction of the
requirements for the degree Doctor of Philosophy

in

Biomedical Sciences

by

Antonio G. Soto

Committee in charge:

Professor JoAnn Trejo, Chair
Professor Joan Heller Brown
Professor Jeffrey D. Esko
Professor Tracy M. Handel
Professor Judith A. Varner

2013

The Dissertation of Antonio G. Soto is approved, and it is acceptable in quality and form for publication on microfilm and electronically:

_____

_____

_____

_____

_____

Chair

University of California, San Diego

2013

DEDICATION

This dissertation is dedicated to my entire family who were integral in providing a loving environment in which to thrive. For my aunts, uncles, and cousins who always supported and looked out for the "baby" of the family. For my grandparents, who instilled in my parents the importance of education, which, in turn was passed onto me. For my mother, Carmen Soto, who was diagnosed with rheumatoid arthritis when I was eight years old. She continues a battle that would slow down many other people. My mother has been and always will be an infinite source of inspiration for me. She taught me never to let life get you down and how to handle adversity. For my father, Gregory Soto, who from the beginning chose family over work. My father spent countless hours coaching my youth sports teams throughout my entire childhood. He taught me the importance of hard work and dedication, along with many life lessons I have taken to heart. For my big brother, Salvador Soto, who made sure I took a break from time to time. He frequently reminded me that life is more than just books and beakers. He taught me the importance of finding time to enjoy life. For my dog, Lady, who taught me so much more than just how to be a good pet owner.

For all my friends, who along the way encouraged me, gave me support, made me laugh when I was down, and gave me a shoulder to lean on. Especially those at Coastal German Shepherd Rescue, who were my family away from my family, providing me with a place to rest and recuperate.

For everything, past, present, and future, I thank you all.

TABLE OF CONTENTS

LIST OF ABBREVIATIONS

A	alanine
ALIX	ALG-2-interacting protein X
APC	activated protein C
ATP	adenosine triphosphate
BRET	bioluminescence resonance energy transfer
cAMP	3’-5’-cyclic adenosine monophosphate
CARB	carbachol
DAG	diacyl glycerol
ECL	extracellular loop
Ede	edelfosine
EE	EEEEYMPME epitope tag
EEA1	early endosome antigen-1
EGFR	epidermal growth factor receptor
ELISA	enzyme-linked immunosorbent assay
Endo H	endoglycosidase H
ERK	extracellular signal-regulated kinase
ESCRT	endosomal sorting complexes required for transport
FLAG	DYKDDDDK epitope tag
GDP	guanosine diphosphate
GEF	guanine nucleotide exchange factor
GPCR	G protein-coupled receptor
GRK	G protein-coupled receptor kinase

GST	glutathione S-transferase
GTP	guanosine triphosphate
HA	hemagglutinin
IP	inositol phosphates
KLK	kallikrien
MAP	mitogen-activated protein
MMP	matrix metalloproteinase
N	asparagine
NTer	N-terminus
PAR	protease-activated receptor
PI	phosphatidylinositol
PIP_2	phosphatidylinositol 4,5-bisphosphate
PKC	protein kinase C
PLC	phospholipase C
PNGase F	peptide-N-glycosidase F
Rac1	Ras-related C3 botulinum toxin substrate 1
RBD	Rho binding domain
RhoA	Ras homolog gene family, member A
Rluc	Renilla luciferase
siRNA	small interfering ribonucleic acid
α-Th	thrombin
TNC	tunicamycin
UT	untransfected

WT	wild-type
YFP	yellow fluorescent protein

LIST OF FIGURES & TABLES

ACKNOWLEDGEMENTS

I would like to thank the BMS graduate program, especially Gina, Leanne, and Kathy for all their help through the years. I would also like to thank the UCSD pharmacology department staff members, who were all extremely helpful during my time in the lab.

I would like to thank all the members of the Trejo Lab for helpful and insightful discussions throughout my entire graduate career. In particular, I would like to thank both Drs. Mike Dores and Buxin Chen. The two post docs who really took it upon themselves to take me under their wings and mentor me. Their involvement in my progression as a scientist was crucial to get to where I am today.

I would like to thank my thesis advisor, Dr. JoAnn Trejo, for allowing me to join the lab and for her guidance throughout my graduate years. The freedom she gave me to develop my own project and not just continue previous work done in the lab was a special and rewarding experience that I am extremely thankful for.

I would like to extend a special thank you to all the members of my thesis committee, Drs. Joan Heller Brown, Jeffrey D. Esko, Tracy M. Handel and Judith A. Varner for advice, suggestions and guidance in helping me in the development of my thesis project. My committee meetings were always thought provoking and helpful. On a personal note, I would like to especially thank Dr. Joan Heller Brown who was my SPAC advisor. Her sincere dedication and care for the students in the BMS program is the reason I am here today.

The contents of Chapter 2, in part, have been published: **Soto, A.G.,** and Trejo, J. (2010) N-Linked glycosylation of protease-activated receptor-1 second extracellular

loop: a critical determinant for ligand-induced receptor activation and internalization. *Journal of Biological Chemistry,* 285(24), 18781-93. The dissertation author was the primary investigator and author of this paper. All co-authors have given written permission for its use and the reproduction of all associated data in this dissertation.

The contents of Chapter 3, in part, have been published: **Soto, A.G.,** and Trejo, J. (2010) N-Linked glycosylation of protease-activated receptor-1 second extracellular loop: a critical determinant for ligand-induced receptor activation and internalization. *Journal of Biological Chemistry, 285*(24), 18781-93. The dissertation author was the primary investigator and author of this paper. All co-authors have given written permission for its use and the reproduction of all associated data in this dissertation.

The contents of Chapter 4, in full, is in preparation: **Soto, A.G.,** Smith, T.H., and Trejo, J. (2013) An N-linked Glycosylation Switch for GPCR-G Protein Coupling Specificity. *Journal TBD*. The dissertation author was the primary investigator and author of this paper. All co-authors have given written permission for its use and the reproduction of all associated data in this dissertation.

This work was supported National Institutes of Health grant HL073328 (J.Trejo) and an American Heart Association Established Investigator Award (J.Trejo). A. G. Soto was supported by a T32 NIGMS Pharmacological Sciences Training Grant. The authors have no conflict of interest to declare.

VITA

2008 B.S. Biochemistry, California Polytechnic State University, San Luis Obispo

2013 Ph.D. Biomedical Sciences, University of California San Diego

PUBLICATIONS

Soto, A.G., Smith, T.H., and Trejo, J. (2013) An N-linked Glycosylation Switch for GPCR-G Protein Coupling Specificity. *Journal TBD*. *In preparation*

Grimsey, N., **Soto, A.G.**, and Trejo, J. Regulation of protease-activated receptor signaling by post-translational modifications. *IUBMB Life.* 2011 June; 63(6):403-411.

Soto A.G., Trejo, J. N-linked glycosylation of protease-activated receptor-1 second extracellular loop: a critical determinant for ligand-induced receptor activation and internalization *J Biol Chem.* 2010 June 11; 285(24):18781-18793.

ABSTRACTS

A.G. Soto and J. Trejo. Regulation of protease-activated receptor-1 signaling by extracellular loop 2 N-linked glycosylation: A possible bias signaling "switch"? American Society for Cell Biology ASCB, San Francisco, CA December 2012.

MAC travel award recipient.

A.G. Soto and J. Trejo. Regulation of protease-activated receptor-1 signaling and trafficking by extracellular loop 2 N-linked glycosylation. Experimental Biology FASEB, San Diego, CA April 2012.

A.G. Soto and J. Trejo. Regulation of protease-activated receptor-1 signaling and trafficking by extracellular loop 2 N-linked glycosylation. Keystone Symposia on G-protein coupled receptors, Banff, Alberta, Canada February 2012.

Minority travel award recipient.

A.G. Soto and J. Trejo. N-linked glycosylation of protease-activated receptor-1 regulates receptor activation and internalization. Experimental Biology FASEB, Washington, DC April 2011.

MARC travel award recipient.

A.G. Soto and J. Trejo. N-linked glycosylation of PAR1: sweet new findings of signal regulation. American Society for Cell Biology ASCB, San Diego, CA December 2009.

ABSTRACT OF THE DISSERTATION

N-linked glycosylation regulates protease-activated receptor-1 trafficking and signaling

by

Antonio G. Soto

Doctor of Philosophy in Biomedical Sciences

University of California, San Diego, 2013

Professor JoAnn Trejo, Chair

G protein-coupled receptors (GPCRs) are a superfamily of seven transmembrane receptors that respond to a diverse array of stimuli, regulate a multitude of physiological responses and are the targets of most drugs used clinically. Activated GPCRs undergo conformational changes, facilitating activation of specific heterotrimeric G protein subtypes by functioning as a guanine-nucleotide exchange factor (GEF) facilitating exchange of GDP for GTP on the Gα subunit resulting in dissociation of βγ subunits and downstream signaling. GPCR signal termination is mediated by desensitization and internalization. Interestingly, certain GPCRs have the capacity to couple to multiple distinct G protein subtypes even in the same cell.

However, the mechanisms that specify GPCR-G protein coupling to specific subtypes remains poorly understood. Many GPCRs are modified by N-linked glycosylation but whether this modification contributes to GPCR signal regulation has yet to be fully explored. In the work described in the thesis I examined whether N-linked glycosylation of protease-activated receptor-1 (PAR1), a GPCR for the coagulant protease thrombin, regulated receptor function. I found that PAR1 is extensively glycosylated on the N-terminus and extracellular loop two (ECL2), with ECL2 serving as the major site for N-linked glycosylation. I also discovered that N-linked glycosylation of PAR1 at the N-terminus is important for transport to the cell surface, whereas glycosylation at ECL2 makes important contributions to receptor activation. Activation of PAR1 occurs via proteolytic cleavage of the N-terminus resulting in the generation of a new N-terminus, which functions as a tethered ligand by binding intramolecularly to ECL2 to facilitate transmembrane signaling. I discovered that N-linked glycosylation at ECL2 regulates G protein coupling specificity. PAR1 wild-type displayed preferential coupling to $G_{12/13}$ versus G_q, whereas a PAR1 mutant lacking N-linked glycosylation at ECL2 exhibited enhanced coupling to G_q versus $G_{12/13}$. Intriguingly, both PAR1 wild-type and mutant coupled comparably to G_i protein. In summary, the work in this thesis describes a function for N-linked glycosylation of PAR1 in regulating receptor-G protein coupling specificity and provides the first molecular insight into mechanisms that can influence activated GPCR biased coupling to specific G protein subtypes.

Chapter 1:

An introduction to protease-activated receptor-1, a member of the G protein-coupled receptor superfamily

1.1 Introduction

The G protein-coupled receptor (GPCR) superfamily is the largest class of signaling receptors in the mammalian genome, respond to a variety of extracellular stimuli and elicit a diverse array of cellular responses. GPCRs are involved in many physiological processes and have been implicated in numerous disease states. Thus, a better understanding of the mechanisms that regulate GPCR signaling is critical and will aid in the development of new therapeutics to prevent and treat various diseases. N-linked glycosylation occurs via the covalent attachment of saccharides to asparagine residues during protein translation and is a modification that frequently occurs with mammalian GPCRs. The work presented in this thesis is focused on examining the function of N-linked glycosylation in the regulation of the G protein-coupled protease-activated receptor-1 (PAR1) signaling.

1.1.2 PAR1 discovery and mechanism of activation

The protease-activated GPCR family includes four members: PAR1, PAR2, PAR3 and PAR4. PARs are uniquely activated via a proteolytic cleavage mechanism. PAR1 was discovered nearly 20 years ago by Coughlin and colleagues in an attempt to identify a receptor that conferred thrombin signaling in platelets. These investigators employed an expression cloning strategy that utilized mRNA isolated from a megakaryocytic cell line and *Xenopus* oocytes (1). The isolated cDNA encoding a functional thrombin receptor contained an LDPR/S sequence present in the N-terminus that resembled the thrombin cleavage site in the zymogen Protein C (LDPR/I). Mutation of the critical arginine (R) within the putative cleavage site of

PAR1 ablated thrombin signaling. Moreover, a synthetic peptide that mimicked the first six amino acids of the newly generated N-terminus was shown to fully activate PAR1 independent of thrombin and receptor cleavage (2). However, thrombin is more efficient than synthetic peptide agonist at activation of PAR1. The LDPR/S sequence of PAR1 is essential for thrombin recognition and cleavage. Thrombin also contains an anion-binding exosite that interacts with an acidic hirudin-like sequence in the N-terminus of PAR1 (**Fig. 1, blue highlight**). The hirudin-like sequence is present in both PAR1 and PAR3, but not in PAR4 and confers thrombin high affinity binding. PAR2 is not cleaved nor activated by thrombin (3). Thus, PAR1 carries its own ligand, which is unveiled following thrombin cleavage. The important discovery of PAR1 provided an explanation for thrombin-induced cellular responses and uncovered a novel mechanism for the activation of cells by proteases, which is critical for platelet aggregation and other cellular responses implicated in normal physiology and disease.

Cleavage of PAR1 results in the generation of a tethered ligand that binds intramolecularly to the body of the receptor to promote transmembrane signaling (**Fig. 2**). Previous studies using PAR1 chimeric receptors showed that the second extracellular loop (ECL2) is important for species-specific ligand docking interactions (4, 5). Additional work using PAR1 chimeric receptors and alanine scanning mutagenesis revealed that glutamate (E) at position 260 in ECL2 is crucial for ligand interaction and receptor activation (6). In the same study further examination of amino acids surrounding E260 revealed a possible role for these residues in ligand interaction and receptor activation. Of note is the asparagine at position 259, which is part of a

NXS/T N-linked glycosylation consensus sequence. These results suggest a potential role for PAR1 ECL2 N-linked glycosylation in tethered ligand interactions.

1.1.3 PAR1 activation by multiple proteases

Thrombin, while the most efficient at cleaving PAR1, is not the only protease that can activate the receptor. In addition to thrombin, plasmin is able to cleave PAR1 at multiple sites in the N-terminus that either activate or incapacitate the receptor (7) (**Fig. 1**). Certain kallikreins also have the ability to cleave PAR1 at multiple sites within the N-terminus (8, 9). Kallikreins have also been shown to induce PAR1 signaling in various cell types, including cancer cells (10-12). Other proteases, although unable to cleave at multiple sites like plasmin and the kallikreins, are also able to cleave and activate PAR1. Activated protein C (APC) cleaves PAR1 at R46, a distinct site downstream of the R41 thrombin cleavage site and activates signaling important for endothelial barrier stability and recovery (13-15) (**Fig. 1**). Matrix metalloprotease-1 (MMP1) cleaves PAR1 after aspartate (D) at position 39 upstream of the thrombin cleavage site and induces signaling responses that appear to contribute to sepsis and cancer progression (16-19) (**Fig.1**). In addition, several other proteases have been reported to cleave PAR1, but the mechanism of activation and consequences on cell signaling is not clearly established (**Table 1**). The distinct cleavage sites of APC and MMP1 result in the generation of unique N-terminal tethered ligands that may stabilize different active PAR1 conformations to facilitate distinct cellular responses. The ability of distinct ligands to induce different GPCR signaling responses is a phenomenon that has been termed “biased agonism” or

"functional selectivity" (20, 21). Thus, the expression profile of PAR1 and repertoire of activating proteases will dictate how the receptor functions in different cell types and tissues.

1.1.4 PAR1 expression and function

PAR1 is highly expressed in endothelial cells and platelets and has an integral role in vascular biology by mediating responses important for hemostasis, thrombosis, inflammation, and embryonic development (3, 22-24). PAR1 is also expressed in fibroblasts, smooth muscle cells, epithelial cells, astrocytes and other cell types and mediates diverse cellular responses. To assess PAR1 function the gene encoding the receptor was deleted in mice. PAR1 knockout mice have severe defects in vascular development with 50% lethality occurring by midgestation (25). The expression of PAR1 in endothelial cells was able to rescue the embryonic lethality phenotype (24, 26), indicating that endothelial PAR1 is critical for vascular development. Studies using PAR1 knockout fibroblasts showed loss of thrombin signaling, indicating an important role for PAR1 in mediating thrombin signaling in this particular cell type. However, platelets deficient in PAR1 expression were still able to respond to thrombin (24). These results led to the search for and subsequent discovery of PAR3 and PAR4, as well as species-specific differences in PAR1 expression in mouse versus human platelets. PAR1 is critical for human platelet activation and endothelial barrier regulation as well as smooth muscle cell (27) and fibroblast (28) cell proliferation and migration . Thus, PAR1 is expressed in many different cell types and plays an

important role in cellular responses important for vascular physiology making it an important drug target.

Thrombin activates PAR1 and PAR4 in human platelets, which initiates signaling cascades leading to Ca^{2+} mobilization, secretion of autocrine activators, expression of adhesion molecules at the cell surface, and cell shape change, which promote platelet aggregation (23). PAR1 is activated by low thrombin concentrations, due to the high affinity interaction between the hirudin-like sequence in the N-terminus and thrombin's anionic binding exosite, leading to rapid and transient signaling responses (29, 30). PAR4 is a low affinity thrombin receptor, lacks a hirudin-like sequence within its N-terminus and thus requires high thrombin concentrations for activation and leads to prolonged signaling responses (31-33). In human endothelial cells, PAR1 and PAR3 are important for endothelial barrier regulation (34, 35). A previous study showed that PAR1 and PAR3 form heterodimers in endothelial cells, which appears to increase G_{13} protein coupling versus the PAR1 protomer (36). In addition, PAR3 coexpression modulated PAR1-activated increase in endothelial permeability (36).

In addition to its role in the vasculature, PAR1 has been implicated in cancer progression. PAR1 is overexpressed in different types of cancer including aggressive melanoma, colon cancer, prostate cancer and invasive breast cancer (3, 37). The overexpression of PAR1 in NIH 3T3 fibroblasts induces transformation, while expression of PAR1 in non-invasive MCF7 breast carcinoma is sufficient to promote growth and invasion using mammary fat pad xenografts and immune-deficient mice (38, 39). Moreover, antisense or RNAi-mediated reduction of PAR1 expression has

been shown to decrease invasiveness of breast carcinoma cell lines *in vitro* (40). The mechanisms by which PAR1 is able to contribute to tumor progression may differ depending on tumor type and the tumor microenvironment. For example, PAR1 promotes cell motility through transactivation of EGFR in renal carcinoma (41), while defects in PAR1 trafficking lead to persistent EGFR/ErbB2 tranasctivation and prolonged ERK1/2 signaling which promotes breast carcinoma invasion and tumor growth in vivo (40). The diversity of PAR1 signaling is partly due to its promiscuous nature and ability to couple to multiple different heterotrimeric G protein subtypes.

1.1.5 PAR1 signaling

PAR1 has the capacity to signal through multiple G-protein subtypes including G_q, G_i, and $G_{12/13}$ (37, 42-46) (**Fig. 2**). G-proteins are comprised of three different subunits including the α, β, and γ subunits. Activated GPCRs function as guanine-nucleotide exchange (GEFs) and promote the exchange of GDP for GTP on the α subunit resulting in dissociation of the βγ subunits and effector coupling. PAR1 activation of G_q leads to phospholipase C (PLC)-mediated generation of phosphoinositides and calcium mobilization (47, 48). G_i activation induced by PAR1 leads to inhibition of cAMP accumulation (48), whereas $G_{12/13}$ activation couples to Rho GEFs leading to RhoA activation (49, 50). The molecular mechanisms by which PAR1 is capable of coupling to distinct G-protein subtypes in the same cell are not clearly understood. It is possible that distinct populations of PAR1 exist and each has a different preference for certain G-protein subtypes due to location, oligomerization, or perhaps differences in posttranslational modifications of the receptor.

The capacity of a given receptor to signal through different pathways depending on the activating ligand is a processed termed “biased signaling”. In many cases, activation of GPCRs with certain ligands has been shown to promote signaling through either G-protein or β-arrestin signal transduction pathways (51-53). PAR1 has been shown to elicit biased responses depending on the activating protease. In endothelial cells, thrombin activation of PAR1 promotes preferential coupling to G_q and $G_{12/13}$ leading to Ca^{2+} increases and RhoA signaling causing transient disruption of the endothelial barrier (23, 54, 55). Conversely, APC stimulated activation of PAR1 results in Rac1 signaling and promotes endothelial barrier maintenance (55, 56). APC-activation of PAR1 occurs in caveolar microdomains and involves β-arrestin recruitment of dishevelled-2, which promotes Rac1 activation and endothelial barrier stabilization (55, 57). The mechanism responsible for segregating PAR1 into distinct microdomains is not known. It is possible that PAR1 posttranslational modifications contribute to biased signaling and localization to distinct plasma membrane microdomains, but this has yet to be fully investigated.

1.1.6 Regulation of PAR1 signaling

Due to the irreversible proteolytic activation of PAR1 signaling is tightly regulated through rapid desensitization and endocytic trafficking. Similar to other GPCRs, activated PAR1 is rapidly phosphorylated and binds β-arrestins, which promotes desensitization by uncoupling the receptor from G-protein signaling at the plasma membrane (58-61). The major sites of PAR1 phosphorylation occur on multiple serine and threonine residues (**Fig. 1**) within its C-tail domain and

phosphorylation is mediated by the G-protein coupled receptor kinase-3 (GRK3) and GRK5 (62, 63). A PAR1 mutant in which all serine and threonine residues were mutated to alanine displayed major defects in signaling and receptor internalization (62). Interestingly, PAR1 phosphorylation cluster mutants, in which only specific serines and threonines were mutated to alanine, showed that different sites may mediate internalization versus desensitization (62). In contrast to most GPCRs, PAR1 internalization is not mediated by β-arrestins, although β-arrestins are essential for receptor desensitization (58). The mechanistic basis for this phenomenon is not known.

In addition to desensitization, internalization of activated PAR1 from the cell surface is important for removing activated receptor from signaling effectors. After internalization, activated PAR1 is then efficiently sorted to lysosomes and degraded (37), a process important for preventing previously activated receptors from returning to the cell surface and continuing to signal. PAR1 displays constitutive and agonist-induced internalization. Constitutive internalization of PAR1 is mediated by the clathrin adaptor AP-2, rather than β-arrestins (64). In contrast, activated PAR1 internalization is mediated by the clathrin adaptors AP-2 and epsin-1 (65), which recognize distinct phosphorylation and ubiquitination sorting signals. Constitutive internalization of PAR1 provides the cell with an intracellular pool of naïve receptors that recycle to the cell surface and is important for resensitizing cells to thrombin signaling and occurs independent of *de novo* receptor synthesis (64, 66, 67).

In addition to AP-2, constitutive internalization of unactivated PAR1 is regulated by ubiquitination. PAR1 contains multiple lysine residues within its

cytoplasmic loop and C-tail, which serves as the major site for ubiquitination (**Fig. 1**). Ubiquitin is a 76 amino acid protein that is covalently linked to lysine residues of GPCRs and is best known to facilitate receptor lysosomal sorting via interaction with ESCRT proteins (68, 69). However, ubiquitination of PAR1 is important for retention at the cell surface since an ubiquitination-deficient receptor mutant containing lysine to arginine mutations showed enhanced constitutive internalization and this phenotype was rescued by an in-frame fusion of a single ubiquitin moiety to the C-tail domain (70). Interestingly, the PAR1 lysine-less mutant did not show a defect in agonist-induced degradation and led to the search for an ubiquitin-independent degradation pathway for GPCRs. Recent studies from our lab revealed that ALIX and AP-3 adaptor proteins mediate PAR1 lysosomal sorting independent of ubiquitination (71, 72), a pathway that may be applicable to a subset of GPCRs containing ALIX recognition motifs.

In addition to ubiquitination, palmitoylation of PAR1 is important for proper trafficking of the receptor. PAR1 contains two highly conserved C-tail cysteines that serve as sites for palmitoylation. Palmitoylation is a posttranslational modification in which palmitic acid is covalently attached to a cysteine residue of a protein. PAR1 harbors two highly conserved C-tail cysteines that are located between a proximal and distal tyrosine-based motif, which are binding sites for AP-2 and AP-3. The distal tyrosine based motif was previously shown to be important for AP-2 interaction with PAR1 and essential for constitutive internalization (64). The proximal tyrosine-based motif of PAR1 was subsequently shown to be important for AP-3 interaction and proper lysosomal sorting and degradation of the receptor (72). A PAR1 mutant

defective in palmitoylation displayed aberrant trafficking indicating that this posttranslational modification is important for proper utilization of the two tyrosine-based motifs by AP-2 and AP-3 (73). Thus, palmitoylation of PAR1 is critical for appropriate cell surface expression.

Phosphorylation, ubiquitination and palmitoylation control PAR1 surface expression and signaling following activation of the receptor and occur on cytoplasmic regions of the receptor. However, N-linked glcyosylation is a modification that occurs at consensus sequences within the extracellular domains of GPCRs. PAR1 contains five N-linked glycosylation consensus sites (**Fig. 1**). Interestingly, two of the N-linked glycosylation consensus sites are localized within the second extracellular loop, a domain critical for ligand interactions with receptor (4-6). The function of PAR1 N-linked glycosylation in the regulation of receptor signaling has not been thoroughly investigated.

1.1.7 N-linked glycosylation and GPCRs

N-linked glycosylation is a posttranslational modification that occurs during protein biogenesis. Throughout the endoplasmic reticulum and golgi apparatus multiple different enzymes facilitate the covalent attachment of saccharides to proteins that contain the NXS/T consensus site (where X is any amino acid except proline). A review of multispanning transmembrane protein glycosylation revealed that approximately 92% (211/229) of the GPCRs examined contained at least one N-linked glycosylation consensus site within the N-terminus of the receptor, and of the 92% only one-third contained additional sites outside the N-terminus (74). The actual

sites that are modified may be attributed partially to the location of the consensus site within the GPCR, with sites that are close to the membrane being less likely to be modified by glycosylation. Thus, not all consensus sites found within GPCRs may be glycosylated. Unlike other posttranslational modifications, N-linked glycosylation of GPCR results in a significant increase in the apparent molecular weight of the receptor as assessed by SDS-PAGE due to additional mass and charge. PAR1 has been reported to migrate as a high ~75 kDa molecular weight protein, although its predicted molecular weight based on the number of amino acids is ~38 kDa. However, PAR1 is reduced to its predicted molecular weight after glycosidase treatment suggesting that the contribution of the N-linked glycans on PAR1 result in a significant increase in apparent molecular weight (75, 76). There are six saccharides that are commonly found within mammalian N-linked glycosylation of proteins (**Table 2**). During protein processing the addition of N-linked glycans is heterogenous and can result in distinct populations of receptors that are differentially modified. It is possible that this heterogeneity may account for some of the differences seen in PAR1 band pattern formation observed in different studies.

N-linked glycosylation of GPCRs, similar to other transmembrane proteins, is important for proper processing and stability. Several studies have shown that alteration of N-linked glycosylation either by mutation or use of inhibitors caused a decrease in the amount of GPCR surface expression (77-80). Thus, attempts to understand the function of GPCR N-linked glycosylation function with mutants that exhibit defects in stability or expression is problematic. However, in other studies a function for N-linked glycosylation has been linked to GPCR ligand interactions,

receptor activation and internalization (81-85). Given substantial contribution of N-linked glycosylation, it is possible that this modification will impact not only GPCR interaction with its ligand but other proteins as well. Although there are relatively few reports on GPCR N-linked glycosylation, the function of this modification remains an important topic for the further understanding of GPCR biology.

1.1.8 Rationale and significance

Most GPCRs contain putative N-linked glycosylation sites, however, studies conducted to determine whether N-linked glycosylation affects GPCR coupling to specific G-protein subtypes are lacking. While there are reports that N-linked glycosylation is important for proper transport of certain GPCRs to the cell surface, these studies did not examine the influence on ligand interactions with the receptors. All members of the PAR family contain at least one consensus site for N-linked glycosylation, however, the function of this modification has not been extensively studied in PARs with the exception of PAR2, which is not a thrombin receptor (86). PAR4 has one N-linked glycosylation site within the N-terminus, PAR3 has two sites within the N-terminus and one within ECL3, but the function of N-linked glycosylation has not been studied. PAR2 has one N-linked glycosylation within the N-terminus and one within ECL2 (87). Compton and colleagues showed through the use of sialidase, tunicamycin, and mutatgenesis that N-linked glycosylation plays a role in protease specificity. Removal of glycosylation granted tryptase the ability to cleave and activate PAR2, while not affecting trypsin cleavage or activation of the receptor (87). Previous studies on PAR1 N-linked glycosylation suggest an important

role in surface expression. In the study Jurkat cells treated with tunicamycin, which globally disrupts N-linked glycosylation, PAR1 expression was drastically reduced compared to control (88). In more recent work, mutations of the various N-linked glycosylation sites within the N-terminus were shown to govern receptor disarming to trypsin, thermolysin, and the neutrophil proteinases elastase and proteinase 3 (89). These findings suggest that PAR1 is glycosylated at the N-terminus but precisely how this posttranslational modification affects receptor function has not been thoroughly examined.

The work described in this dissertation investigated the role of N-linked glycosylation in the regulation of PAR1 signaling and trafficking. I defined for the first time that PAR1 is modified by N-linked glycosylation on both the N-terminus and ECL2, with ECL2 serving as the major site of N-linked glycosylation (90). I also demonstrated that N-linked glycosylation differentially regulates PAR1 signaling and trafficking (90). N-linked glycosylation of PAR1 at the N-terminus is important for trafficking to the cell surface, whereas N-linked glycosylation at ECL2 affects receptor coupling to G_q stimulated phosphoinositide hydrolysis signaling. I also made the novel discovery that N-linked glycosylation at ECL2 influences the capacity of PAR1 to couple to distinct G protein subtypes. This work provides the first insight into the molecular basis of GPCR-G protein coupling specificity (**Fig. 4**), which may be relevant to the molecular basis of biased signaling.

1.2 Figures

Table 1.1: PAR1 N-terminus is cleaved by multiple protease

Protease	Activation	Reference
Thrombin	+	(1)
Meziothrombin/ Meziothrombin desF1	+	(91), (92)
Granzyme A	+	(93)
Plasmin	+/-	(7)
APC-EPCR	+	(13), (94)
Trypsin	+/-	(95)
Factor Xa	+	(96), (97)
KLK1, 14	+/-	(8), (9)
KLK4, 5, 6	+	(10), (9)
MMP-1	+	(18), (19)
Cathepsin G	+/-	(98)
Proatherocytin	+	(99)
Pen C 13	+	(100)
ADAM17	-	(101)
Proteinase 3	-	(89)
Elastase	-	(89)

+ indicates a protease that cleaves and activates the receptor
- indicates a protease that cleaves and disarms the receptor
APC-ECPR = activated protein C-endothelial protein C receptor, KLK = kallikrein, MMP = matrix mettaloproteinase, ADAM = a disintegrin and metalloproteinase domain-containing protein. Adapted from: Adams *et al.* (2011) *Pharmacol Ther* **3**, 248-82.

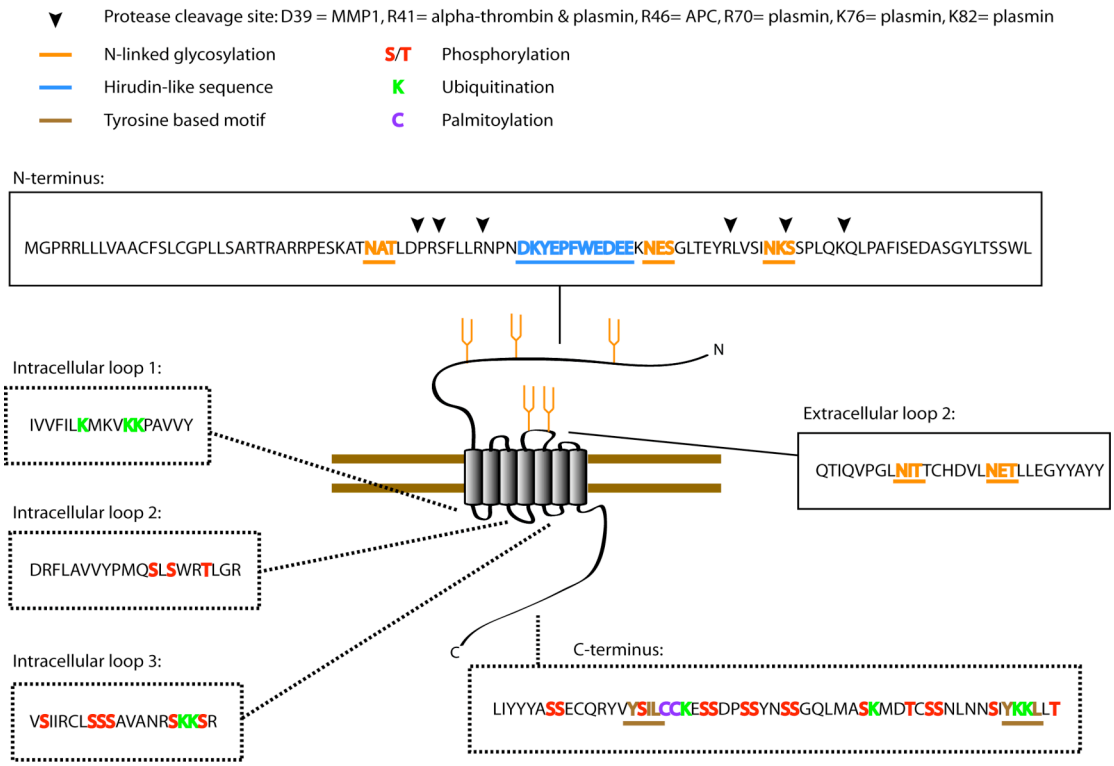

Figure 1.1: Receptor modifications and motifs that are important for PAR1 signal regulation. Similar to other GPCRs PAR1 can be modified by numerous different posttranslational modifications, which play a role in receptor signal regulation. In additional, the tyrosine based motifs within PAR1 C-terminus are known to be important for AP2 interaction. Highlighted in orange are N-linked glycosylation consensus sequences of which PAR1 has five.

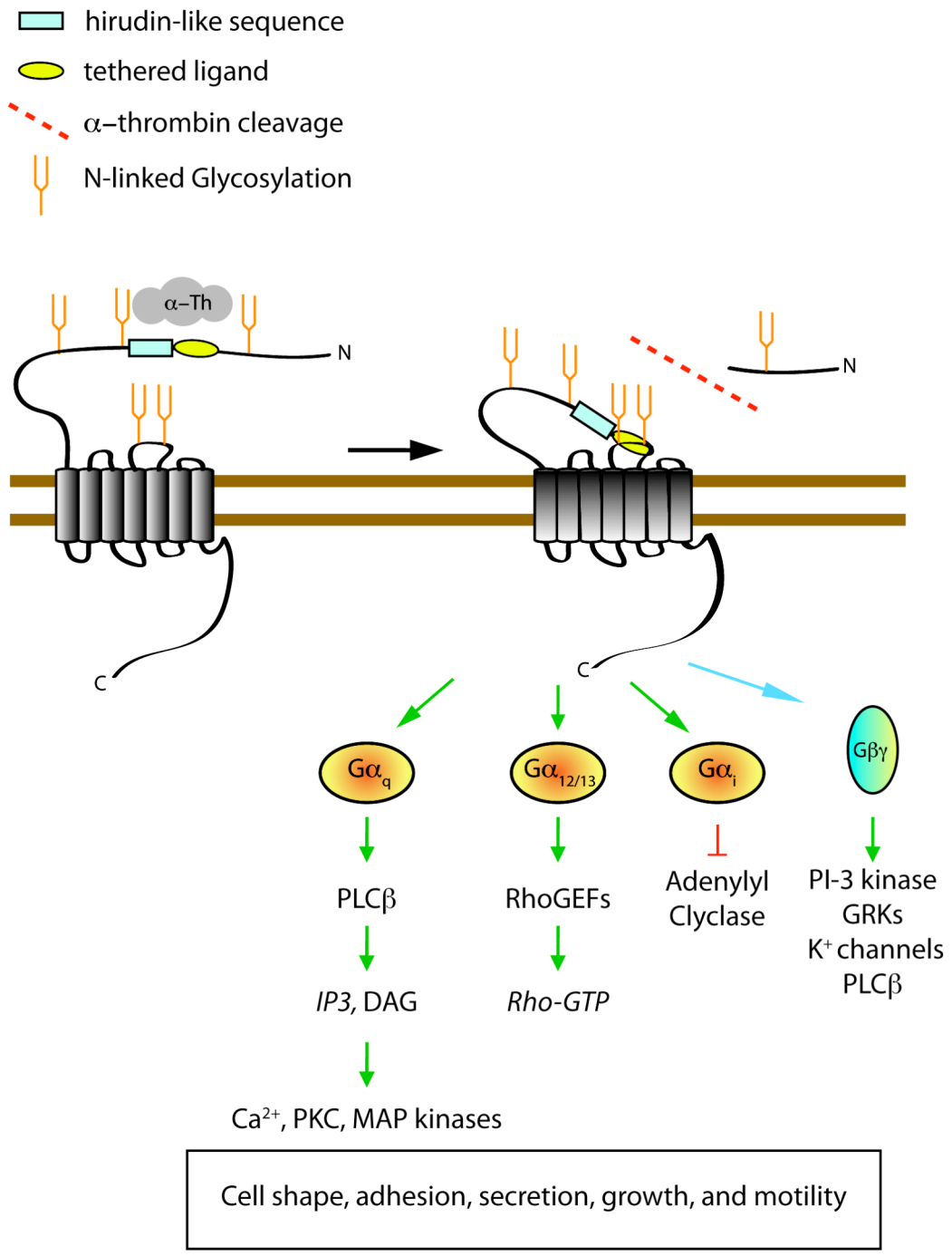

Figure 1.2: Activation of PAR1 and G protein signaling. After thrombin cleavage the new N-terminus acts as a tethered ligand that docks intramolecularly. Extracellular loop 2 is thought to play a critical role in ligand docking. After docking of the tethered ligand the receptor undergoes a conformational change that initiates G protein signaling. PAR1 couples to multiple heterotrimeric G protein subtypes after activation including G_q, G_i, and $G_{12/13}$ and results in diverse cellular responses.

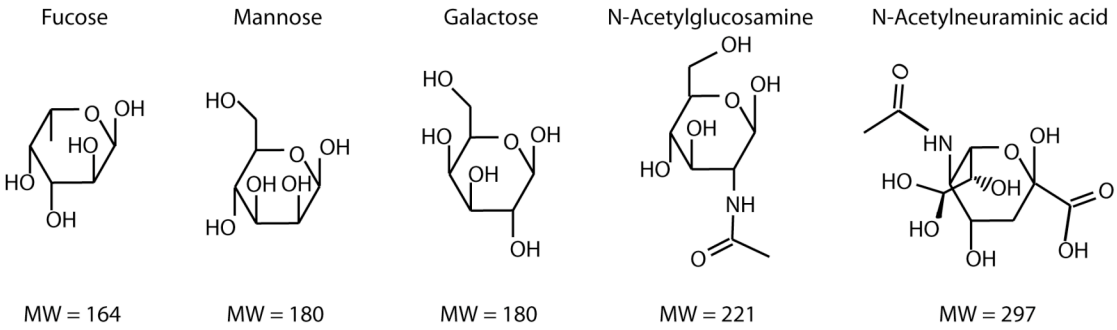

Figure 1.3: Common monosaccharides of vertebrate N-linked glycosylation. The five monosaccharides that are commonly found in vertebrate N-linked glycosylation are represented with the anomeric hydroxyl group in the beta position. Lister below each monosaccharide is approximate molecular weight. Glucose is not listed as it is only part of the 14 saccharide precursor that is transferred to the asparagines and is trimmed later in processing.

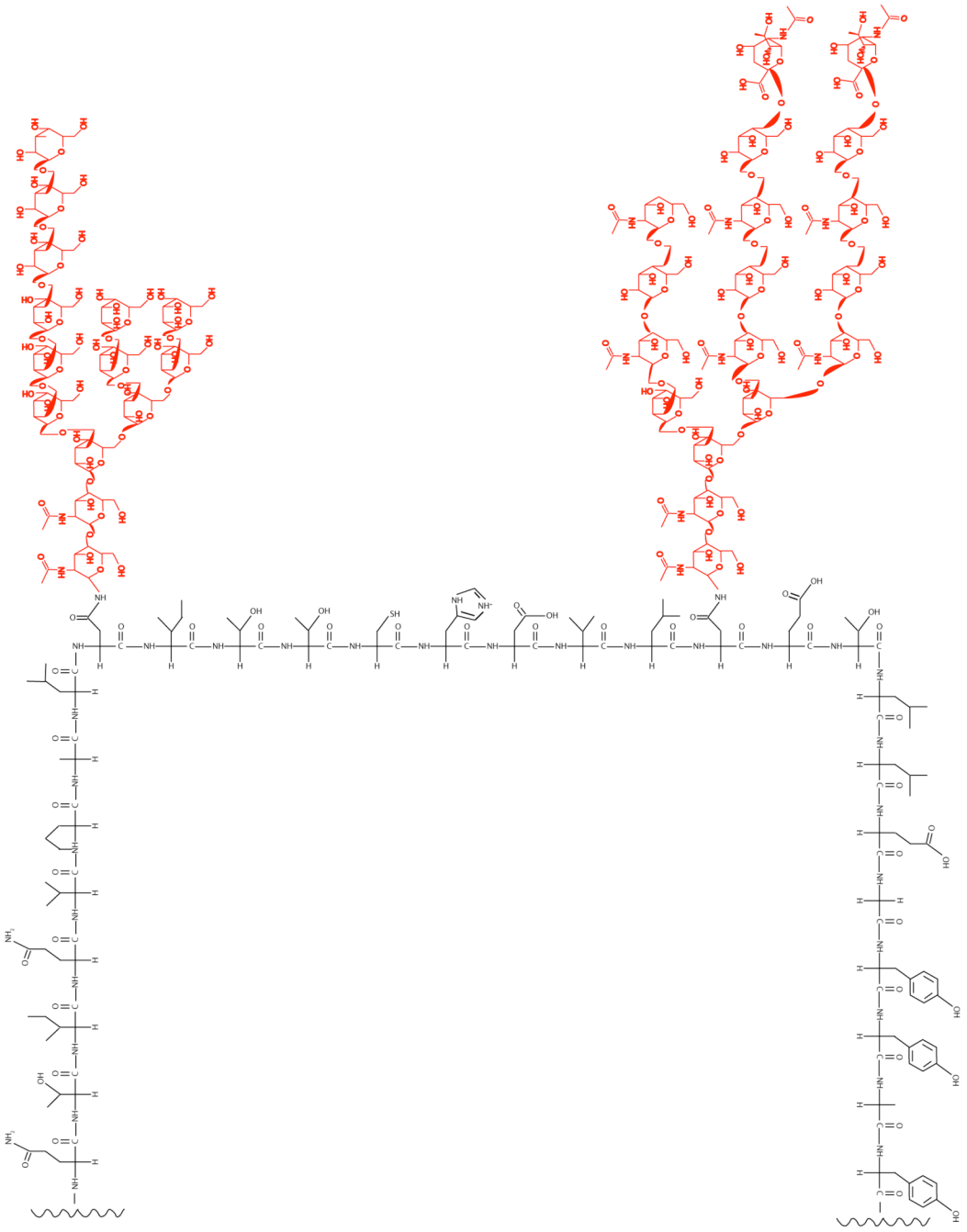

Figure 1.4: Model of PAR1 second extracellular loop amino acids with N-linked glycans. Shown is a model of the 28 amino acids of the second extracellular loop of PAR1. N-linked glycosylation moieties are highlighted in red. The first N-linked glycan is the 14 saccharide "core" structure that is first transferred to the asparagines during biogenesis in the endoplasmic reticulum and is composed of 2 N-acetylglucosamie, 9 mannose, and 3 glucose. The second N-linked glycan is more representative of a complex N-linked glycan that may be found in vertebrates.

1.3 References

1. Vu, T. K., Hung, D. T., Wheaton, V. I., and Coughlin, S. R. (1991) Molecular cloning of a functional thrombin receptor reveals a novel proteolytic mechanism of receptor activation. *Cell* **64**, 1057-1068

2. Vassallo, R. R., Jr., Kieber-Emmons, T., Cichowski, K., and Brass, L. F. (1992) Structure-function relationships in the activation of platelet thrombin receptors by receptor-derived peptides. *J Biol Chem* **267**, 6081-6085

3. Adams, M. N., Ramachandran, R., Yau, M. K., Suen, J. Y., Fairlie, D. P., Hollenberg, M. D., and Hooper, J. D. (2011) Structure, function and pathophysiology of protease activated receptors. *Pharmacol Ther* **130**, 248-282

4. Gerszten, R. E., Chen, J., Ishi, M., Ishi, K., Wang, L., Nanevicz, T., Turck, C.W., Vu, T.K.H., and Coughlin, S.R. (1994) Specificty of the thrombin receptor for agonist peptide is defined by its extracellular surface. *Nature* **368**, 648-651

5. Lerner, D. J., Chen, M., Tram, T., and Coughlin, S. R. (1996) Agonist recognition by proteinase-activated receptor 2 and thrombin receptor. Importance of extracellular loop interactions for receptor function. *J Biol Chem* **271**, 13943-13947

6. Nanevicz, T., Ishii, M., Wang, L., Chen, M., Chen, J., Turck, C. W., Cohen, F. E., and Coughlin, S. R. (1995) Mechanisms of thrombin receptor agonist specificity. Chimeric receptors and complementary mutations identify an agonist recognition site. *J Biol Chem* **270**, 21619-21625

7. Kuliopulos, A., Covic, L., Seeley, S. K., Sheridan, P. J., Helin, J., and Costello, C. E. (1999) Plasmin desensitization of the PAR1 thrombin receptor: kinetics, sites of truncation, and implications for thrombolytic therapy. *Biochemistry* **38**, 4572-4585

8. Oikonomopoulou, K., Hansen, K. K., Saifeddine, M., Vergnolle, N., Tea, I., Blaber, M., Blaber, S. I., Scarisbrick, I., Diamandis, E. P., and Hollenberg, M. D. (2006) Kallikrein-mediated cell signalling: targeting proteinase-activated receptors (PARs). *Biol Chem* **387**, 817-824

9. Oikonomopoulou, K., Hansen, K. K., Saifeddine, M., Vergnolle, N., Tea, I., Diamandis, E. P., and Hollenberg, M. D. (2006) Proteinase-mediated cell signalling: targeting proteinase-activated receptors (PARs) by kallikreins and more. *Biol Chem* **387**, 677-685

10. Mize, G. J., Wang, W., and Takayama, T. K. (2008) Prostate-specific kallikreins-2 and -4 enhance the proliferation of DU-145 prostate cancer cells through protease-activated receptors-1 and -2. *Mol Cancer Res* **6**, 1043-1051

11. Vandell, A. G., Larson, N., Laxmikanthan, G., Panos, M., Blaber, S. I., Blaber, M., and Scarisbrick, I. A. (2008) Protease-activated receptor dependent and independent signaling by kallikreins 1 and 6 in CNS neuron and astroglial cell lines. *J Neurochem* **107**, 855-870

12. Abdallah, R. T., Keum, J. S., El-Shewy, H. M., Lee, M. H., Wang, B., Gooz, M., Luttrell, D. K., Luttrell, L. M., and Jaffa, A. A. (2010) Plasma kallikrein promotes epidermal growth factor receptor transactivation and signaling in vascular smooth muscle through direct activation of protease-activated receptors. *J Biol Chem* **285**, 35206-35215

13. Schuepbach, R. A., Madon, J., Ender, M., Galli, P., and Riewald, M. (2012) Protease-activated receptor-1 cleaved at R46 mediates cytoprotective effects. *J Thromb Haemost* **10**, 1675-1684

14. Ruf, W., Furlan-Freguia, C., and Niessen, F. (2009) Vascular and dendritic cell coagulation signaling in sepsis progression. *J Thromb Haemost* **7 Suppl 1**, 118-121

15. Griffin JH, F. J., Gale AJ, Mosnier LO (2007) Activated protein C. *J Thromb Haemost* **5**, 73-80

16. Yang, E., Boire, A., Agarwal, A., Nguyen, N., O'Callaghan, K., Tu, P., Kuliopulos, A., and Covic, L. (2009) Blockade of PAR1 signaling with cell-penetrating pepducins inhibits Akt survival pathways in breast cancer cells and suppresses tumor survival and metastasis. *Cancer Res* **69**, 6223-6231

17. Du, X., Wang, S., Lu, J., Cao, Y., Song, N., Yang, T., Dong, R., Zang, L., Yang, Y., Wu, T., and Li, J. (2011) Correlation between MMP1-PAR1 axis and clinical outcome of primary gallbladder carcinoma. *Jpn J Clin Oncol* **41**, 1086-1093

18. Trivedi, V., Boire, A., Tchernychev, B., Kaneider, N.C., Leger, A.J., O' Callaghan, K., Covic, L., and Kuliopulos, A. (2009) Platelet matrix metalloprotease-1 mediates thrombogenesis by activating PAR1 at a cryptic ligand site. *Cell* **137**, 332-343

19. Austin, K. M., Covic, L., and Kuliopulos, A. (2013) Matrix metalloproteases and PAR1 activation. *Blood* **121**, 431-439

20. Mailman, R. B. (2007) GPCR functional selectivity has therapeutic impact. *Trends Pharmacol Sci* **28**, 390-396

21. Kenakin, T., and Christopoulos, A. (2013) Signalling bias in new drug discovery: detection, quantification and therapeutic impact. *Nat Rev Drug Discov* **12**, 205-216

22. Koukos, G., Sevigny, L., Zhang, P., Covic, L., and Kuliopulos, A. (2011) Serine and metalloprotease signaling through PAR1 in arterial thrombosis and vascular injury. *IUBMB Life* **63**, 412-418

23. Coughlin, S. R. (2005) Protease-activated receptors in hemostasis, thrombosis and vascular biology. *J Thromb Haemost* **3**, 1800-1814

24. Connolly, A. J., Ishihara, H., Kahn, M. L., Farese, R. V., Jr., and Coughlin, S. R. (1996) Role of the thrombin receptor in development and evidence for a second receptor. *Nature* **381**, 516-519

25. Darrow, A. L., Fung-Leung, W. P., Ye, R. D., Santulli, R. J., Cheung, W. M., Derian, C. K., Burns, C. L., Damiano, B. P., Zhou, L., Keenan, C. M., Peterson, P. A., and Andrade-Gordon, P. (1996) Biological consequences of thrombin receptor deficiency in mice. *Thromb Haemost* **76**, 860-866

26. Griffin, C. T., Srinivasan, Y., Zheng, Y. W., Huang, W., and Coughlin, S. R. (2001) A role for thrombin receptor signaling in endothelial cells during embryonic development. *Science* **293**, 1666-1670

27. McNamara, C. A., Sarembock, I. J., Gimple, L. W., Fenton, J. W., 2nd, Coughlin, S. R., and Owens, G. K. (1993) Thrombin stimulates proliferation of cultured rat aortic smooth muscle cells by a proteolytically activated receptor. *J Clin Invest* **91**, 94-98

28. Chen, L. B., and Buchanan, J. M. (1975) Mitogenic activity of blood components. I. Thrombin and prothrombin. *Proc Natl Acad Sci U S A* **72**, 131-135

29. Vu, T. K., Wheaton, V. I., Hung, D. T., Charo, I., and Coughlin, S. R. (1991) Domains specifying thrombin-receptor interaction. *Nature* **353**, 674-677

30. Ishii, K., Gerszten, R., Zheng, Y. W., Welsh, J. B., Turck, C. W., and Coughlin, S. R. (1995) Determinants of thrombin receptor cleavage. Receptor domains involved, specificity, and role of the P3 aspartate. *J Biol Chem* **270**, 16435-16440

31. Xu, W. F., Andersen, H., Whitmore, T. E., Presnell, S. R., Yee, D. P., Ching, A., Gilbert, T., Davie, E. W., and Foster, D. C. (1998) Cloning and characterization of human protease-activated receptor 4. *Proc Natl Acad Sci U S A* **95**, 6642-6646

32. Kahn, M. L., Zheng, Y. W., Huang, W., Bigornia, V., Zeng, D., Moff, S., Farese, R. V., Jr., Tam, C., and Coughlin, S. R. (1998) A dual thrombin receptor system for platelet activation. *Nature* **394**, 690-694

33. Covic, L., Gresser, A. L., and Kuliopulos, A. (2000) Biphasic kinetics of activation and signaling for PAR1 and PAR4 thrombin receptors in platelets. *Biochemistry* **39**, 5458-5467

34. Ramachandran, R. (2012) Developing PAR1 antagonists: minding the endothelial gap. *Discov Med* **13**, 425-431

35. Kalashnyk, O., Petrova, Y., Lykhmus, O., Mikhalovska, L., Mikhalovsky, S., Zhukova, A., Gnatenko, D., Bahou, W., Komisarenko, S., and Skok, M. (2013) Expression, function and cooperating partners of protease-activated receptor type 3 in vascular endothelial cells and B lymphocytes studied with specific monoclonal antibody. *Mol Immunol* **54**, 319-326

36. McLaughlin, J. N., Patterson, M. M., and Malik, A. B. (2007) Protease-activated receptor-3 (PAR3) regulates PAR1 signaling by receptor dimerization. *Proc Natl Acad Sci U S A* **104**, 5662-5667

37. Arora, P., Ricks, T. K., and Trejo, J. (2007) Protease-activated receptor signalling, endocytic sorting and dysregulation in cancer. *J Cell Sci* **120**, 921-928

38. Martin, C. B., Mahon, G. M., Klinger, M. B., Kay, R. J., Symons, M., Der, C. J., and Whitehead, I. P. (2001) The thrombin receptor, PAR-1, causes transformation by activation of Rho-mediated signaling pathways. *Oncogene* **20**, 1953-1963

39. Boire, A., Covic, L., Agarwal, A., Jacques, S., Sherifi, S., and Kuliopulos, A. (2005) PAR1 is a matrix metalloprotease-1 receptor that promotes invasion and tumorigenesis of breast cancer cells. *Cell* **120**, 303-313

40. Booden, M. A., Eckert, L. B., Der, C. J., and Trejo, J. (2004) Persistent signaling by dysregulated thrombin receptor trafficking promotes breast carcinoma cell invasion. *Mol Cell Biol* **24**, 1990-1999

41. Bergmann, S., Junker, K., Henklein, P., Hollenberg, M. D., Settmacher, U., and Kaufmann, R. (2006) PAR-type thrombin receptors in renal carcinoma

cells: PAR1-mediated EGFR activation promotes cell migration. *Oncol Rep* **15**, 889-893

42. Benka, M. L., Lee, M., Wang, G.R., Buckman, S., Burlacu, A., Cole, L., DePina, A., Dias, P., Granger, A., Grant, B., et al (1995) The thrombin receptor in human platelets is coupled to a GTP binding protein of the G alpha q family. *FEBS lett.* **363**, 49-52

43. Majumdar, M., Seasholtz, T. M., Buckmaster, C., Toksoz, D., and Brown, J. H. (1999) A rho exchange factor mediates thrombin and Galpha(12)-induced cytoskeletal responses. *J Biol Chem* **274**, 26815-26821

44. Baffy, G., Yang, L., Raj, S., Manning, D.R., and Williamson, J.R. (1994) G protein coupling to the thrombin receptor in Chinese hamster lung fibroblasts. *J Biol Chem.* **269**, 8483-8487

45. Offermanns, S., Toombs, C. F., Hu, Y. H., and Simon, M. I. (1997) Defective platelet activation in G alpha(q)-deficient mice. *Nature* **389**, 183-186

46. Macfarlane, S. R., Seatter, M. J., Kanke, T., Hunter, G. D., and Plevin, R. (2001) Proteinase-activated receptors. *Pharmacol Rev* **53**, 245-282

47. Vaidyula, V. R., and Rao, A. K. (2003) Role of Galphaq and phospholipase C-beta2 in human platelets activation by thrombin receptors PAR1 and PAR4: studies in human platelets deficient in Galphaq and phospholipase C-beta2. *Br J Haematol* **121**, 491-496

48. Hung, D. T., Wong, Y. H., Vu, T. K., and Coughlin, S. R. (1992) The cloned platelet thrombin receptor couples to at least two distinct effectors to stimulate phosphoinositide hydrolysis and inhibit adenylyl cyclase. *J Biol Chem* **267**, 20831-20834

49. Offermanns, S., Laugwitz, K. L., Spicher, K., and Schultz, G. (1994) G proteins of the G12 family are activated via thromboxane A2 and thrombin receptors in human platelets. *Proc Natl Acad Sci U S A* **91**, 504-508

50. Coughlin, S. R. (2000) Thrombin signalling and protease-activated receptors. *Nature* **407**, 258-264

51. Violin, J. D., and Lefkowitz, R. J. (2007) Beta-arrestin-biased ligands at seven-transmembrane receptors. *Trends Pharmacol Sci* **28**, 416-422

52. Luttrell, L. M., and Kenakin, T. P. (2011) Refining efficacy: allosterism and bias in G protein-coupled receptor signaling. *Methods Mol Biol* **756**, 3-35

53. Maudsley, S., Patel, S. A., Park, S. S., Luttrell, L. M., and Martin, B. (2012) Functional signaling biases in G protein-coupled receptors: Game Theory and receptor dynamics. *Mini Rev Med Chem* **12**, 831-840

54. Komarova, Y. A., Mehta, D., and Malik, A. B. (2007) Dual regulation of endothelial junctional permeability. *Sci STKE* **2007**, re8

55. Russo, A., Soh, U. J., Paing, M. M., Arora, P., and Trejo, J. (2009) Caveolae are required for protease-selective signaling by protease-activated receptor-1. *Proc Natl Acad Sci U S A* **106**, 6393-6397

56. Russo, A., Soh, U. J., and Trejo, J. (2009) Proteases display biased agonism at protease-activated receptors: location matters! *Mol Interv* **9**, 87-96

57. Soh, U. J., and Trejo, J. (2011) Activated protein C promotes protease-activated receptor-1 cytoprotective signaling through beta-arrestin and dishevelled-2 scaffolds. *Proc Natl Acad Sci U S A* **108**, E1372-1380

58. Paing, M. M., Stutts, A.B., Kohout, T.A., Lefkowitz, R.J., and Trejo, J. (2002) beta-arrestins regulate protease-activated receptor-1 desensitization but not internalization or down-regulation. *The Journal of Biological Chemistry* **277**, 1292-1300

59. Ishii, K., Hein, L., Kobilka, B., and Coughlin, S. R. (1993) Kinetics of thrombin receptor cleavage on intact cells. Relation to signaling. *J Biol Chem* **268**, 9780-9786

60. Ishii, K., Chen, J., Ishii, M., Koch, W. J., Freedman, N. J., Lefkowitz, R. J., and Coughlin, S. R. (1994) Inhibition of thrombin receptor signaling by a G-protein coupled receptor kinase. Functional specificity among G-protein coupled receptor kinases. *J Biol Chem* **269**, 1125-1130

61. Chen, C. H., Paing, M. M., and Trejo, J. (2004) Termination of protease-activated receptor-1 signaling by beta-arrestins is independent of receptor phosphorylation. *J Biol Chem* **279**, 10020-10031

62. Hammes, S. R., Shapiro, M. J., and Coughlin, S. R. (1999) Shutoff and agonist-triggered internalization of protease-activated receptor 1 can be separated by mutation of putative phosphorylation sites in the cytoplasmic tail. *Biochemistry* **38**, 9308-9316

63. Tiruppathi, C., Yan, W., Sandoval, R., Naqvi, T., Pronin, A. N., Benovic, J. L., and Malik, A. B. (2000) G protein-coupled receptor kinase-5 regulates thrombin-activated signaling in endothelial cells. *Proc Natl Acad Sci U S A* **97**, 7440-7445

64. Paing, M. M., Johnston, C. A., Siderovski, D. P., and Trejo, J. (2006) Clathrin adaptor AP2 regulates thrombin receptor constitutive internalization and endothelial cell resensitization. *Mol Cell Biol* **26**, 3231-3242

65. Chen, B., Dores, M. R., Grimsey, N., Canto, I., Barker, B. L., and Trejo, J. (2011) Adaptor protein complex-2 (AP-2) and epsin-1 mediate protease-activated receptor-1 internalization via phosphorylation- and ubiquitination-dependent sorting signals. *J Biol Chem* **286**, 40760-40770

66. Hein, L., Ishii, K., Coughlin, S. R., and Kobilka, B. K. (1994) Intracellular targeting and trafficking of thrombin receptors. A novel mechanism for resensitization of a G protein-coupled receptor. *J Biol Chem* **269**, 27719-27726

67. Shapiro, M. J., and Coughlin, S. R. (1998) Separate signals for agonist-independent and agonist-triggered trafficking of protease-activated receptor 1. *J Biol Chem* **273**, 29009-29014

68. Clague, M. J., and Urbe, S. (2010) Ubiquitin: same molecule, different degradation pathways. *Cell* **143**, 682-685

69. Dores, M. R., and Trejo, J. (2012) Ubiquitination of G protein-coupled receptors: functional implications and drug discovery. *Mol Pharmacol* **82**, 563-570

70. Wolfe, B. L., Marchese, A., and Trejo, J. (2007) Ubiquitination differentially regulates clathrin-dependent internalization of protease-activated receptor-1. *J Cell Biol* **177**, 905-916

71. Dores, M. R., Chen, B., Lin, H., Soh, U. J., Paing, M. M., Montagne, W. A., Meerloo, T., and Trejo, J. (2012) ALIX binds a YPX(3)L motif of the GPCR PAR1 and mediates ubiquitin-independent ESCRT-III/MVB sorting. *J Cell Biol* **197**, 407-419

72. Dores, M. R., Paing, M. M., Lin, H., Montagne, W. A., Marchese, A., and Trejo, J. (2012) AP-3 regulates PAR1 ubiquitin-independent MVB/lysosomal sorting via an ALIX-mediated pathway. *Mol Biol Cell* **23**, 3612-3623

73. Canto, I., and Trejo, J. (2013) Palmitoylation of protease-activated receptor-1 regulates adaptor protein complex-2 and -3 interaction with tyrosine-based motifs and endocytic sorting. *J Biol Chem*

74. Landolt-Marticorena, C., and Reithmeier, R. A. (1994) Asparagine-linked oligosaccharides are localized to single extracytosolic segments in multi-span membrane glycoproteins. *Biochem J* **302 (Pt 1)**, 253-260

75. Vouret-Craviari, V., Grall, D., Chambard, J. C., Rasmussen, U. B., Pouyssegur, J., and Van Obberghen-Schilling, E. (1995) Post-translational and activation-dependent modifications of the G protein-coupled thrombin receptor. *J Biol Chem* **270**, 8367-8372

76. Mize, G. J., Harris, J. E., Takayama, T. K., and Kulman, J. D. (2008) Regulated expression of active biotinylated G-protein coupled receptors in mammalian cells. *Protein Expr Purif* **57**, 280-289

77. Roy, S., Perron, B., and Gallo-Payet, N. (2010) Role of asparagine-linked glycosylation in cell surface expression and function of the human adrenocorticotropin receptor (melanocortin 2 receptor) in 293/FRT cells. *Endocrinology* **151**, 660-670

78. Lanctot, P. M., Leclerc, P. C., Escher, E., Leduc, R., and Guillemette, G. (1999) Role of N-glycosylation in the expression and functional properties of human AT1 receptor. *Biochemistry* **38**, 8621-8627

79. Whitaker, G. M., Lynn, F. C., McIntosh, C. H., and Accili, E. A. (2012) Regulation of GIP and GLP1 receptor cell surface expression by N-glycosylation and receptor heteromerization. *PLoS One* **7**, e32675

80. Wheatley, M., and Hawtin, S. R. (1999) Glycosylation of G-protein-coupled receptors for hormones central to normal reproductive functioning: its occurrence and role. *Hum Reprod Update* **5**, 356-364

81. Kohno, T., Wada, A., and Igarashi, Y. (2002) N-glycans of sphingosine 1-phosphate receptor Edg-1 regulate ligand-induced receptor internalization. *FASEB J* **16**, 983-992

82. Cho, D. I., Min, C., Jung, K. S., Cheong, S. Y., Zheng, M., Cheong, S. J., Oak, M. H., Cheong, J. H., Lee, B. K., and Kim, K. M. (2012) The N-terminal region of the dopamine D2 receptor, a rhodopsin-like GPCR, regulates correct integration into the plasma membrane and endocytic routes. *Br J Pharmacol* **166**, 659-675

83. Zhang, Z., Austin, S. C., and Smyth, E. M. (2001) Glycosylation of the human prostacyclin receptor: role in ligand binding and signal transduction. *Mol Pharmacol* **60**, 480-487

84. Hsiao, C. C., Cheng, K. F., Chen, H. Y., Chou, Y. H., Stacey, M., Chang, G. W., and Lin, H. H. (2009) Site-specific N-glycosylation regulates the GPS auto-proteolysis of CD97. *FEBS Lett* **583**, 3285-3290

85. Walsh, M. T., Foley, J. F., and Kinsella, B. T. (1998) Characterization of the role of N-linked glycosylation on the cell signaling and expression of the human thromboxane A2 receptor alpha and beta isoforms. *J Pharmacol Exp Ther* **286**, 1026-1036

86. Compton, S. J. (2003) Glycosylation and Proteinase-Activated Receptor Function. *Drug Development Research* **59**, 350-354

87. Compton, S. J., Renaux, B., Wijesuriya, S. J., and Hollenberg, M. D. (2001) Glycosylation and the activation of proteinase-activated receptor 2 (PAR(2)) by human mast cell tryptase. *Br J Pharmacol* **134**, 705-718

88. Tordai, A., Brass, L. F., and Gelfand, E. W. (1995) Tunicamycin inhibits the expression of functional thrombin receptors on human T-lymphoblastoid cells. *Biochem Biophys Res Commun* **206**, 857-862

89. Xiao, Y. P., Morice, A. H., Compton, S. J., and Sadofsky, L. (2011) N-linked glycosylation regulates human proteinase-activated receptor-1 cell surface expression and disarming via neutrophil proteinases and thermolysin. *J Biol Chem* **286**, 22991-23002

90. Soto, A. G., and Trejo, J. (2010) N-linked glycosylation of protease-activated receptor-1 second extracellular loop: a critical determinant for ligand-induced receptor activation and internalization. *J Biol Chem* **285**, 18781-18793

91. Kaufmann, R., Hoffmann, J., Ramakrishnan, V., and Nowak, G. (1998) Intermediates of prothrombin activation induce intracellular calcium mobilization in rat aortic smooth muscle cells. *Thromb Haemost* **80**, 1018-1021

92. Kaufmann, R., Zieger, M., Tausch, S., Henklein, P., and Nowak, G. (2000) Meizothrombin, an intermediate of prothrombin activation, stimulates human glioblastoma cells by interaction with PAR-1-type thrombin receptors. *J Neurosci Res* **59**, 643-648

93. Suidan, H. S., Bouvier, J., Schaerer, E., Stone, S. R., Monard, D., and Tschopp, J. (1994) Granzyme A released upon stimulation of cytotoxic T lymphocytes activates the thrombin receptor on neuronal cells and astrocytes. *Proc Natl Acad Sci U S A* **91**, 8112-8116

94. Riewald, M., Petrovan, R. J., Donner, A., Mueller, B. M., and Ruf, W. (2002) Activation of endothelial cell protease activated receptor 1 by the protein C pathway. *Science* **296**, 1880-1882

95. Knecht, W., Cottrell, G. S., Amadesi, S., Mohlin, J., Skaregarde, A., Gedda, K., Peterson, A., Chapman, K., Hollenberg, M. D., Vergnolle, N., and Bunnett, N. W. (2007) Trypsin IV or mesotrypsin and p23 cleave protease-activated receptors 1 and 2 to induce inflammation and hyperalgesia. *J Biol Chem* **282**, 26089-26100

96. Riewald, M., Kravchenko, V. V., Petrovan, R. J., O'Brien, P. J., Brass, L. F., Ulevitch, R. J., and Ruf, W. (2001) Gene induction by coagulation factor Xa is mediated by activation of protease-activated receptor 1. *Blood* **97**, 3109-3116

97. Camerer, E., Kataoka, H., Kahn, M., Lease, K., and Coughlin, S. R. (2002) Genetic evidence that protease-activated receptors mediate factor Xa signaling in endothelial cells. *J Biol Chem* **277**, 16081-16087

98. Wilson, T. J., Nannuru, K. C., and Singh, R. K. (2009) Cathepsin G recruits osteoclast precursors via proteolytic activation of protease-activated receptor-1. *Cancer Res* **69**, 3188-3195

99. Laing, G. D., Compton, S. J., Ramachandran, R., Fuller, G. L., Wilkinson, M. C., Wagstaff, S. C., Watson, S. P., Kamiguti, A. S., Theakston, R. D., and Senis, Y. A. (2005) Characterization of a novel protein from Proatheris superciliaris venom: proatherocytin, a 34-kDa platelet receptor PAR1 agonist. *Toxicon* **46**, 490-499

100. Chiu, L. L., Perng, D. W., Yu, C. H., Su, S. N., and Chow, L. P. (2007) Mold allergen, pen C 13, induces IL-8 expression in human airway epithelial cells by activating protease-activated receptor 1 and 2. *J Immunol* **178**, 5237-5244

101. Ludeman, M. J., Zheng, Y. W., Ishii, K., and Coughlin, S. R. (2004) Regulated shedding of PAR1 N-terminal exodomain from endothelial cells. *J Biol Chem* **279**, 18592-18599

Chapter 2:

Characterization of PAR1 N-linked glycosylation

2.1 Abstract

N-linked glycosylation is a post-translational modification that occurs on GPCRs at the consensus sequence N-X-S/T (where X is any amino acid except proline). PAR1 contains five N-linked glycosylation consensus sites: three residing in the N-terminus and two localized on the surface of the second extracellular loop (ECL2). However, the function of PAR1 N-linked glycosylation is not known. We thus sought to determine if PAR1 is glycosylated and the impact of glycosylation on receptor trafficking and signaling. Here, we report that PAR1 is extensively modified by N-linked glycosylation. We found that both the PAR1 N-terminus and ECL2 serve as sites for N-linked glycosylation, with the ECL2 more extensively glycosylated than ECL2. However, mutation of the PAR1 N-linked glycosylation sites revealed that N-terminal glycosylation and ECL2 glycosylation have different functions in the regulation of receptor signaling and trafficking. In this chapter, we described the initial characterization of PAR1 N-linked glycosylation.

2.2 Introduction

The posttranslational modification of nascent proteins by N-linked glycosylation occurs via covalent attachment of saccharides to asparagine (N) residues of the consensus site N-X-S/T (where X is any amino acid except proline, S is serine and T is threonine)(1) . A diverse array of GPCRs are post-translationally modified by N-linked glycosylation during biogenesis (2-5). N-linked glycosylation occurs in the endoplasmic reticulum and *trans*-Golgi network concurrent with translation and folding of nascent proteins. This process involves numerous enzymes and the

attachment of carbohydrate chains to nascent transmembrane proteins and occurs in an ordered fashion. During N-linked glycosylation, glycosyltransferases add carbohydrates to growing carbohydrate chains, while glycosidases remove carbohydrates from the modified protein. Carbohydrates are able to form a variety of bonds and branching networks making N-linked glycosylation highly heterogeneous (6). Consequently, GPCRs can be differentially glycosylated in different tissues and cell types (7-11), most likely depending on the enzyme expression profile and the availability of substrate carbohydrates. This raises the possibility that PAR1 may exist as a differentially glycosylated species in different tissues or cell types. Whether this could affect PAR1 localization, ligand interactions, G-protein coupling, or other facets of receptor function has not been examined.

Although N-linked glycosylation of GPCRs is critical for biogenesis and appropriate trafficking to the cell surface, it has other functions in GPCR regulation. N-linked glycosylation within the N-terminus of CD97, an adhesion GPCR, has been shown to regulate auto proteolysis of the receptor (12). Internalization of the dopamine D_2 receptor and the sphingosine 1-phosphate receptor, endothelial differentiation gene-1 product (Edg-1), are affected by N-linked glycosylation (13, 14). In addition, N-linked glycosylation can also have affects on GPCR signaling, as is the case for the prostacyclin receptor and the thromboxane A2 receptor (15, 16). Whereas N-linked glycosylation of PAR2, a GPCR related to PAR1 appears to affect protease recognition (17, 18). Incubation of PAR2 with tunicamycin, a drug that globally inhibits N-linked glycosylation, or mutation of the putative N-linked glycosylation site within the N-terminus altered the capacity of trypsin, but not tryptase to cleave and

activate the receptor. In addition, treatment of PAR2 with sialidase, an enzyme that cleaves terminal sialic acids, resulted in a similar effect. These findings suggest that N-linked glycan modification of PAR1 could modulate receptor function in different ways.

Most GPCRs contain at least one consensus site for N-linked glycosylation that resides within the N-terminus (19). However, human PAR1 contains five potential N-linked glycosylation consensus sites: three within the N-terminus and two are localized in ECL2. Several studies have suggested that PAR1 is highly glycosylated in different cell types based on a shift in its apparent molecular weight following glycosidase treatment (20-22). In yeast *S. cerevisiae*, which are unable to glycosylate the receptor, PAR1 migrates as a single band close to its predicted molecular weight rather than a broad high molecular weight species typically observed in mammalian cells (21). Moreover, global disruption of glycoprotein synthesis with the drug tunicamycin greatly diminished surface expression of PAR1 in Jurkat T lymphocyte cells (23), suggesting that N-linked glycosylation of PAR1 is important for proper trafficking to the cell surface. However, the actual sites of PAR1 N-linked glycosylation and the importance of such sites in the regulation of receptor signaling and trafficking have not been determined.

In the work presented here we show that PAR1 is highly modified by N-linked glycosylation. Both the N-terminus and the ECL2 of PAR1 are targeted for N-linked glycosylation, with the ECL2 sites contributing more to the overall glycosylation status of the receptor than the N-terminal sites. In addition, we show that N-linked glycosylation of PAR1 at the N-terminus is important for the proper processing and

export to the cell surface, similar to that observed with most GPCRs. Intriguingly, however, N-linked glycosylation of PAR1 at ECL2 appears to modulate receptor signaling. The later finding serves as a foundation for further studies of N-linked glycosylation of PAR1 at ECL2 on biased signaling that are described in Chapters 3 and 4.

2.3 Materials and methods

Reagents and Antibodies- Human α-thrombin was obtained from Enzyme Research Laboratories (South Bend, IN). The PAR1-activating peptide SFLLRN was synthesized as the carboxyl amide and purified by reverse phase high-pressure chromatography at Tufts University Core Facility (Boston, MA). PNGase F, Sialidase, and Endo H were purchased from New England Biolabs, Inc. (Ipswich, MA). Tunicamycin and carbachol was obtained from Sigma-Aldrich (St. Louis, MO). Rabbit polyclonal anti-FLAG antibody and mouse monoclonal M1 and M2 anti- FLAG antibodies were purchased from Sigma- Aldrich. The anti-PAR1 WEDE mouse antibody was purchased from Beckman Coulter (Fullerton, CA). Anti-PAR1 rabbit polyclonal antibody was previously described (24). Mouse anti-early endosome antigen-1 (EEA-1) and *trans*-Golgi network (TGN) 230 antibodies were purchased from BD Transduction Laboratories (Lexington, KY). Goat anti-mouse IgG antibody was purchased from Thermo Scientific (Rockford, IL). Horse-radish peroxidase (HRP)-conjugated goat anti-mouse and goat anti-rabbit antibodies were purchased from Bio-Rad Laboratories (Richmond, CA).

cDNAs and Cell lines- A cDNA encoding human PAR1 with an N-terminal FLAG epitope sequence cloned into pBJ vector was previously described (25) and used in these studies. Mutations were introduced into FLAG-tagged PAR1 by site-directed mutagenesis using the QuikChange Mutagenesis kit (Stratagene) and confirmed by dideoxy sequencing (Moores Cancer Center Core Facility, La Jolla, CA). HeLa cells stably expressing FLAG-tagged PAR1 wild-type and mutants were generated and maintained as previously described (25). The human umbilical vein endothelial-derived EA.hy926 cells were grown and cultured as we previously described (26).

HeLa cells were transiently transfected with a total plasmid amount of 0.4 μg per 24-well or 2 μg per six-well using Lipofectamine reagent (Invitrogen) according to the manufacturer's instructions and were assayed 48 h after transfection.

PAR1 Sequence Alignment- A sequence alignment was performed using the EMBL-EBI ClustalW2 program. *Rattus norvegicus* (NCBI Reference Sequence: NM_012950.2), *Mus musculus* (NCBI Reference Sequence: NM_010169.3), *Cricetulus longicaudatus* (GenBank: X61958.1), *Homo sapiens* (NCBI Reference Sequence: NM_001992.3), *Papio hamadryus* (GenBank: AF028727.1), *Equuas caballus* (NCBI Reference Sequence: XM_001503957.2), *Canis lupis familiaris* (NCBI Reference Sequence: XM_546059.2), *Xenopus laevis* (NCBI Reference Sequence: NM_001085783.1), *Gallus gallus* (NCBI Reference Sequence:

XM_424799.3), *Macaca mulatta* (GenBank: EHH26595.1), *Sus scrofa* (NCBI Reference Sequence: NP_001231301.1), *Boas taurus* (NCBI Reference Sequence: NP_001096567.1), *Bos grunniens mutus* (GenBank: ELR60449.1), *Heterocephalus glaber* (GenBank: EHB00368.1), *Mustela putorius furo* (GenBank: AER98213.1), *Danio rerio* (NCBI Reference Sequence: NP_001108318.1), *Gorilla gorilla gorilla* (NCBI Reference Sequence: XP_004058710.1), *Pongo abelii* (NCBI Reference Sequence: XP_002815710.1), *Pan troglodytes* (NCBI Reference Sequence: XP_526888.3), *Nomascus leucogenys* (NCBI Reference Sequence: XP_003261537.1), *Papio anubis* (NCBI Reference Sequence: XP_003899888.1), *Cavia porcellus* (XP_003470285.1), *Callithrix jacchus* (NCBI Reference Sequence: XP_002744891.1), *Cricetulus griseus* (NCBI Reference Sequence: XP_003498759.1), *Saimiri boliviensis boliviensis* (NCBI Reference Sequence: XP_003921004.1), *Loxodonta Africans* (NCBI Reference Sequence: XP_003408011.1), *Monodelphis domestica* (NCBI Reference Sequence: XP_001362837.2), *Otolemur garnetti* NCBI Reference Sequence: XP_003785973.1), *Felis catus* (NCBI Reference Sequence: XP_003981132.1), *Ovis aries* (NCBI Reference Sequence: XP_004010905.1).

PAR1 Immunoprecipitation and Immunoblotting- HeLa cells stably expressing FLAG-tagged PAR1 wild-type or mutants were plated at 5 X 10^5 cells per well in 6-well culture dishes and grown overnight at 37°C. Cells were washed, incubated with or without agonists diluted in DMEM containing 1 mg/ml BSA and 10 mM HEPES, pH 7.4 for various times at 37°C. Cells were then washed with cold PBS and lysed with

Triton X-100 lysis buffer (50 mM Tris-HCl pH 7.4, 100 mM NaCl, 5 mM EDTA, 50 mM NaF, 10 mM NaPP, 1% Triton X-100) containing freshly added protease inhibitors. Cell lysates were solubilized for 1.5 h at 4°C and clarified by centrifugation at 14,000 rpm for 20 min at 4°C. The total amount of protein in cell lysates was quantified using a Bicinchoninic acid (BCA) Protein Assay Reagent (Thermo Scientific) and equivalent amounts of lysates were used for immunoprecipitation with the M2 anti-FLAG antibody or goat anti-mouse IgG control. Immunoprecipitates were analyzed by SDS-PAGE, transferred to membranes and PAR1 was detected by immunoblotting. Immunoblots were developed with Enhanced Chemiluminescence (GE Healthcare, Piscataway, NJ), imaged by autoradiography and quantitated with ImageJ software.

Cell Surface ELISA- HeLa cells stably expressing FLAG-tagged PAR1 wild-type or mutants were plated at 1 X 10^5 cells per well in a fibronectin coated 24-well culture dish and grown overnight at 37°C. Cells were washed in serum- free DMEM, then treated with thrombin diluted in DMEM/ BSA/HEPES at 37°C for various times. After treatments, cells were placed on ice, washed with PBS and then fixed with 4% paraformaldehyde (PFA) for 5 min at 4°C. Cells were washed, and then incubated with polyclonal anti-FLAG antibody diluted 1:1000 or rabbit polyclonal anti-PAR1 C5433 diluted 1:250 in DMEM/BSA/HEPES for 1 h at room temperature. Cells were washed and then incubated with secondary HRP-conjugated goat anti-rabbit antibody for 1 h at room temperature and washed extensively. The amount of secondary

antibody bound was determined by incubation with 1-Step ABTS (2,2-azinobis-3-ethylbenz-thiazoline-6- sulfonic acid) (Thermo Scientific) substrate for 10 to 20 min at 25 °C. An aliquot was removed, and the optical density (OD) determined at 405 nm using a Molecular Devices SpectraMax Plus microplate reader.

Deglycosylation of PAR1- HeLa cells stably expressing FLAG-tagged PAR1 or FLAG-PAR2 wild- type were plated at 5 X 10^5 cells per well in 6-well dishes or 1.0 X 10^5 cells per well in 24-well culture dishes coated with fibronectin and grown overnight at 37°C. Cells were washed, and then treated with 0.5 μg/ml tunicamycin (diluted in DMSO) or vehicle control in serum-free DMEM for 16 h at 37°C. After incubation, cells were either lysed with Triton lysis buffer, processed and immunoblotted for PAR1 expression or fixed with 4% PFA and processed for cell surface ELISA as described above.

Glycosidase Incubations- For PNGase F treatments, cells stably expressing FLAG-tagged PAR1 or endogenous PAR1 were plated at 5 X 10^5 cells per well in a 6-well culture dish and grown overnight at 37°C. Cells were lysed with Triton lysis buffer, processed and then immunoprecipitated with M2 anti-FLAG antibody, anti-PAR1 WEDE antibody, or goat anti-mouse IgG as described above. PAR1 immunoprecipitates were then resuspended in 100 μl of 1X glycoprotein denaturing buffer (0.5% SDS, 40 mM DTT), heated at 100°C for 10 min, vortexed, and then

centrifuged for 30 sec at 25°C. Beads were resuspended and 20 μl aliquots were added to each reaction tube. PNGase F reaction mixture was prepared using 2 μl enzyme per 20 μl sample volume and added to reaction tubes. Samples were incubated at 37°C for various times then an equal volume of 2X sample buffer (62.5 mM Tris-HCl, 10% glycerol, 5% SDS, 0.01% bromophenol blue) was added and the analysis of PAR1 was determined by immunoblotting. HeLa cells stably expressing FLAG-tagged PAR1 wild-type or mutant were prepared as described for the PNGase F assay. Sialidase, EndoH, and PNGase F reaction mixtures were prepared using 4 μl, 2 μl, or 2 μl of the enzymes, respectively, per 20 μl sample volume and added to reaction tubes. Samples were incubated at 37°C for 16 h and then an equal volume of 2X sample buffer was added. PAR1 was then analyzed by immunoblotting.

Phosphoinositide Hydrolysis- HeLa cells stably expressing FLAG-tagged PAR1 wild-type or mutants were plated at 1 X 10^5 cells per well in a fibronectin coated 24-well culture dish and grown overnight at 37°C. Cells were then labeled with 1 μCi/ml of *myo*-[^{3}H]inositol (American Radiolabeled Chemicals, St. Louis, MO) diluted in serum- and inositol-free DMEM containing 1 mg/ml BSA overnight. Cells were washed, treated with or without agonists in DMEM media containing 20 mM lithium chloride (LiCl) for 60 min at 37°C and accumulated [^{3}H]inositol phosphates (IPs) were measured as described (24).

Data Analysis- Data were analyzed using GraphPad Prism software 4.0, and statistical analysis was determined using the Prism data analysis tool as noted. Statistical analysis was determined by performing student's *t* test, one-way ANOVA and Dunnett multiple comparison test, or two-way ANOVA and Bonferroni post-tests.

2.4 Results

2.4.1 Conservation of PAR1 N-linked glycosylation sites

There are five consensus sites for N-linked glycosylation of PAR1, three are localized in the N-terminus and two reside within the second extracellular loop. We first determined whether the five N-linked glycosylation consensus sites of PAR1 were conserved between species using Clustal W2 alignment **(Fig. 2.1A and B)**. An analysis of thirty PAR1 sequences from different species revealed that the N-linked glycosylation consensus sites with the most conservation occurred at the third N-terminal site and the fourth site residing in ECL2 **(Fig. 2.1A and B).** Interestingly, *Rattus norvegicus, Mus Musculus*, and *Gallus gallus* all contained three N-linked glycosylation sites within their N-terminus although they did not align with the human PAR1 N-terminal sites using Clustal W2 alignment analysis. All of the thirty PAR1 sequences contained N-terminal glycosylation sites and only three had a single site in the N-terminus. Only two PAR1 species lacked N-linked glycosylation sites in ECL2 and five species had only one site in this domain. Intriguingly, the two cold-blooded animals *Xenopus laevus* and *Danio rerio* had only one N-linked glycosylation site in the N-terminus and ECL2, but the physiological relevance of this occurrence remains

unknown. Whether the putative N-linked glycosylation sites of PAR1 are each modified by glycosylation or have specific functions important for regulation of PAR1 signaling and trafficking is not known.

2.4.2 PAR1 is modified by N-linked glycosylation

Next, we examined the glycosylation status of human PAR1 ectopically expressed in HeLa cells by examining its susceptibility to cleavage by PNGase F, an enzyme that cleaves all N-linked glycosylation except for those with an alpha-(1,3)-linked core fucose modification. HeLa cells expressing FLAG-tagged PAR1 were lysed and immunoprecipitated with M2 anti-FLAG antibody or IgG control and then incubated with PNGase F for various times at 37°C. In untreated control cells, PAR1 migrated as a broad band between ~64 and 98 kDa **(Fig. 2.2A, lane 3)**, consistent with that observed previously (25), but significantly greater than the predicted molecular weight of ~40 kDa. In contrast, after incubation with PNGase F, PAR1 migrated comparable to its predicted molecular weight of ~40 kDa **(Fig. 2.2A, lanes 4-6)**, suggesting that PAR1 is modified extensively by N-linked glycosylation. We then examined N-linked glycosylation of endogenous PAR1 expressed in human endothelial EA.hy926 cells. Endogenous PAR1 immunoprecipitated from human endothelial cells also migrated as a high molecular broad band that was reduced to its' predicted molecular weight after PNGase F treatment **(Fig. 2.2B, lanes 2-4)**. Thus, PAR1 is glycosylated in two different cell types that express the receptor exogenously and endogenously.

To further confirm that PAR1 is modified by N-linked glycosylation, we examined the mobility of PAR1 following treatment with tunicamycin, a drug that blocks the first step of glycoprotein synthesis and functions as a global inhibitor of N-linked glycosylation. In cells treated with tunicamycin, PAR1 migrated at ~40 kDa **(Fig. 2.2C, lane 4)** similar to that observed with PNGase F treatment **(Fig. 2.2A)**, and distinct from the broad high molecular weight band observed with untreated PAR1. These findings strongly suggest that PAR1 is extensively glycosylated, and is consistent with that previously reported (20-22).

2.4.3 N-linked glycosylation of PAR1 is required for export to the cell surface

N-linked glycosylation of many transmembrane proteins, including GPCRs, is important for proper folding during translation and export to the cell surface (27, 28). Thus, we determined whether global disruption of PAR1 N- linked glycosylation affected receptor export to the cell surface using tunicamycin. PAR1 cell surface expression was substantially reduced in tunicamycin treated cells compared to untreated control cells **(Fig. 2.3)**, suggesting that global disruption of PAR1 N-linked glycosylation affects transport of the receptor to the cell surface as previously reported (23). To control for pleiotropic effects of tunicamycin on protein transport, we examined cell surface expression of PAR2. In contrast to PAR1, PAR2 surface expression was surprisingly unaffected in tunicamycin treated HeLa cells **(Fig. 2.3)**. Immunoblot analysis confirmed efficient degylcosylation of PAR2 after tunicamycin treatment **(Fig. 2.3, *inset*)**. These findings suggest that glycosylation of PAR1, but not

PAR2, is important for export to the cell surface in HeLa cells. However, whether N-linked glycosylation of PAR1 occurs largely at the N- terminus, second extracellular loop or both is not known.

2.4.4 The N-terminus and ECL2 of PAR1 are modified by N-linked glycosylation

In order to determine which sites of PAR1 are modified by N-linked glycosylation, we first individually mutated the critical asparagine (N) to alanine (A) of each of the N-linked glycosylation consensus sites in the PAR1 N-terminus and ECL2 **(Fig. 2.4A)**. We used an N-terminal FLAG-tagged human PAR1 construct for our studies. However, insertion of the N-terminal FLAG tag into PAR1 inadvertently disrupted the first N-linked glycosylation site. Therefore, we re-created the site by inserting an asparagine at position 35 (N35) to determine if this site contributes to PAR1 N-linked glycosylation (**Fig. 2.4A**). An alanine was also introduced into PAR1 at this site (N35A) and used as a control. We transiently expressed PAR1 variants containing single site mutations in HeLa cells and used immunoblot analysis to determine which mutants, if any, showed a shift in mobility compared to wild-type receptor. Neither the FLAG-tagged PAR1 N35 nor N35A mutations displayed affects on receptor mobility compared to wild-type PAR1 **(Fig. 2.4B, lanes 3-5)**. Other individual point mutants of the N-terminus caused minimal changes in PAR1 mobility assessed by immunoblot **(Fig 2.4B, lanes 4,6-7)**, however, when all N-terminal sites were mutated together in a mutant designated NA NTer we observed a shift in receptor mobility **(Fig 2.4C, lane 6)** consistent with a defect in glycosylation. These

data indicate that N-linked glycosylation of PAR1 occurs at the N-terminus. Interestingly, a PAR1 mutant in which the two asparagine residues of the consensus sites in extracellular loop 2 were mutated to alanine (NA ECL2) exhibited the greatest shift in mobility **(Fig 2.4C, lane 7)**. Thus, PAR1 appears to be modified by N-linked glycosylation at both the N-terminus and ECL2, however the ECL2 serves as the major site for N-linked glycosylation. We next examined the function of PAR1 NA NTer and NA ECL2 PAR1 mutants, since single site mutations appeared to have minimal affects on PAR1 overall glycosylation status.

2.4.5 Glycosylation of the N-terminus of PAR1 is important for export to the cell surface

To ascertain the function of N-terminal *versus* ECL2 glycosylation of PAR1, we first determined whether mutants were expressed at the cell surface comparable to wild-type PAR1 by quantifying the amount of cell surface receptor with ELISA. Interestingly, cells expressing the NA NTer PAR1 mutant showed significantly less cell surface expression compared to PAR1 wild-type (WT) or NA ECL2 mutant **(Fig. 2.5A)**, suggesting that glycosylation of the PAR1 N-terminus facilitates export to the cell surface. To confirm whether PAR1 NA NTer transport is aberrant we examined the subcellular distribution of PAR1 at steady state by immunofluorescence microscopy. Both PAR1 wild-type and mutants localized to the cell surface in unpermeabilized cells **(Fig. 2.5B, top panels)**. Interestingly, however, a substantial amount of PAR1 NA NTer mutant was retained in an intracellular compartment

compared to wild-type or NA ECL2 mutant **(Fig. 2.5B, lower panels)**. We next examined the localization of PAR1 NA NTer to specific intracellular compartments. Confocal microscopy studies revealed that intracellular PAR1 NA NTer localized primarily to the *trans* Golgi network indicated by marked co-localization with TGN230 and minimally to endocytic vesicles co-stained with EEA1 **(Fig. 2.5C)**. These findings suggest that glycosylation of the PAR1 N-terminus is critical for efficient export to the cell surface.

2.4.6 PAR1 NA NTer and ECL2 mutants are partially glycosylated

We next evaluated the sensitivity of PAR1 NA NTer and ECL2 mutants to cleavage by various glycosidases to determine whether the mutant receptors indeed retained N-linked glycosylation and the nature of the glycosylation modifications. The mobility of PAR1 wild-type and mutants were unchanged after incubation with sialidase **(Fig. 2.6A lanes 2, 6 and 2.6B lanes 6, 10)**. Treatment with endoglycosidase H (Endo H) caused a shift in the mobility of the immature receptor form that appears as a minor species migrating below the fully glycosylated PAR1 wild-type and mutants **(Fig. 2.6A lanes 3, 7 and 2.6B lanes 7, 11)**. Interestingly, incubation with PNGase F caused a dramatic shift in mobility of PAR1 wild-type, NA NTer and NA ECL2 mutants to the predicted molecular weight of the unmodified receptor **(Fig. 2.6A lanes 4, 8 and 2.6B lanes 8, 12)**. These findings lend further support to the idea that the PAR1 N-terminus and ECL2 domains are both functional targets for

modification with N-linked glycosylation.

2.4.7 PAR1 NA NTer and ECL2 exhibit similar rates of thrombin cleavage compared to wild-type receptor

To determine whether glycosylation affects the capacity of thrombin to cleave PAR1, we examined the kinetics of thrombin-mediated cleavage of the PAR1 NA NTer and NA ECL2 mutants. HeLa cells stably expressing similar surface levels of either FLAG-tagged PAR1 wild-type or mutants were incubated with a low (1 nM) and a high (10 nM) concentration of thrombin for various times at 37°C, and the rate of PAR1 cleavage was monitored by measuring the loss of FLAG epitope by ELISA. PAR1 wild-type, NA ECL2 and NA NTer mutants were efficiently cleaved with similar kinetics at maximal and sub-maximal doses of thrombin **(Fig 2.7A and Fig 2.7B)**. While the rates of thrombin cleavage of PAR1 were unchanged by the mutations there was still the possibility of differences in tethered ligand docking interactions with the receptor that could lead to changes in signaling.

2.4.8 PAR1 NA ECL2 signaling is markedly enhanced compared to wild-type receptor

To determine whether N-linked glycosylation of PAR1 of the N-terminus or the ECL2 has a function in receptor signaling we examined the capacity of activated

wild-type and mutant receptors to stimulate phosphoinositide (PI) hydrolysis. Activated PAR1-stimulated PI hydrolysis occurs predominantly by $G\alpha_q$ coupling to PLC-β, as well as G $\alpha_{12/13}$ and PLC-ε, mediated hydrolysis of phosphoinositides (5, 29, 30). Cells expressing comparable surface levels of either PAR1 wild-type, NA NTer or NA ECL2, were incubated with a saturating concentration of thrombin for 1 h at 37°C and total [^{3}H]IPs were measured. After 60 min of thrombin exposure, a ~2.5-fold increase in PI hydrolysis was detected in wild-type PAR1 expressing cells, whereas a significantly greater ~4.2-fold increase in signaling was measured in cells expressing the PAR1 NA ECL2 mutant lacking N-linked glycosylation in the second extracellular loop **(Fig. 2.8A)**. In cells expressing similar amounts of both PAR1 wild-type and NA ECL2 mutant, stimulation of endogenous muscarinic acetylcholine receptors with carbachol resulted in comparable changes in PI hydrolysis **(Fig. 2.8A)**, indicating that there are no cell clone specific defects in G protein signaling. Moreover, the activation of PAR1 with the peptide agonist SFLLRN also caused enhanced signaling of PAR1 NA ECL2 compared to wild-type PAR1 **(Fig. 2.8A)**. In contrast to PAR1 NA ECL2 mutant, thrombin-activation of PAR1 NA NTer caused a significant but modest increase in signaling compared to wild-type receptor **(Fig. 2.8B)**. Together these data suggest that N-linked glycosylation of PAR1 at ECL2 has a predominant effect on receptor stimulated G-protein signaling.

2.5 Discussion

In the present study, we sought to characterize N-linked glycosylation of PAR1 by identifying the major sites of glycosylation and the function of receptor glycosylation. We found that PAR1 is extensively glycosylated in transfected cells and native cell systems. The glycosylation of PAR1 was shown to occur mainly at ECL2 via two consensus sites, whereas the sites in the N-terminus contributed less overall to the glycosylation status of the receptor. Glycosylation of PAR2 at the N-terminus has been shown to modulate export to the cell surface (17) and specificity of distinct proteases to cleave and activate the receptor (18), however, virtually nothing is known about the function of PAR1 N-linked glycosylation. The studies presented in this chapter now indicate that glycosylation of PAR1 is required for efficient trafficking to the cell surface, similar to that reported for other GPCRs (31-33). In addition, glycosylation of PAR1 at ECL2 appears to make important contributions to activated receptor stimulation of G protein signaling, which cannot be attributed to defects in the ability of thrombin to cleave the receptor. These findings suggest that N-linked glycosylation of PAR1 at the N-terminus versus ECL2 serve distinct function in regulation of receptor function.

Most mammalian GPCRs harbor N-linked glycosylation sites within their N-terminal extracellular domain, whereas glycosylation occurs less commonly on the extracellular loops linking the transmembrane helices. Despite the presence of three N-linked glycosylation consensus sites in the N-terminus, we found that modification of the PAR1 N- terminus with glycosylation does occur, but contributes minimally to the overall glycosylation status of the receptor. However, like many other mammalian

GPCRs, our findings suggest that N- linked glycosylation of the PAR1 N-terminus is important for receptor trafficking through the biosynthetic pathway and export to the cell surface. Calnexin and calreticulin are chaperone proteins that retain unfolded or unassembled N-linked glycoproteins in the endoplasmic reticulum and may be important for proper trafficking of PAR1 through the endoplasmic reticulum and Golgi apparatus but this remains to be determined. We also show that mutations in N-linked glycosylation sites at the N-terminus or ECL2 of PAR1 does not completely abrogate glycosylation of the receptor, indicating that these receptor mutants are still capable of being processed by the diverse set of enzymes involved in N-linked glycosylation formation in the endoplasmic reticulum and Golgi.

In addition to thrombin, many other proteases including serine, cysteine and metalloproteases can cleave and activate PARs (26, 34-36). These proteases can function as soluble enzymes similar to thrombin or require membrane-associated cofactors that facilitate membrane localization and/or allosterically modulate protease activity. Interestingly, an N-linked glycosylation site present in the N-terminus of PAR2 appears to regulate signaling by the serine protease tryptase but not trypsin or synthetic peptide agonist (17, 18), suggesting that glycosylation of PARs at the N-terminus can dictate protease specificity. Thrombin binds to and cleaves PAR1 with exquisite specificity and recognizes both the N-terminal LDPR/S cleavage site and an acidic region C-terminal to the cleavage site termed the hirudin-like sequence (37). Our results indicate that PAR1 is glycosylated at the N-terminus albeit considerably less than that observed at ECL2. In addition, the PAR1 NA NTer mutant lacking all

potential sites of N-linked glycosylation in the N-terminus was cleaved by thrombin as efficiently as wild-type receptor. These findings suggest that N-linked glycosylation is not critical for thrombin cleavage of PAR1, but whether N-linked glycosylation of the PAR1 N-terminus affects the capacity of other proteases, such as activated protein C or matrix metalloprotease-1, to cleave and activate PAR1 is not known. However, a recent study reported that N-terminal glycosylation of PAR1 affected the capacity of trypsin, thermolysin and neutrophil proteinases to cleave the receptor at non-activating sites (38), suggesting that N-linked glycosylation within the N-terminus may protect PAR1 from aberrant cleavage by certain proteases.

Our studies also identified for the first time the major sites of PAR1 N-linked glycosylation and suggest a function for N-linked glycosylation of ECL2 in regulation of receptor signaling. In contrast, the glycosylation of the PAR1 N-terminus appears to function primarily in proper processing and trafficking of the receptor through the biosynthetic pathway to the cell surface. The modest affect observed with PAR1 NA NTer mutant on signaling may also suggest that glycosylation at these sites may have a role in signal regulation as well, but perhaps through a distinct mechanism than glycosylation at ECL2. It remains to be determined whether PAR1 is differentially modified by N-linked glycosylation at the N-terminus and/or ECL2 in different tissues, distinct cell types or perhaps in disease states.

2.6 Acknowledgements

This work was supported by National Institutes of Health grant HL073328 (J. Trejo) and an American Heart Association Established Investigator Award (J. trejo). A. G. Soto was supported by a T32 NIGMS Pharmocological Sciences Training Grant. The authors have no conflict of interest to declare.

The contents of Chapter 2, in part, have been published: **Soto, A.G.,** and Trejo, J. (2010) N-Linked glycosylation of protease-activated receptor-1 second extracellular loop: a critical determinant for ligand-induced receptor activation and internalization. *Journal of Biological Chemistry,* 285(24), 18781-93. The dissertation author was the primary investigator and author of this paper. All co-authors have given written permission for its use and the reproduction of all associated data in this dissertation.

2.7 Figures

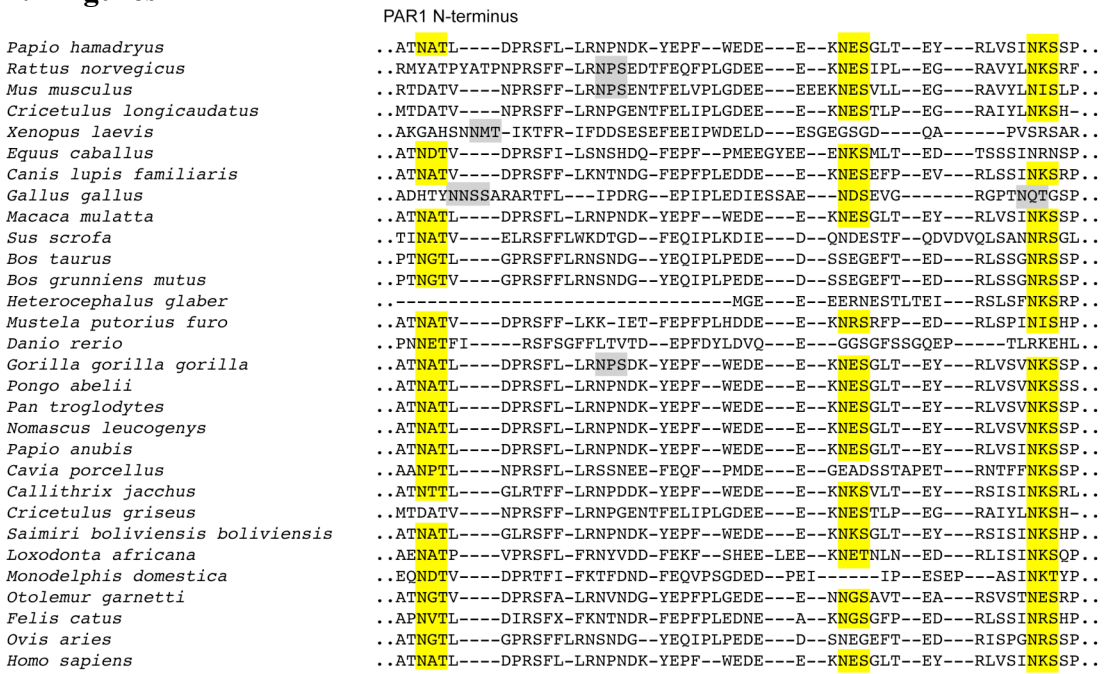

Figure 2.1A: Conservation of PAR1 N-linked glycosylation sites within the N-terminus. Thirty N-terminal sequences of PAR1 from different species were aligned using Clustal W2 alignment analysis. The conserved N-linked glycosylation sites are highlighted in yellow. N-linked glycosylation sites not conserved in the human PAR1 sequence are highlighted in grey. See Materials and methods section for NCBI accession numbers.

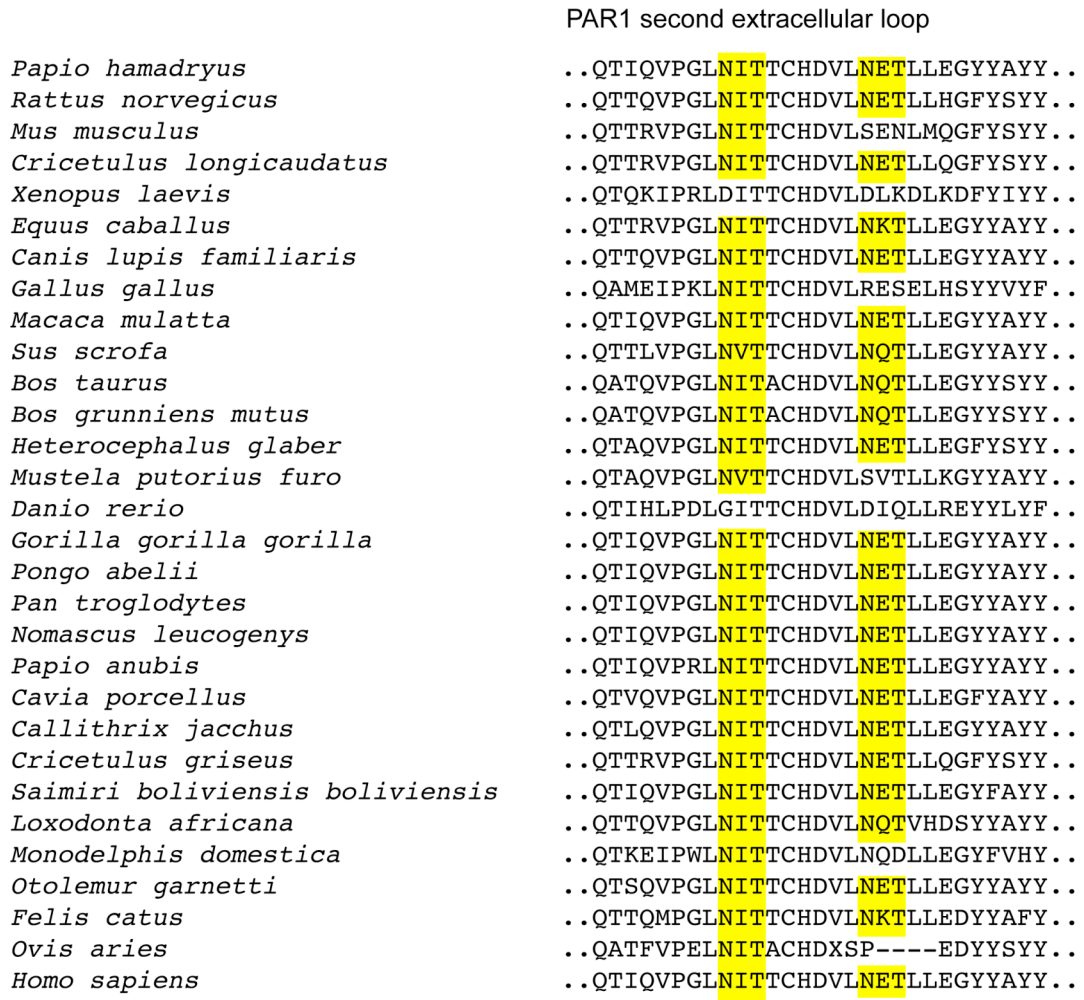

Figure 2.1B: Conservation of PAR1 second extracellular loop N-linked glycosylation sites. Thirty PAR1 ECL2 sequences from different species were aligned. The conserved N-linked glycosylation sites are highlighted in yellow. See Materials and methods section for NCBI accession numbers.

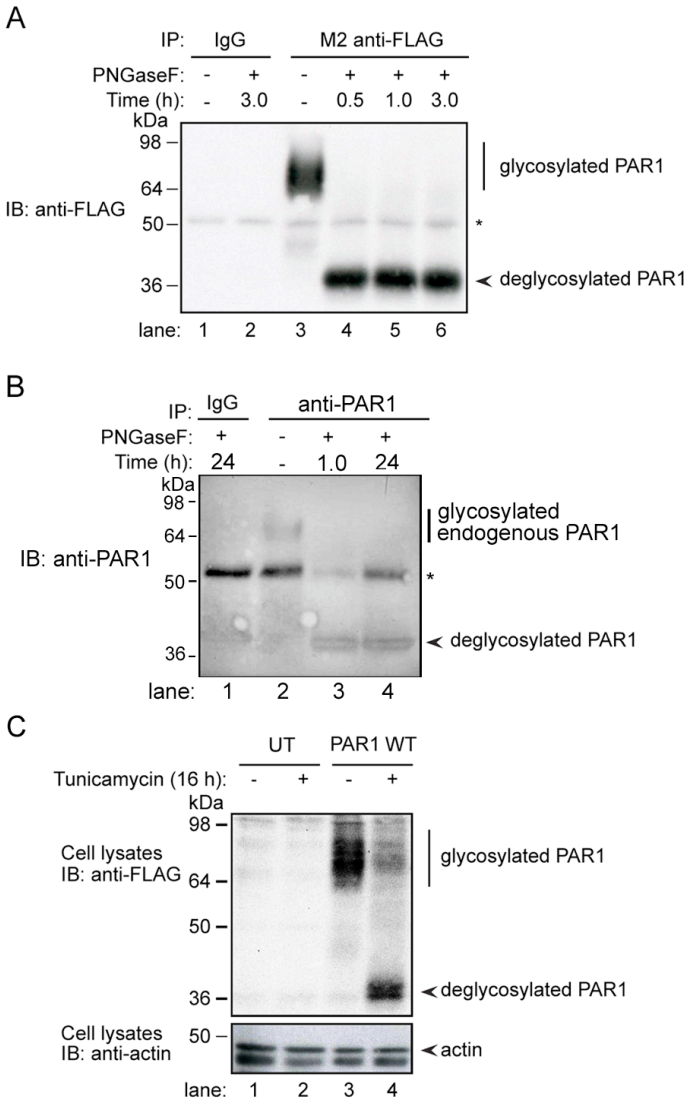

Figure 2.2: PAR1 is highly glycosylated in HeLa and endothelial cells. (*A*) HeLa cells stably expressing FLAG-tagged wild-type PAR1 were lysed and immunoprecipitated with either M2 anti-FLAG antibody or IgG control. Immunoprecipitates were treated with PNGase F for the indicated times at 37°C. Samples were then processed and immunoblotted with rabbit polyclonal anti-FLAG antibody to detect PAR1. Similar findings were observed in three independent experiments. The *asterisk* indicates the detection of a non-specific FLAG positive band. (*B*) Endogenous PAR1 was immunoprecipitated from lysates prepared from EA.hy926 human endothelial cells, treated with PNGaseF, processed and detected by immunoblotting with an anti-PAR1 polyclonal antibody. (*C*) HeLa cells stably expressing FLAG-tagged wild-type PAR1 and untransfected (UT) control cells were treated with DMSO (-) or tunicamycin (+, 0.5 μg/ml) for 16 h in serum-free media at 37°C. Total cell lysates were immunoblotted with rabbit polyclonal anti-FLAG antibody to detect PAR1. The membranes were then stripped and re-probed for actin to control for equal loading. Similar findings were observed in three independent experiments.

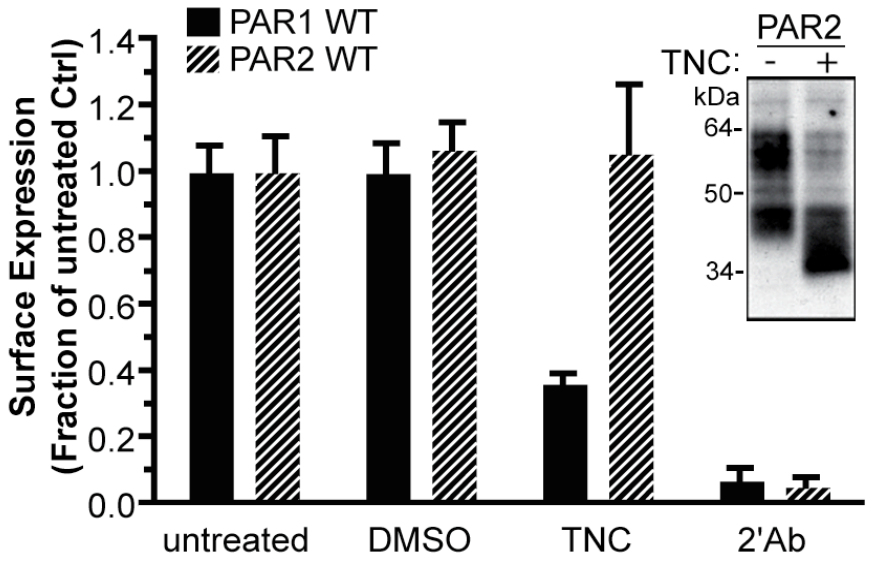

Figure 2.3: N-linked glycosylation is important for PAR1 but not PAR2, surface expression. HeLa cells stably expressing FLAG-tagged wild-type (WT) PAR1 or PAR2 were left untreated or treated with either DMSO or tunicamycin (TNC) (0.5 μg/ml) for 16 h in serum-free media at 37°C. The amount of receptor expressed on the cell surface was detected by ELISA. The secondary antibody (2' Ab) control represents cells not incubated with primary antibody. The data shown (mean ± S.D.; *n*=3) are expressed as the fraction of untreated control and are the averages of three independent experiments. The *inset* shows the mobility of PAR2 in control (-) and tunicamycin (+) treated cells.

A.

```
PAR1 N-Terminus:
WT           ..ATNATLDPRSFLLRNPNDKYEPFWEDEEKNESGLTEYRLVSINKSSP..
FLAG WT      ..DVDATLDPRSFLLRNPNDKYEPFWEDEEKNESGLTEYRLVSINKSSP..
FLAG N35     ..DVDNATLDPRSFLLRNPNDKYEPFWEDEEKNESGLTEYRLVSINKSSP..
FLAG N35A    ..DVDAATLDPRSFLLRNPNDKYEPFWEDEEKNESGLTEYRLVSINKSSP..
FLAG N62A    ..DVDATLDPRSFLLRNPNDKYEPFWEDEEKAESGLTEYRLVSINKSSP..
FLAG N75A    ..DVDATLDPRSFLLRNPNDKYEPFWEDEEKNESGLTEYRLVSIAKSSP..
FLAG NA NTer ..DVDATLDPRSFLLRNPNDKYEPFWEDEEKAESGLTEYRLVSIAKSSP..

PAR1 second extracellular loop:
WT           ..QTIQVPGLNITTCHDVLNETLLEGYYAYY..
FLAG WT      ..QTIQVPGLNITTCHDVLNETLLEGYYAYY..
FLAG N250A   ..QTIQVPGLAITTCHDVLNETLLEGYYAYY..
FLAG N259A   ..QTIQVPGLNITTCHDVLAETLLEGYYAYY..
FLAG NA ECL2 ..QTIQVPGLAITTCHDVLAETLLEGYYAYY..
```

B.

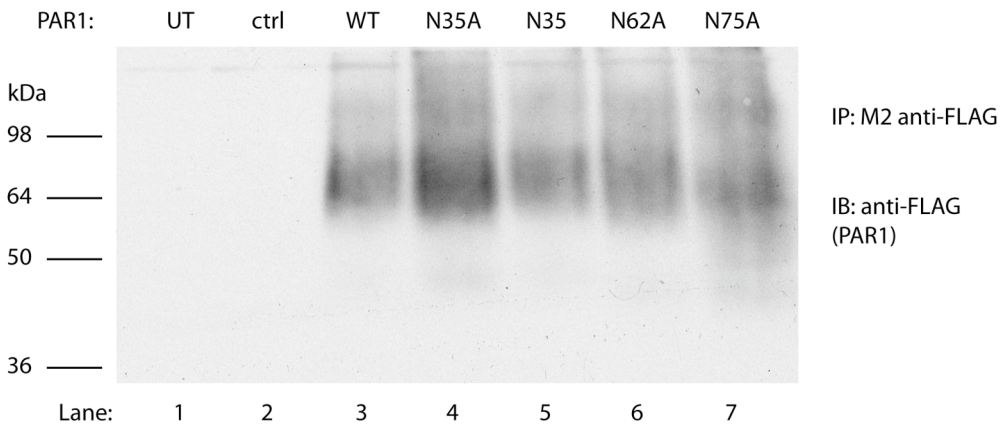

C.

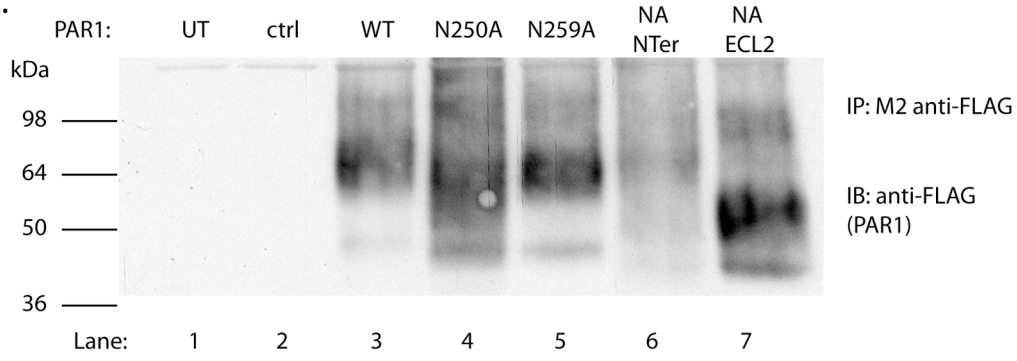

Figure 2.4: PAR1 N-linked glycosylation mutants. (*A*) Nomenclature and corresponding amino acid sequence of FLAG-PAR1 N-linked glycosylation mutants. (*B* and *C*) HeLa cells were transiently transfected with the various FLAG-tagged PAR1 constructs as indicated. After 48 h, cells were lysed and immunoprecipitated with M2 anti-FLAG antibody. Samples were then processed and immunoblotted with rabbit polyclonal anti-FLAG antibody to detect PAR1. UT = untransfected. Ctrl = PBJ vector.

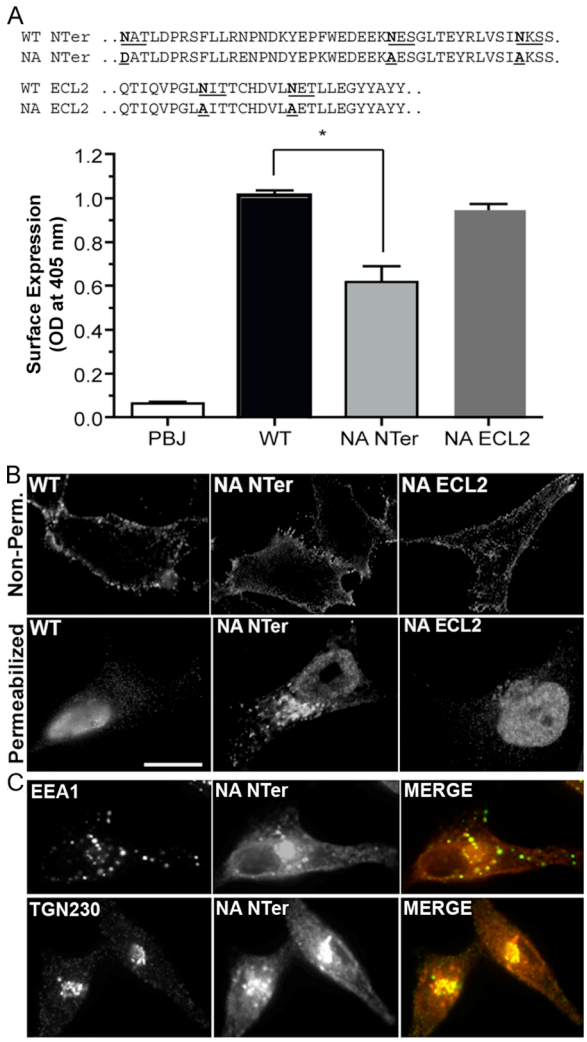

Figure 2.5: PAR1 harboring mutations in the N terminus or ECL2 N-linked glycosylation consensus sites are differentially transported to the cell surface. (*A*) HeLa cells were transiently transfected with FLAG-tagged PAR1 wild-type (WT), NA NTer, NA ECL2 mutant, or pBJ vector, and the amount of cell surface expression was determined by ELISA. The data shown (mean± S.D.; *n*_3) are expressed as the absorbance (*OD*) values measured at 405 nm. Similar findings were observed in three independent experiments. A significant difference between PAR1 WT and NA NTer cell surface expression was detected (*, p <0.01) by Dunnett's multiple comparison tests. (*B*) HeLa cells expressing FLAG-tagged PAR1 WT, NA NTer, or NA ECL2 were fixed and either left alone (unpermeabilized) or treated with 10 nM thrombin, which cleaves off the FLAG epitope from cell surface PAR1, and then permeabilized (*Perm*), processed, and immunostained for PAR1 using a polyclonal anti-FLAG antibody. Under these conditions only PAR1 present in intracellular compartments protected from thrombin cleavage will be detected with the anti-FLAG antibody. The cells were imaged by confocal microscopy. *Scale bar*, 10 μm. (*C*), PAR1 NA NTer-expressing HeLa cells were fixed, permeabilized, and immunostained for PAR1 NA NTer or endogenous EEA1 or TGN230 and examined by confocal microscopy. The images shown are representative of many cells examined. Co-localization of PAR1 NA NTer with endogenous TGN230 is indicated by the *yellow color* in the merged image.

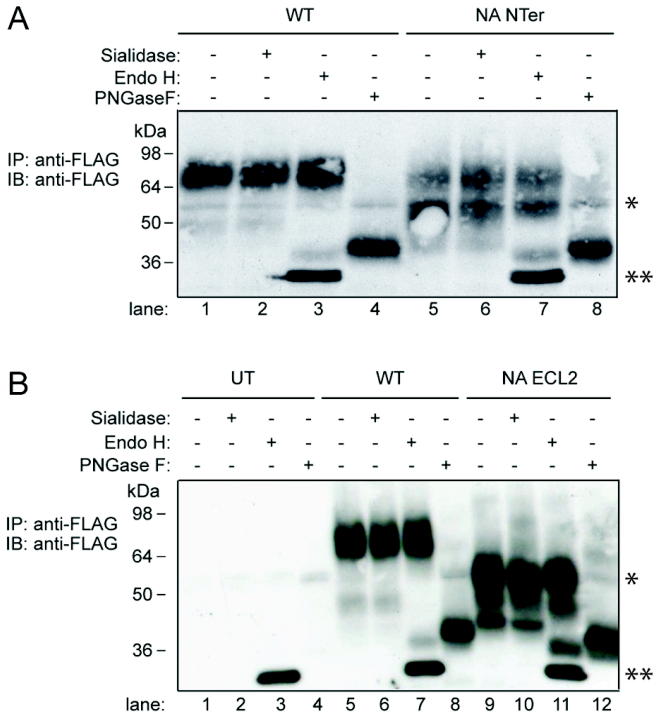

Figure 2.6: NA NTer and NA ECL2 PAR1 mutants are glycosylated. HeLa cells stably expressing FLAG-tagged PAR1 wild-type (WT), NA NTer mutant (*A*), NA ELC2 mutant (*B*) or untransfected (UT) control cells were lysed, processed and PAR1 immunoprecipitated using M2 monoclonal anti-FLAG antibody. Immunoprecipitates were treated with the indicated enzyme for 16 h at 37°C. Immunoprecipitates were resolved by SDS-PAGE and PAR1 was detected by immunoblotting with rabbit polyclonal anti-FLAG antibody. Similar findings were observed in multiple independent experiments. The single asterisk indicates the detection of a nonspecific FLAG-positive band, and the double asterisks denote a nonspecific FLAG-positive band only detected in samples treated with endoglycosidase H (Endo H).

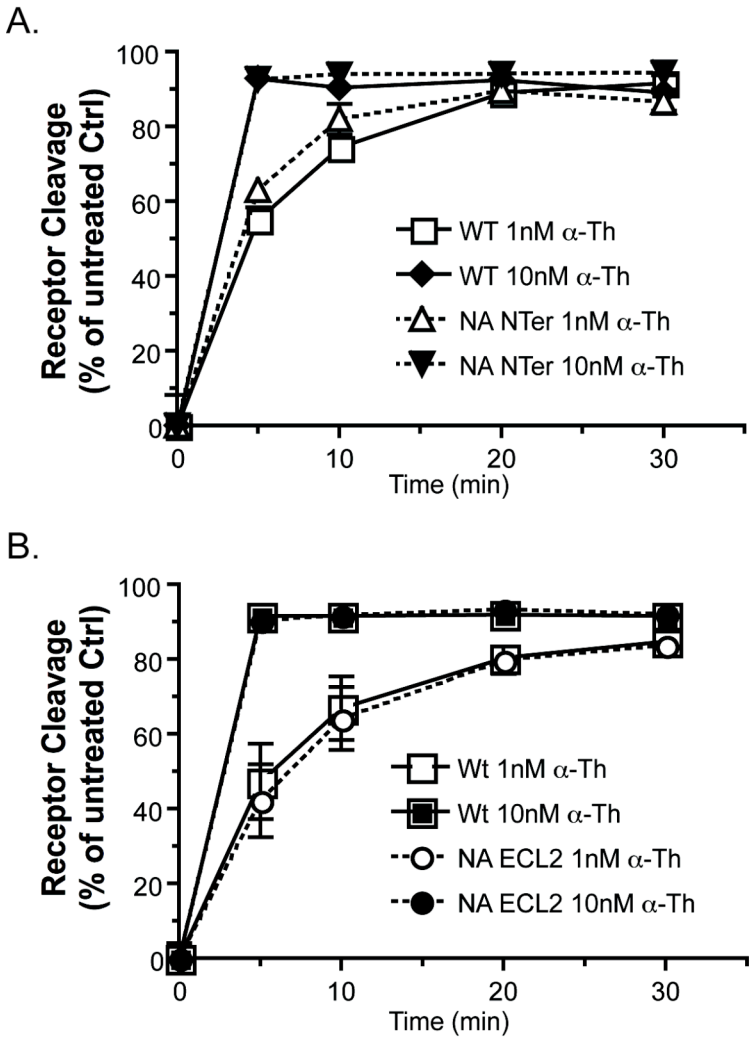

Figure 2.7: PAR1 NA NTer and NA ECL2 mutants display similar thrombin cleavage rates. HeLa cells stably expressing similar amounts of FLAG-tagged PAR1 wild-type (WT) or NA NTer (*A*) or NA ECL2 (*B*) mutant were serum starved for 30 min then treated with media containing 1 nM or 10 nM thrombin (α-Th) for various times at 37°C. After incubations, cells were washed, fixed and uncleaved PAR1 was detected with anti-FLAG antibody by cell surface ELISA. The data shown (mean ± S.D.; *n*=3) are expressed as the percent of receptor cleaved = 100* (average untreated value -value at x min)/(average untreated value) and are the averages from three independent experiments performed in triplicate.

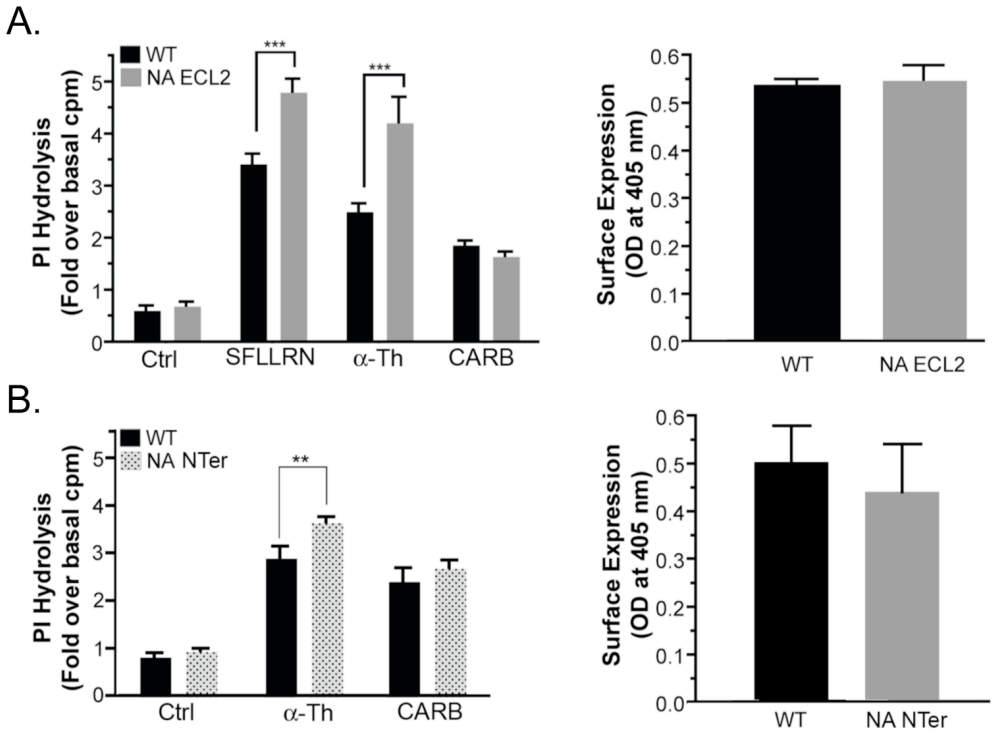

Figure 2.8: PAR1 N-linked glycosylation mutants display markedly enhanced PI hydrolysis signaling compared to the wild-type receptor. HeLa cells stably expressing similar surface levels of FLAG-tagged PAR1 wild-type (WT), NA NTer (*A*) or NA ECL2 (*B*) mutant labeled with *myo*-[^{3}H]inositol were incubated with media containing LiCl alone (Ctrl) or media containing LiCl and 100 μM SFLLRN, 10 nM thrombin (α–Th), or 500 μM carbachol (CARB) for 60 min at 37°C. The amounts of accumulated [^{3}H]IPs were then measured. The data shown (mean ± S.D.; *n*=3) are expressed as the fold increase in [^{3}H]IPs accumulation over basal amounts and are the averages from three independent experiments performed in triplicate. The difference in agonist-induced signaling at PAR1 WT and NA ECL2 mutant was significant (***, $p < 0.001$) by two-way ANOVA and Bonferroni post-tests. The amounts of PAR1 WT, NA NTer and NA ECL2 mutant expressed at the cell surface was determined by ELISA.

2.8 References

1. Jones, J., Krag, S. S., and Betenbaugh, M. J. (2005) Controlling N-linked glycan site occupancy. *Biochim Biophys Acta* **1726**, 121-137

2. Minegishi, T., Delgado, C., and Dufau, M. L. (1989) Phosphorylation and glycosylation of the luteinizing hormone receptor. *Proc Natl Acad Sci U S A* **86**, 1470-1474

3. Rands, E., Candelore, M. R., Cheung, A. H., Hill, W. S., Strader, C. D., and Dixon, R. A. (1990) Mutational analysis of beta-adrenergic receptor glycosylation. *J Biol Chem* **265**, 10759-10764

4. Wheatley, M., and Hawtin, S. R. (1999) Glycosylation of G-protein-coupled receptors for hormones central to normal reproductive functioning: its occurrence and role. *Hum Reprod Update* **5**, 356-364

5. Coughlin, S. R. (2000) Thrombin signalling and protease-activated receptors. *Nature* **407**, 258-264

6. Ohtsubo, K., and Marth, J. D. (2006) Glycosylation in cellular mechanisms of health and disease. *Cell* **126**, 855-867

7. Henkel, W., Rauterberg, J., and Stirtz, T. (1976) Isolation of a crosslinked cyanogen-bromide peptide from insoluble rabbit collagen. Tissue differences in hydroxylation and glycosylation of the crosslink. *Eur J Biochem* **69**, 223-231

8. Rougon, G., Deagostini-Bazin, H., Hirn, M., and Goridis, C. (1982) Tissue- and developmental stage-specific forms of a neural cell surface antigen linked to differences in glycosylation of a common polypeptide. *EMBO J* **1**, 1239-1244

9. Serrano, R., Barrenetxe, J., Orbe, J., Rodriguez, J. A., Gallardo, N., Martinez, C., Andres, A., and Paramo, J. A. (2009) Tissue-specific PAI-1 gene expression and glycosylation pattern in insulin-resistant old rats. *Am J Physiol Regul Integr Comp Physiol* **297**, R1563-1569

10. West, M. B., Segu, Z. M., Feasley, C. L., Kang, P., Klouckova, I., Li, C., Novotny, M. V., West, C. M., Mechref, Y., and Hanigan, M. H. (2010) Analysis of site-specific glycosylation of renal and hepatic gamma-glutamyl transpeptidase from normal human tissue. *J Biol Chem* **285**, 29511-29524

11. Davies, L. R., and Varki, A. (2013) Why Is N-Glycolylneuraminic Acid Rare in the Vertebrate Brain? *Top Curr Chem*

12. Hsiao, C. C., Cheng, K. F., Chen, H. Y., Chou, Y. H., Stacey, M., Chang, G. W., and Lin, H. H. (2009) Site-specific N-glycosylation regulates the GPS auto-proteolysis of CD97. *FEBS Lett* **583**, 3285-3290

13. Kohno, T., Wada, A., and Igarashi, Y. (2002) N-glycans of sphingosine 1-phosphate receptor Edg-1 regulate ligand-induced receptor internalization. *FASEB J* **16**, 983-992

14. Cho, D. I., Min, C., Jung, K. S., Cheong, S. Y., Zheng, M., Cheong, S. J., Oak, M. H., Cheong, J. H., Lee, B. K., and Kim, K. M. (2012) The N-terminal region of the dopamine D2 receptor, a rhodopsin-like GPCR, regulates correct integration into the plasma membrane and endocytic routes. *Br J Pharmacol* **166**, 659-675

15. Walsh, M. T., Foley, J. F., and Kinsella, B. T. (1998) Characterization of the role of N-linked glycosylation on the cell signaling and expression of the human thromboxane A2 receptor alpha and beta isoforms. *J Pharmacol Exp Ther* **286**, 1026-1036

16. Zhang, Z., Austin, S. C., and Smyth, E. M. (2001) Glycosylation of the human prostacyclin receptor: role in ligand binding and signal transduction. *Mol Pharmacol* **60**, 480-487

17. Compton, S. J., Sandhu, S., Wijesuriya, S. J., and Hollenberg, M. D. (2002) Glycosylation of human proteinase-activated receptor-2 (hPAR2): role in cell surface expression and signalling. *Biochem J* **368**, 495-505

18. Compton, S. J., Renaux, B., Wijesuriya, S. J., and Hollenberg, M. D. (2001) Glycosylation and the activation of proteinase-activated receptor 2 (PAR(2)) by human mast cell tryptase. *Br J Pharmacol* **134**, 705-718

19. Landolt-Marticorena, C., and Reithmeier, R. A. (1994) Asparagine-linked oligosaccharides are localized to single extracytosolic segments in multi-span membrane glycoproteins. *Biochem J* **302** (Pt 1), 253-260

20. Vouret-Craviari, V., Grall, D., Chambard, J. C., Rasmussen, U. B., Pouyssegur, J., and Van Obberghen-Schilling, E. (1995) Post-translational and activation-dependent modifications of the G protein-coupled thrombin receptor. *J Biol Chem* **270**, 8367-8372

21. Kuliopulos, A., Covic, L., Seeley, S. K., Sheridan, P. J., Helin, J., and Costello, C. E. (1999) Plasmin desensitization of the PAR1 thrombin receptor: kinetics, sites of truncation, and implications for thrombolytic therapy. *Biochemistry* **38**, 4572-4585

22. Mize, G. J., Harris, J. E., Takayama, T. K., and Kulman, J. D. (2008) Regulated expression of active biotinylated G-protein coupled receptors in mammalian cells. *Protein Expr Purif* **57**, 280-289

23. Tordai, A., Brass, L. F., and Gelfand, E. W. (1995) Tunicamycin inhibits the expression of functional thrombin receptors on human T-lymphoblastoid cells. *Biochem Biophys Res Commun* **206**, 857-862

24. Paing, M. M., Johnston, C. A., Siderovski, D. P., and Trejo, J. (2006) Clathrin adaptor AP2 regulates thrombin receptor constitutive internalization and endothelial cell resensitization. *Mol Cell Biol* **26**, 3231-3242

25. Trejo, J., Altschuler, Y., Fu, H. W., Mostov, K. E., and Coughlin, S. R. (2000) Protease-activated receptor-1 down-regulation: a mutant HeLa cell line suggests novel requirements for PAR1 phosphorylation and recruitment to clathrin-coated pits. *J Biol Chem* **275**, 31255-31265

26. Russo, A., Soh, U. J., Paing, M. M., Arora, P., and Trejo, J. (2009) Caveolae are required for protease-selective signaling by protease-activated receptor-1. *Proc Natl Acad Sci U S A* **106**, 6393-6397

27. Helenius, A. (1994) How N-linked Oligosaccharides Affect Glycoprotein Folding in the Endoplasmic Reticulum. *Molecular Biology of the Cell* **5**, 253-265

28. Dennis, J. W., Lau, K.S., Demetriou, M., and Nabi, I.R. (2009) Adaptive Regulation at the Cell Surface By N-Glycosylation. *Traffic* **10**, 1569-1578

29. Taylor, S. J., Chae, H. Z., Rhee, S. G., and Exton, J. H. (1991) Activation of the beta 1 isozyme of phospholipase C by alpha subunits of the Gq class of G proteins. *Nature* **350**, 516-518

30. Hains, M. D., Wing, M. R., Maddileti, S., Siderovski, D. P., and Harden, T. K. (2006) Galpha12/13- and rho-dependent activation of phospholipase C-epsilon by lysophosphatidic acid and thrombin receptors. *Mol Pharmacol* **69**, 2068-2075

31. Lanctot, P. M., Leclerc, P. C., Escher, E., Leduc, R., and Guillemette, G. (1999) Role of N-glycosylation in the expression and functional properties of human AT1 receptor. *Biochemistry* **38**, 8621-8627

32. Roy, S., Perron, B., and Gallo-Payet, N. (2010) Role of asparagine-linked glycosylation in cell surface expression and function of the human

adrenocorticotropin receptor (melanocortin 2 receptor) in 293/FRT cells. *Endocrinology* **151**, 660-670

33. Whitaker, G. M., Lynn, F. C., McIntosh, C. H., and Accili, E. A. (2012) Regulation of GIP and GLP1 receptor cell surface expression by N-glycosylation and receptor heteromerization. *PLoS One* **7**, e32675

34. Trivedi, V., Boire, A., Tchernychev, B., Kaneider, N.C., Leger, A.J., O' Callaghan, K., Covic, L., and Kuliopulos, A. (2009) Platelet matrix metalloprotease-1 mediates thrombogenesis by activating PAR1 at a cryptic ligand site. *Cell* **137**, 332-343

35. Chambers, R. C., and Scotton, C. J. (2012) Coagulation cascade proteinases in lung injury and fibrosis. *Proc Am Thorac Soc* **9**, 96-101

36. Austin, K. M., Covic, L., and Kuliopulos, A. (2013) Matrix metalloproteases and PAR1 activation. *Blood* **121**, 431-439

37. Jacques, S. L., LeMasurier, M., Sheridan, P. J., Seeley, S. K., and Kuliopulos, A. (2000) Substrate-assisted catalysis of the PAR1 thrombin receptor. Enhancement of macromolecular association and cleavage. *J Biol Chem* **275**, 40671-40678

38. Xiao, Y. P., Morice, A. H., Compton, S. J., and Sadofsky, L. (2011) N-linked glycosylation regulates human proteinase-activated receptor-1 cell surface expression and disarming via neutrophil proteinases and thermolysin. *J Biol Chem* **286**, 22991-23002

Chapter 3:

N-linked glycosylation of PAR1 ECL2: A critical determinant for ligand-induced receptor activation and internalization

3.1 Abstract

PAR1 is cleaved by thrombin, revealing a new N-terminus that acts as a tethered ligand that binds intramolecularly to the second extracellular loop (ECL2) of the receptor to elicit transmembrane signaling. Once activated, PAR1 undergoes conformational changes that exposes cytoplasmic surfaces to facilitate interaction with heterotrimeric G proteins. Activated PAR1 is then phosphorylated and ubiquitinated and recruited to clathrin-coated pits by the endocytic adaptor proteins AP-2 and epsin-1, which are critical for receptor internalization. In the present chapter we examined whether N-linked glycosylation of PAR1 at ECL2 affects receptor-stimulated PI hydrolysis, an effect attributed mainly to G_q coupling, and internalization. Here, we report that N-linked glycosylation of PAR1 enhances the capacity of the receptor to efficiently couple to G_q-stimulated PI hydrolysis and impairs the ability of the receptor to engage the endocytic machinery, which resulted in slowed agonist-induced receptor internalization.

3.2 Introduction

PAR1 is activated when the N-terminus is cleaved by thrombin, which creates a new N-terminus that acts as a tethered ligand that binds intramolecularly to the receptor to initiate transmembrane signaling (1). Activated PAR1 signals through multiple heterotrimeric G-protein subtypes including G_q, $G_{i/o}$ and $G_{12/13}$ to promote diverse cellular responses in various cell types (2-5). The current model for activation

of GPCR signaling posits that agonist binding within the receptor helical core triggers rearrangements of transmembrane helices that exposes cytoplasmic domains to initiate G protein activation (6, 7). However, for the class B GPCRs whose natural ligands are peptide hormones, the extracellular domains have a critical role in ligand binding (8). In addition, recent studies of class A GPCRs also indicate that ligands interact with their extracellular domains (9-14). PAR1 is a class A Rhodopsin-like GPCR that is activated through peptide agonist interaction with the receptor extracellular surface domains. Specifically, the PAR1 second extracellular loop (ECL2) is critical for species-specific ligand interactions and peptide agonist recognition (15, 16). Indeed the recent high-resolution X-ray structure of PAR1 is consistent with tethered ligand interactions with the surface of ECL2 (17). An interesting feature of the ECL2 of human PAR1 is the inclusion of two N-linked glycosylation consensus sites, however, the function of glycosylation in regulation of PAR1 signaling and trafficking has not been thoroughly examined.

After activation, PAR1 is rapidly desensitized from G protein signaling by phosphorylation and β-arrestin binding (18, 19). In addition to desensitization, PAR1 internalization and lysosomal degradation are critical for termination of G protein signaling (20, 21). PAR1 displays two modes of internalization that proceed through a clathrin- and dynamin-dependent pathway independent of β-arrestins (18). Constitutive internalization of unactivated PAR1 is mediated by the clathrin adaptor protein complex-2 (AP-2), which binds directly to a tyrosine-based motif localized within the receptor C-tail domain (22). However, AP-2 depletion only partially

inhibited agonist-induced internalization of PAR1, suggesting a function for other clathrin adaptors in this process. Indeed, activated PAR1 internalization is mediated by AP-2 and epsin-1, which bind to discrete phosphorylation and ubiquitination endocytic signals (23). Constitutive internalization of PAR1 is important for generating an intracellular pool of receptor that can replenish the cell surface and is essential for resensitizing cells to thrombin signaling (22, 24, 25). Internalization and lysosomal degradation of activated PAR1 is critical for termination of signaling, since a PAR1 mutant that internalizes and recycles can continue to signal even in the absence of thrombin (20, 21). Whether signaling by PAR1 can modulate the endocytic machinery to affect receptor internalization or lysosomal sorting has not been previously examined.

In the present work, we examine for the first time the function of N-linked glycosylation of the PAR1 ECL2 in the regulation of receptor signaling and trafficking. PAR1 NA ECL2 mutant displays impaired agonist-induced internalization, whereas constitutive internalization remained intact. In addition, proteolytic activation of PAR1 NA ECL2 mutant exhibited a marked increase in G_q-stimulated PI signaling that is not due to defects in desensitization or signal termination. Rather, the PAR1 NA ECL2 mutant exhibits a greater efficacy in activation of G_q protein mediated signaling response. In addition, impaired PAR1 internalization was not a result of enhanced PI hydrolysis, since perturbation of PI hydrolysis by phospholipase C (PLC) inhibition with edelfosine or G_q siRNA knockdown failed to rescue the phenotype. These findings suggest that glycosylation of PAR1 at ECL2 influences tethered ligand

interactions with the surface of ECL2 that enhances the stabilization of an active receptor conformation.

3.3 Materials and methods

Reagents and Antibodies- Human α-thrombin was obtained from Enzyme Research Laboratories (South Bend, IN). The PAR1-activating peptide, SFLLRN, was synthesized as the carboxyl amide and purified by reverse phase high-pressure chromatography at Tufts University Core Facility (Boston, MA). Cycloheximide, carbachol, epidermal growth factor (EGF), and hirudin were obtained from Sigma-Aldrich (St. Louis, MO). Edelfosine (ET-18-O-CH3; 1-octadecyl-2-O-methyl-glycero-3-phophocholine) was obtained from Calbiochem (San Diego, CA). Rabbit polyclonal anti-FLAG antibody and mouse monoclonal M1 and M2 anti- FLAG antibodies were purchased from Sigma-Aldrich. The anti-PAR1 WEDE mouse antibody was purchased from Beckman Coulter (Fullerton, CA). Anti-PAR1 rabbit polyclonal antibody was previously described (22). The mouse monoclonal AP-50 (μ2) antibody was obtained from BD Biosciences. The mouse monoclonal anti-EGFR LA22 antibody was from Upstate Cell Signaling Solutions (Billerica, MA). The Rabbit polyclonal anti-G_q and anti-epsin-1 (H130) antibodies were from Santa Cruz Biotechnology. Goat anti-mouse IgG antibody was purchased from Thermo Scientific (Rockford, IL). Horse-radish peroxidase (HRP)-conjugated goat anti-mouse and goat anti-rabbit antibodies were purchased from Bio-Rad Laboratories (Richmond, CA).

Cell lines- HeLa cells stably expressing FLAG-tagged PAR1 wild-type and mutants were generated and maintained as previously described (26, 27).

PAR1 Immunoprecipitation and Immunoblotting- HeLa cells stably expressing FLAG-tagged PAR1 wild-type or mutants were plated at 5 X 10^5 cells per well in 6-well culture dishes and grown overnight at 37°C. To assess PAR1 degradation, cells were pretreated with 10 μM cycloheximide for 30 min at 37°C, and then incubated with or without agonists in serum-free media containing 10 μM cycloheximide for various times at 37°C. Cells were washed, solubilized with Triton X-100 lysis buffer (50 mM Tris-HCl pH 7.4, 100 mM NaCl, 5 mM EDTA, 50 mM NaF, 10 mM NaPP, 1% Triton X-100) containing freshly added protease inhibitors. Cell lysates were solubilized for 1.5 h at 4°C and clarified by centrifugation at 14,000 rpm for 20 min at 4°C. The total amount of protein in cell lysates was quantified using a Bicinchoninic acid (BCA) Protein Assay Reagent (Thermo Scientific) and equivalent amounts of lysates were used for immunoprecipitation with the M2 anti-FLAG antibody or goat anti-mouse IgG control. Immunoprecipitates were analyzed by SDS-PAGE, transferred to membranes and PAR1 was detected by immunoblotting with anti-PAR1 antibody. Immunoblots were developed with Enhanced Chemiluminescence (GE Healthcare, Piscataway, NJ), imaged by autoradiography and quantitated with ImageJ software.

Cell Surface ELISA- HeLa cells stably expressing FLAG-tagged PAR1 wild-type or mutant were plated at 1 X 10^5 cells per well in a fibronectin coated 24-well culture dish and grown overnight at 37°C. Cells were washed in serum-free DMEM, then treated with agonists, 100 μM SFLLRN or 10 nM thrombin, diluted in DMEM/ BSA/HEPES at 37°C for various times. After treatments, cells were placed on ice, washed with PBS and then fixed with 4% paraformaldehyde (PFA) for 5 min at 4°C. Cells were washed, and then incubated with polyclonal anti-FLAG antibody diluted 1:1000 or rabbit polyclonal anti-PAR1 C5433 diluted 1:500 in DMEM/BSA/HEPES for 1 h at room temperature. Cells were washed and then incubated with secondary HRP-conjugated goat anti-rabbit antibody for 1 h at room temperature and washed extensively. The amount of secondary antibody bound was determined by incubation with 1-Step ABTS (2,2-azinobis-3-ethylbenz-thiazoline-6- sulfonic acid) (Thermo Scientific) substrate for 10 to 20 min at 25 °C. An aliquot was removed, and the optical density (OD) determined at 405 nm using a Molecular Devices SpectraMax Plus microplate reader.

Phosphoinositide Hydrolysis- HeLa cells stably expressing FLAG-tagged PAR1 wild-type or mutant were plated at 1 X 10^5 cells per well in a fibronectin coated 24-well culture dish and grown overnight at 37°C. Cells were then labeled with 1 μCi/ml of *myo*-[^{3}H]inositol (American Radiolabeled Chemicals, St. Louis, MO) diluted in serum- and inositol-free DMEM containing 1 mg/ml BSA overnight. Cells were washed, treated with or without agonists in DMEM media containing 20 mM lithium

chloride (LiCl) for various times at 37°C and accumulated [^{3}H]inositol phosphates (IPs) were measured as described (18). To determine whether recycling of activated PAR1 continued to signal, cells labeled with *myo*-[^{3}H]inositol were treated with DMEM with or without 10 nM thrombin for 1 h at 37°C. Cells were washed, and medium was replaced with new media containing 20 mM LiCl and cells were incubated for 1 h at 37°C and accumulated [^{3}H]IPs were measured as described (18).

In edelfosine experiments, HeLa cells stably expressing FLAG-tagged wild-type or mutant were plated in fibronectin coated 24-well culture dish and grown overnight. Cells were pretreated with 10 μM edelfosine for 90 min at 37°C then treated with DMEM media containing agonist and edelfosine or edelfosine alone for 5 min. Cells were then processed for PI hydrolysis or cell surface ELISA as described above.

G_q siRNA knockdown- HeLa cells stably expressing FLAG-tagged PAR1 wild-type or mutant were plated in fibronectin coated 24-well culture dish and grown overnight. Cells were then transfected with 100 nM nonspecific or $G_{q/11}$ specific siRNAs using Lipofectamine 2000 or Oligofectamine according to the manufacturer's instructions (Invitrogen) and knockdown allowed to proceed for 72 h before assaying cell surface ELISA or PI hydrolysis as described above. The nonspecific siRNA 5'-CUACGUCCAGGAGCGCACC-3' and $G_{q/11}$ specific siRNA 5'-GAUGUUCGUGGACCUGAAC-3' were synthesized by Dharmacon (Lafayette, CO).

Immunofluorescence Microscopy – HeLa cells stably expressing FLAG-PAR1 wild-type and mutant were plated at a density of 1.5 X 10^5 cells per well on fibronectin coated glass coverslips in 12-well dishes. Cells were labeled with rabbit polyclonal anti-FLAG antibody for 1 h on ice, washed and then treated with or without agonist and then chilled on ice. Cells were fixed with 4% PFA for 5 min on ice then permeabilized with 100% methanol, washed and immunostained with anti-AP-2 or anti-epsin-1 antibodies and processed for confocal microscopy as described (26). Images were collected using an Olympus DSU spinning disk confocal microscope configured with a PlanApo 60X oil objective and a Hamamatsu ORCA-ER digital camera. Fluorescent images of X-Y sections at 0.28 μm were collected using Intelligent Imaging Innovations Slidebook 4.2 software and composite configured using Adobe Photoshop CS3.

Data Analysis- Data were analyzed using GraphPad Prism software 4.0, and statistical analysis was determined using the Prism data analysis tool as noted. Statistical analysis was determined by performing student's *t*-test, one-way ANOVA and Dunnett multiple comparison test, or two-way ANOVA and Bonferroni post-tests.

3.4 Results

3.4.1 PAR1 NA ECL2 mutant signals with greater efficacy compared to wild-type receptor

We previously showed that the PAR1 NA ECL2 mutant displays enhanced PI hydrolysis after a 60 min incubation with thrombin compared to wild-type receptor **(see Fig 2.8)**. To further delineate the signaling phenotype of the NA ECL2 mutant we compared the time-course of thrombin–induced PI hydrolysis in HeLa cells stably expressing similar amounts of PAR1 wild-type and NA ECL2 mutant on the cell surface **(Fig 3.1A)**. Cells were incubated with a saturating concentration of thrombin for various times at 37°C and total [^{3}H]IPs were measured. Interestingly, the PAR1 NA ECL2 mutant displayed a significant difference in the amounts of inositol phosphate accumulation over time compared to wild-type receptor **(Fig 3.1B)**. Next, we examined whether the initial coupling of activated PAR1 wild-type and NA ECL2 mutant to G protein-stimulated PI hydrolysis was affected. The concentration effect curves for thrombin at PAR1 wild-type and mutant deficient in N-linked glycosylation at ECL2 were determined by incubating cells labeled with *myo*-[^{3}H]inositol and varying concentrations of thrombin for 5 min at 37°C, and accumulation of [^{3}H]IPs was measured. The effective concentration of thrombin needed to stimulate half-maximal response after 5 min was significantly different for PAR1 wild-type (1.61 ± 0.14 nM) *versus* NA ECL2 mutant (0.99 ± 0.12) ($p < 0.001$) **(Fig. 3.1C and D)**. Moreover, activation of PAR1 NA ECL2 mutant caused enhanced maximal signaling response compared with wild-type receptor **(Fig. 3.1C)**. Thus, each activated PAR1 mutant lacking N-linked glycosylation in the ECL2 domain appears to couple longer and more robustly to PI hydrolysis before receptor signaling is shut off. These findings

indicate that each activated PAR1 deficient in ECL2 N-linked glycosylation is more efficacious at coupling to G-protein activation than wild-type receptor.

3.4.2 PAR1 NA ECL2 mutant exhibits a distinct desensitization rate compared to wild-type receptor

We next determined whether differences in PAR1 NA ECL2 signaling are due to affects on receptor desensitization. To assess PAR1 desensitization rates, HeLa cells expressing similar surface amounts of PAR1 wild-type and NA ECL2 mutant were exposed to saturating concentrations of thrombin for 10 min at 37°C. The extent of PAR1 signaling activity remaining after various times of thrombin incubation was then determined by the addition of lithium chloride and the amounts of [^{3}H]IPs formed were then measured. Thrombin-induced IP formation is not detectable in the absence of lithium chloride. In PAR1 NA ECL2 mutant-expressing cells the rate of desensitization actually occurred more rapidly compared to cells expressing wild-type receptor **(Fig. 3.2)**. These findings suggest that despite PAR1 NA ECL2 increased rate of desensitization, activated receptor is still able to induce robust activation of G protein signaling.

3.4.3 PAR1 NA ECL2 mutant enhanced signaling is not due to constitutive activation or impaired signal termination

It is conceivable that proteolytically activated PAR1 NA ECL2 mutant can

continue to signal if it remains on the cell surface or if it is internalized and recycled back to the cell surface with its tethered ligand intact (20, 28). Therefore, we examined whether proteolytic activation of PAR1 lacking ECL2 N-linked glycosylation with thrombin induced persistent signaling by assaying the accumulation of [^{3}H]IPs after thrombin removal. HeLa cells expressing comparable amounts of PAR1 wild-type and NA ECL2 mutant labeled with *myo*-[^{3}H]inositol were stimulated with saturating concentrations of thrombin for 1 h at 37°C. In the presence of LiCl, thrombin-stimulated significant increases in [^{3}H]IPs in both PAR1 WT and NA ECL2 expressing cells compared to untreated control cells **(Fig. 3.3).** In cells treated with thrombin the absence of LiCl, PI hydrolysis is stimulated, but [^{3}H]IPs are rapidly metabolized and do not accumulate. To detect ongoing PAR signaling, thrombin was removed and then LiCl was added together with hirudin (a thrombin inhibitor) to allow accumulation of any IPs generated by ongoing phosphoinositide hydrolysis. If receptor signaling were terminated, no IPs would be detected. In cells expressing PAR1 wild-type or NA ECL2 mutant, phosphoinositide hydrolysis in response to thrombin incubation was virtually abolished after agonist removal indicating that receptor signaling was substantially shut-off **(Fig. 3.3)**. Thus, PAR1 NA ECL2 mutant enhanced signaling is not due to constitutive activation or impaired signal termination.

3.4.4 PAR1 NA ECL2 displays a modest decrease in agonist-induced internalization but not constitutive internalization

To determine the role of PAR1 ECL2 N-linked glycosylation in receptor trafficking, we examined both constitutive and agonist-induced internalization. HeLa cells expressing PAR1 wild-type and NA ECL2 mutant were incubated with the M1 anti-FLAG antibody for 1 h at 4°C. Under these conditions only the receptor cohort at the cell surface binds antibody. Cells were washed and then warmed to 37°C for various times to facilitate PAR1 constitutive internalization. Both PAR1 wild-type and NA ECL2 mutant showed a similar slow rate of constitutive internalization with ~12% of the surface receptor cohort being internalized by 20 min **(Fig. 3.4A)**. These findings are consistent with our previously published studies (22, 29) and indicate that PAR1 constitutive internalization occurs independent of N-linked glycosylation of ECL2. In contrast, activation of PAR1 NA ECL2 mutant with either peptide agonist or thrombin caused a marked delay in activated receptor internalization compared to wild-type receptor **(Fig. 3.4B and C).** To exclude the possibility of a global defect in receptor-mediated endocytosis, we also examined internalization of the endogenous epidermal growth factor receptor (EGFR) in the same HeLa cell lines. Activated EGFR showed robust internalization in both PAR1 wild-type and NA ECL2 expressing cell lines indicating that the endocytic machinery is intact and functional **(Fig. 3.4D)**. Thus, impaired agonist-induced PAR1 NA ECL2 mutant internalization suggest that N-linked glycosylation of the second extracellular loop is important for stabilizing an active receptor conformation that is efficiently engaged by the endocytic machinery.

3.4.5 PAR1 NA ECL2 mutant colocation with the endocytic adaptors AP-2 and

epsin-1

We next examined whether activation of PAR1 NA ECL2 mutant resulted in redistribution to clathrin-coated pits containing endocytic adaptors AP-2 and epsin-1 similar to that observed with wild-type receptor (23). HeLa cells expressing FLAG-tagged PAR1 wild-type and NA ECL2 mutant were incubated with anti-FLAG antibody for 1 h 4°C. Under these conditions only the surface PAR1 cohort is labeled with antibody. **(Fig 3.5A and B)**. Cells were then washed to remove unbound antibody and incubated with 100 μM SFLLN for 2 min at 37°C, cells were fixed, processed, immunostained for endogenous AP-2 or epsin-1 and then imaged by confocal microscopy. Activation of wild-type PAR1 for 2 min resulted is substantial colocalization with endogenous AP-2 and epsin-1 **(Fig 3.5A and B)**, consistent with our previously published studies (23). In contrast, however, activation of PAR1 NA ECL2 mutant resulted in less punctae formation and minimal co-localization with either AP-2 or epsin-1 **(Fig 3.5A and B)**. These data provide support for the idea that activated PAR1 NA ECL2 mutant has the capacity to internalize and to associate with AP-2 and epsin-1 but does so less efficiently than wild-type receptor. The mechanism responsible for delayed internalization of activated PAR1 NA ECL2 mutant is not known.

3.4.6 Internalization of PAR1 NA ECL2 is not affected by inhibition of PLC-stimulated PI hydrolysis

Activated PAR1 couples to G_q to stimulate PLC-β-mediated hydrolysis of PIP_2 to generate IPs, but can also utilize a $G_{12/13}$ and PLC-ε pathway for IP generation (30-32). Clathrin-coated pits form at sites enriched in PIP_2 and are the major route for GPCR internalization (33). To determine whether the defect in PAR1 NA ECL2 mutant internalization was related to its capacity to stimulate enhanced PI hydrolysis compared to wild-type receptor, we utilized edelfosine, a pharmacological inhibitor of PLC and examined receptor internalization by ELISA. To ensure that edelfosine was effective at inhibiting PLC we first examined activated PAR1-stimulated PI hydrolysis in HeLa cells labeled with *myo*-[^{3}H]inositol. The expression of PAR1 at the cell surface in edelfosine treated cells was comparable to control cells as determined by ELISA **(Fig 3.6A)**. As expected, pretreatment with edelfosine resulted in virtual ablation of agonist-induced accumulation of [^{3}H]IPs measured after 5 min of agonist stimulation compared to control cells **(Fig 3.6B)**, indicating that edelfosine inhibits PLC activity. To assess internalization, HeLa cells were pretreated with or without 10 μM eldofosine for 90 min at 37°C. Cells were washed and then incubated in the presence or absence of 100 μM SFLLRN or 10 nM thrombin for 5 min at 37°C. Despite the inhibition of PI hydrolysis by edelfosine, agonist-induced internalization of PAR1 wild-type or NA ECL2 mutant were not affected **(Fig 3.6C and D)**, suggesting that receptor-stimulated PI hydrolysis is not linked to internalization.

3.4.7 Internalization of PAR1 NA ECL2 is not affected by inhibition of G_q-mediated PI hydrolysis

To further examine the role of PI hydrolysis in PAR1 internalization we examined the function of G_q, which is the major effector of PLC-stimulated PI hydrolysis induced by activation of PAR1 (5, 34, 35), using siRNA-targeted depletion of endogenous G_q. HeLa cells expressing PAR1 wild-type and NA ECL2 mutant were transfected with 100 nM non-specific siRNA or siRNA targeting G_q for 72 h at 37°C. Cell surface ELISA showed no difference in PAR1 expression in either NS siRNA or G_q siRNA treated cells **(Fig 3.7A)**, however, the immunoblot analysis indicated that expression of endogenous G_q was substantially reduced **(Fig 3.7A, *insert*)**. Cells labeled with *myo*-[^{3}H]inositol were then stimulated with thrombin for 60 min. Cells lacking G_q expression showed substantial inhibition of thrombin-induced [^{3}H]IPs accumulation compared to control cells **(Fig 3.7B)**. In contrast to receptor signaling, depletion of G_q expression had no effect on either PAR1 wild-type or NA ECL2 mutant agonist-induced internalization **(Fig 3.7C)**, suggesting that PI hydrolysis is not the driver of receptor internalization. Together with the PLC inhibitor data, these findings suggest differences in activated PAR1 wild-type and NA ECL2 mutant induced PI hydrolysis is not responsible for modulating receptor internalization.

3.4.8 PAR1 wild-type and NA ECL2 mutant display similar rates of agonist-induced degradation

To determine whether N-linked glycosylation of PAR1 mediates endocytic sorting of the receptor, we compared the rates of agonist-induced PAR1 wild-type and NA ECL2 mutant degradation. HeLa cells expressing FLAG-tagged PAR1 wild-type

and NA ECL2 mutant were incubated with or without agonist for various times at 37°C, and the amount of receptor protein remaining was determined by immunoblot analysis. In cells exposed to agonist for 45 min, a significant decrease in the amount of PAR1 wild-type protein was observed and the detection of receptor protein was virtually abolished at 90 min **(Fig. 3.8A, lanes 3-5 and 3.8B)**, consistent with that previously reported. Interestingly, PAR1 NA ECL2 mutant displayed a rate of agonist-induced degradation comparable to wild-type receptor **(Fig. 3.8A, lanes 6-8 and 3.8B).** These findings suggest that N-linked glycosylation of PAR1 ECL2 is not important for endocytic sorting and lysosomal degradation of activated PAR1.

3.5 Discussion

Unlike most classic reversibly activated GPCRs, PAR1 is irreversibly activated through an unusual proteolytic mechanism that results in the formation of a tethered ligand that binds intramolecularly to the receptor to elicit transmembrane signaling (1). The precise mechanism by which the newly formed tethered ligand interacts with the extracellular surface of PAR1 to induce a signaling response remains poorly understood. GPCRs that belong to class B family of receptors bind peptide hormones presumably through critical interactions with the extracellular portions (36, 37). In addition, the extracellular domains of other non- peptide hormone binding GPCRs belonging to the large class A Rhodopsin-like family of GPCRs have been reported to influence ligand interactions (9-14). In the case of the dopamine, cannabinoid, and adenosine receptor the second extracellular loop was found to participate in ligand

binding, while other extracellular domains participated in ligand recognition of the CCR3 receptor. A more recent study using NMR spectroscopy showed that small molecules that bind within the transmembrane core and display different efficacies towards G protein activation stabilize different conformations of the β2−adrenergic receptor extracellular surface formed by a salt bridge between ECL2 and ECL3 (38). These findings suggest that the extracellular surface of GPCRs is dynamic and can alter receptor conformation and G-protein activation.

Previous studies have shown that the second extracellular loop of PAR1, a class A GPCR, is critical for ligand recognition and signal propagation (15, 16). In these studies, PAR chimera's were generated by substituting various extracellular portions of different species and used to examine species-specific receptor ligand interaction requirements. The results from these studies indicate that the second extracellular loop is a critical portion of the receptor dictating ligand docking and receptor activation. The recent high-resolution structure of PAR1 is consistent with tethered ligand interaction with the surface of extracellular loop 2 (17). Our findings reported here now suggest that glycosylation of the second extracellular loop of PAR1 is also a critical determinant for ligand-induced receptor activation and the fidelity of thrombin signaling. Indeed, in the absence of N-linked glycosylation, activation of PAR1 either proteolytically with thrombin or by the addition of synthetic peptide agonist caused a marked increase in signaling compared to wild-type receptor. Remarkably, enhanced signaling by the PAR1 NA ECL2 mutant was not due to a defect in thrombin cleavage of the receptor or desensitization. Thus, our findings

support the idea that a lack of PAR1 N- linked glycosylation allows the tethered ligand or synthetic peptide agonist to bind the receptor in a manner that induces an active receptor conformation that is more efficient at coupling to G-protein signaling.

In malignant cancer, altered glycosylation of proteins is common and various forms of N-linked glycosylation can be present. The expression of PAR1 is upregulated in many types of invasive cancers including breast cancer due in part to defective receptor trafficking, which leads to persistent signaling, transactivation of ErbB receptors and breast cancer progression (28, 39, 40). Whether defective glycosylation of PAR1 occurs in malignant tumors and contributes to persistent signaling and breast cancer invasion and metastasis has not been examined.

In addition to rapid desensitization, trafficking of PAR1 is critical for the fidelity of receptor signaling. PAR1 displays constitutive internalization, a process important for cellular resensitization (22, 24, 25), and agonist-induced internalization, which is critical for receptor signal termination (20, 21). Interestingly, we found that the initial rate of agonist-induced PAR1 NA ECL2 mutant internalization is impaired compared to wild-type receptor, whereas constitutive internalization remained intact. Moreover, the defect in PAR1 NA ECL2 mutant internalization was observed with thrombin, the physiological relevant agonist, as well as with the synthetic peptide agonist. These findings raise the possibility that glycosylation is important for maintaining distinct active conformations of the receptor that are able to engage the endocytic machinery differently. Both constitutive and agonist-induced PAR1 internalization occur through clathrin-coated pits independent of β–arrestins (18, 26).

Interestingly, constitutive internalization of PAR1 requires the clathrin adaptor AP-2 (22), whereas agonist internalization is specified by both AP-2 and epsin-1 (23). Using confocal microscopy studies we observed that the PAR1 NA ECL2 mutant was still able to interact with both AP-2 and epsin-1, albeit less efficiently than wild-type receptor. The mechanistic basis for delayed internalization of PAR1 NA ECL2 is not known but does not appear to involve differences signaling to PI hydrolysis since perturbation of signaling has no effect on receptor internalization. In contrast to the defects in PAR1 NA ECL2 internalization, we failed to observe any difference between agonist-induced PAR1 wild-type and NA ECL2 mutant lysosomal degradation, suggesting that receptor trafficking through the endocytic pathway occurs independent of receptor glycosylation.

Our studies reveal for the first time a function for PAR1 N-linked glycosylation of the second extracellular loop in regulation of receptor signaling and trafficking. We speculate that N-linked glycosylation of PAR1 influences the active conformation of the receptor following tethered ligand binding that results in less efficient coupling to G_q signaling. The studies described above focused on PAR1 coupling to G_q signaling. However, activated PAR1 is promiscuous and can couple to G_i as well as $G_{12/13}$ proteins in the same cell. Thus, it will be important to determine whether N-linked glycosylation of PAR1 has similar effects on PAR1 coupling to distinct G proteins subtypes and is the topic of Chapter 4.

3.6 Acknowledgements

This work was supported by National Institutes of Health grant HL073328 (J. Trejo) and an American Heart Association Established Investigator Award (J. trejo). A. G. Soto was supported by a T32 NIGMS Pharmocological Sciences Training Grant. The authors have no conflict of interest to declare.

The contents of Chapter 3, in part, have been published: **Soto, A.G.,** and Trejo, J. (2010) N-Linked glycosylation of protease-activated receptor-1 second extracellular loop: a critical determinant for ligand-induced receptor activation and internalization. *Journal of Biological Chemistry, 285*(24), 18781-93. The dissertation author was the primary investigator and author of this paper. All co-authors have given written permission for its use and the reproduction of all associated data in this dissertation.

3.7 Figures

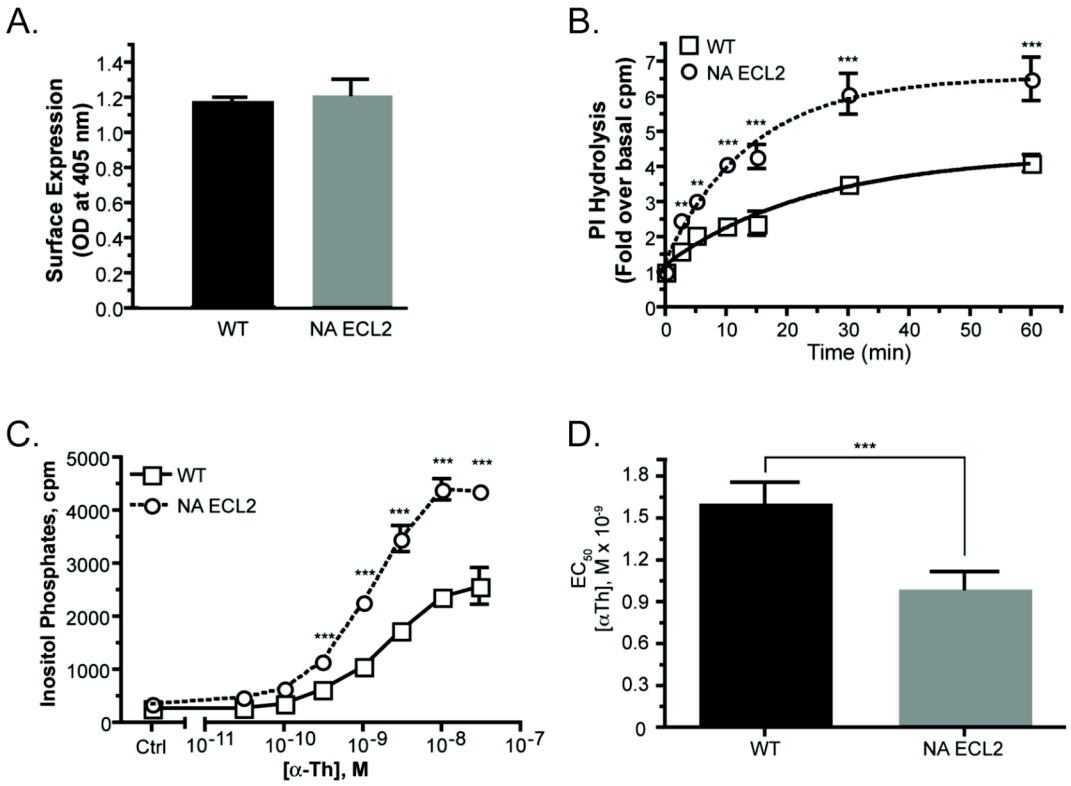

Figure 3.1: PAR1 NA ECL2 mutant signals with greater efficacy compared to wild-type receptor. (*A*) The amounts of PAR1 wild-type (WT) and NA ECL2 mutant expressed at the cell surface was determined by ELISA. (*B*) HeLa cells stably expressing FLAG-tagged PAR1 WT or NA ECL2 mutant labeled with *myo*-[^{3}H]inositol were incubated with 10 nM thrombin (α–Th) for various times at 37°C in media containing LiCl. The data shown (mean ± S.D.; *n*=3) are expressed as the fold increase in [^{3}H]IPs accumulation over basal counts/min and are from one experiment that is representative of multiple independent experiments performed in triplicate. The difference in thrombin-stimulated signaling at PAR1 WT and NA ECL2 mutant at various times was significant (**, $p < 0.01$; ***, $p < 0.001$) by two-way ANOVA and Bonferroni post-tests. (*C*) HeLa cells stably expressing FLAG-tagged PAR1 wild-type (WT) or NA ECL2 mutant labeled with *myo*-[^{3}H]inositol were incubated with media containing various concentrations of thrombin (α–Th) for 5 min at 37°C in media containing LiCl. The data shown (mean ± S.D.; *n*=3) are expressed as the counts/min and are from one experiment that is representative of multiple independent experiments performed in triplicate. The difference in thrombin-stimulated signaling at PAR1 WT and NA ECL2 mutant at various concentrations was significant (***, $p < 0.001$) by two-way ANOVA and Bonferroni post-tests. (*D*) EC_{50} values (mean ± S.D.; *n*=3) for thrombin signaling at PAR1 WT and NA ECL2 mutant was determined from three independent experiments. The difference in thrombin-stimulated EC_{50} was significant (***, $p < 0.001$) by Student's *t* test.

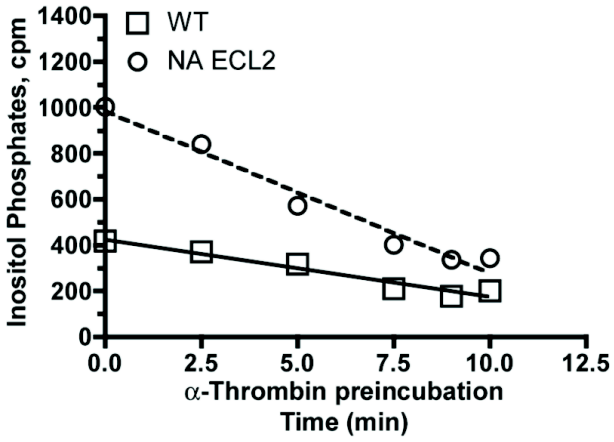

Figure 3.2: PAR1 NA ECL2 mutant exhibits a distinct desensitization rate compared to wild-type receptor. HeLa cells stably expressing similar amounts of FLAG-tagged PAR1 wild-type (WT) or NA ECL2 mutant labeled with *myo*-[^{3}H]inositol were incubated with 10 nM α-thrombin for 10 min at 37°C. Lithium chloride was added after various times of thrombin exposure, and the amounts of [^{3}H]IPs formed were then measured. The data shown (mean ± S.D.; *n*=3) are representative of three independent experiments performed in triplicate.

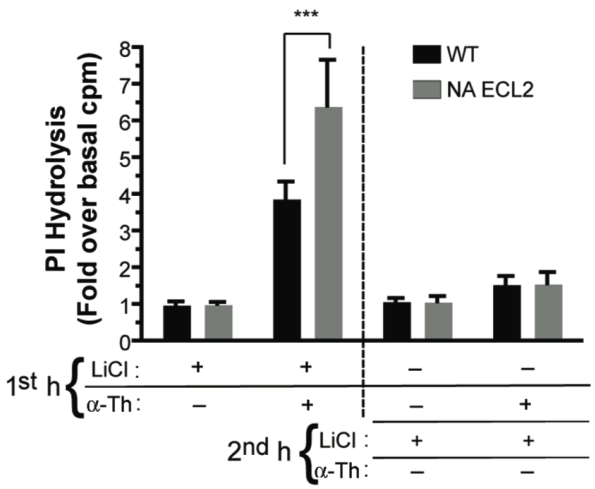

Figure 3.3: PAR1 NA ECL2 mutant enhanced signaling is not due to constitutive activation or impaired signal termination. HeLa cells stably expressing similar amounts of FLAG-tagged PAR1 wild-type (WT) or NA ECL2 mutant labeled with *myo*-[^{3}H]inositol were incubated with media alone or media containing 10 nM α–thrombin (α-Th) in the presence of lithium chloride (LiCl) for 1 h at 37°C (*left bar graphs*). Alternatively, cells were incubated for 1 h at 37 °C in the absence of LiCl with or without 10 nM α-thrombin. These cells were then washed and incubated in new media containing LiCl with 0.5 unit/ml hirudin (thrombin inhibitor) for an additional 1 h at 37°C (*right bar graphs*). The amounts of accumulated [^{3}H]IPs were then measured. The data shown (mean ± S.D.; *n*=3) are expressed as the fold increase in [^{3}H]IP accumulation over basal counts/min and are the averages from three independent experiments. The difference between thrombin-induced signaling in PAR1 WT *versus* NA ECL2 mutant-expressing cells was significant (***, $p < 0.001$) by two-way ANOVA and Bonferroni post-tests.

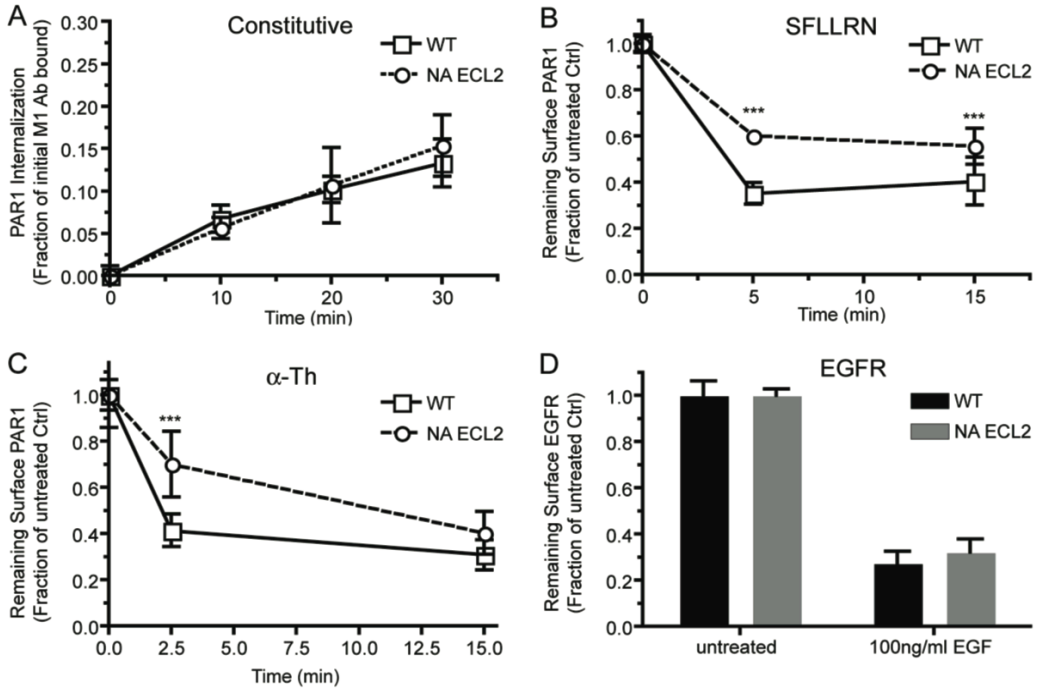

Figure 3.4: PAR1 NA ECL2 displays a modest decrease in agonist-induced internalization but not constitutive internalization. (*A*) HeLa cells stably expressing FLAG-tagged PAR1 wild-type (WT) or NA ECL2 mutant were labeled with M1 anti-FLAG antibody for 1 h at 4°C, washed, and incubated in media without agonist for various times at 37°C. After incubations, cells were stripped of remaining surface bound antibody, and ELISA quantitated internalized antibody. The data shown (mean ± S.D., *n*=3) are expressed as the fraction of initial cell surface receptor-bound antibody corrected for background = ((value at time x – average 0 minute value)/(average untreated value – average 0 minute value)) and are the averages from three independent experiments performed in triplicate. HeLa cells stably expressing similar amounts of FLAG-tagged PAR1 wild-type (WT) or NA ECL2 mutant were serum starved for 30 min then treated with media containing 100 μM SFLLRN (*B*) or 10 nM thrombin (*C*) for various times at 37°C. After incubation cells were washed, fixed and ELISA determined the amount of PAR1 remaining on the cell surface. The data shown (mean ± S.D.; *n*=3) are expressed as the fraction of surface antibody bound of untreated control and are the averages of three separate experiments performed in triplicate. The difference between agonist-induced PAR1 WT and NA ELC2 mutant internalization at various times was significant (***, $p < 0.001$). (*D*) HeLa cells stably expressing PAR1 wild-type or NA ECL2 mutant were serum-starved for 30 min then incubated in media alone (untreated) or media containing 100 ng/ml EGF for 1 h at 37°C and remaining surface EGFR assayed by ELISA. The data shown (mean ± S.D.; *n*=3) are from three independent experiments performed in triplicate.

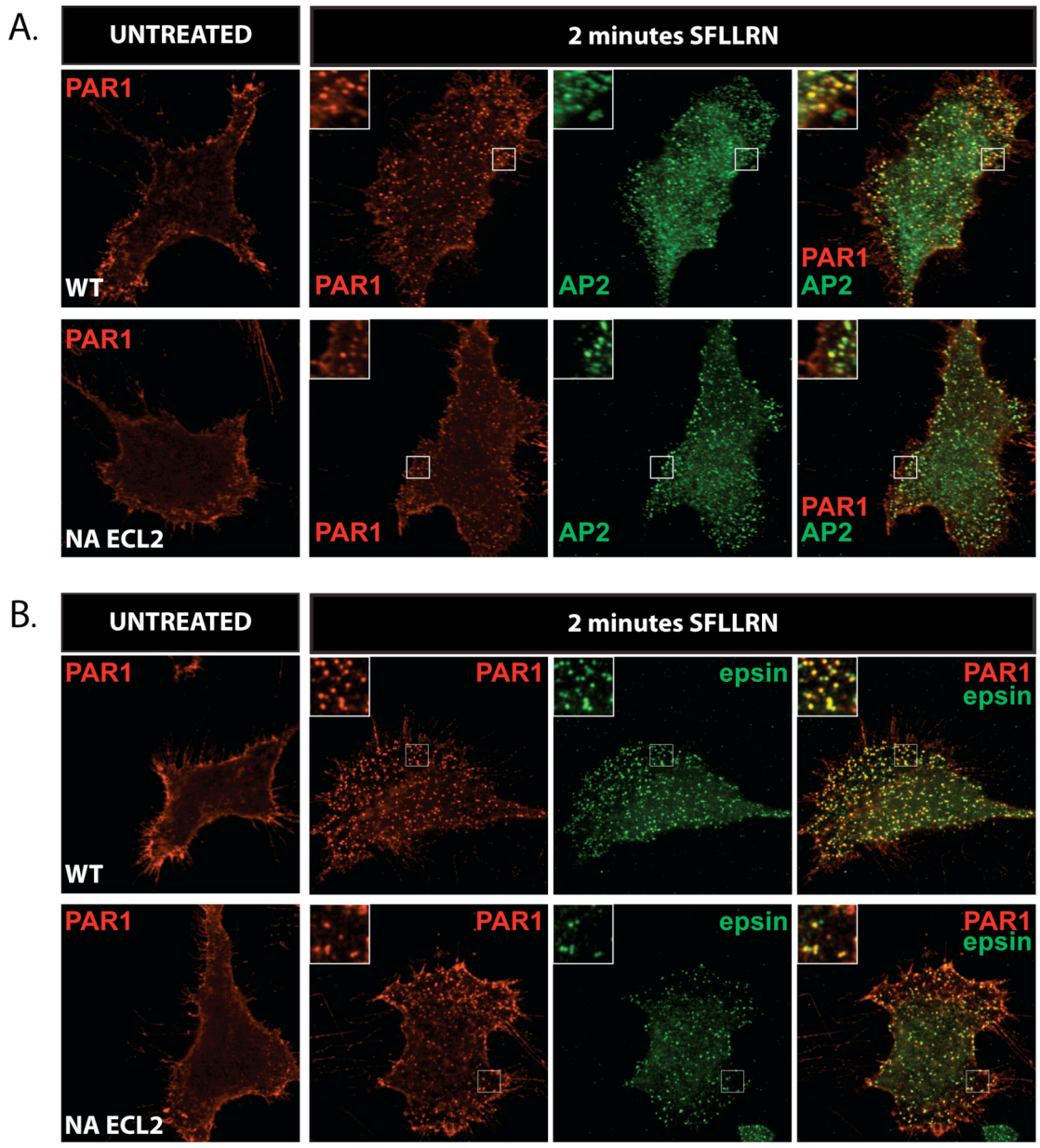

Figure 3.5: PAR1 NA ECL2 mutant colocation with the endocytic adaptors AP-2 and epsin-1. HeLa cells stably expressing FLAG-tagged PAR1 wild-type (WT) or NA ECL2 mutant were labeled with M1 anti-FLAG antibody for 1 h at 4°C, washed, and either incubated in media with 100 μM SFLLRN for 2 min at 37°C or left on ice (untreated). Cells were washed, fixed with 4% PFA, permeabilized with MeOH and then stained for either AP-2 (*A*) or epsin-1 (*B*) and imaged by confocal microscopy. Colocalization is revealed by the yellow color in the merged images. The images are representative of multiple cells imaged from multiple different experiments. *Insets* represent magnification of the boxed areas.

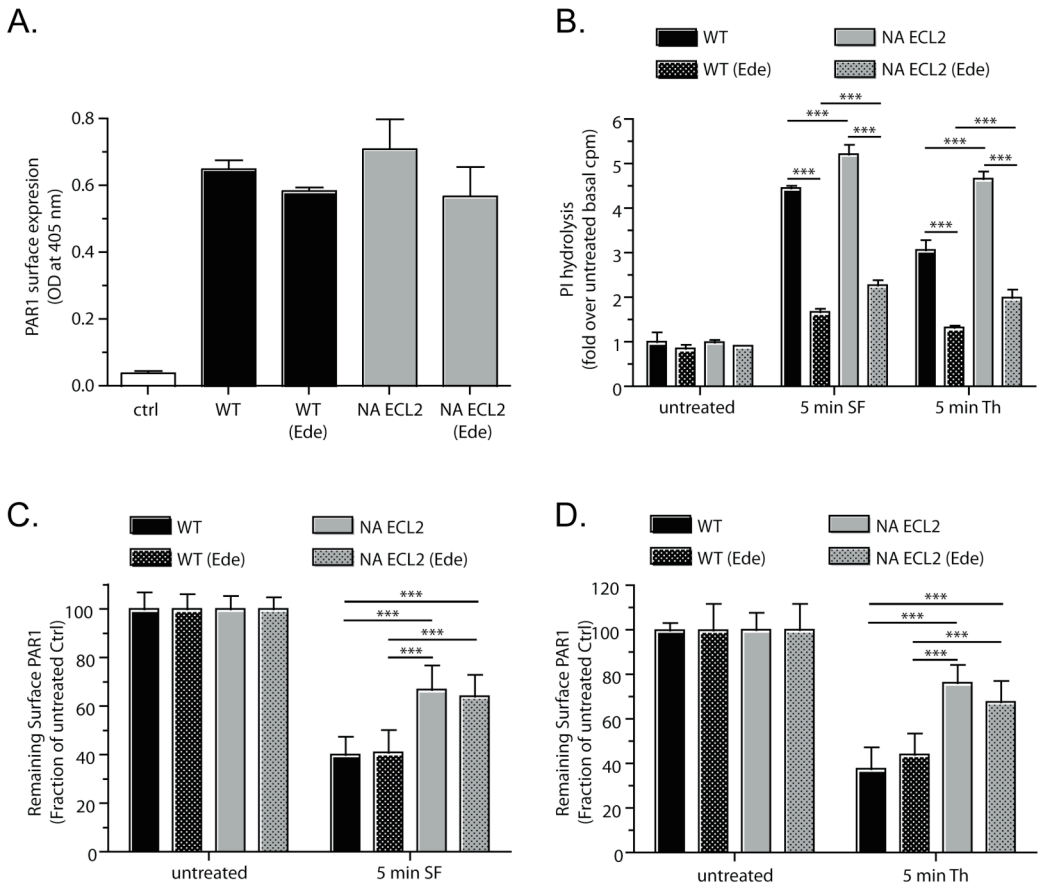

Figure 3.6: Internalization of PAR1 NA ECL2 is not affected by inhibition of PLC-stimulated PI hydrolysis. (*A*) The amounts of PAR1 wild-type (WT) and NA ECL2 mutant expressed at the cell surface after 90 min pretreatment with 10 μM edelfosine (Ede) was determined by ELISA. (*B*) HeLa cells stably expressing similar amounts of FLAG-tagged PAR1 WT or NA ECL2 mutant labeled with *myo*-[^{3}H]inositol were pretreated with 10 μM edelfosine for 90 min at 37°C, then were incubated with either 100 μM SFLLRN (SF) or 10 nM α–thrombin (Th) for 5 min at 37°C in media containing LiCl and edelfosine. The data shown (mean ± S.D.; n=3) are expressed as the fold increase in [^{3}H]IPs accumulation over basal counts/min and are from one experiment that is representative of three independent experiments performed in triplicate. The difference in agonist-stimulated signaling at PAR1 WT and NA was significant (***, $p < 0.001$) by two-way ANOVA and Bonferroni post-tests. HeLa cells stably expressing similar amounts of FLAG-tagged PAR1 WT or NA ECL2 were pretreated with 10 μM edelfosine for 90 min at 37°C, then were incubated with either 100 μM SFLLRN (*C*) or 10 nM α–thrombin (*D*) for 5 min at 37°C and remaining surface receptor was determined by ELISA. The data shown (mean ± S.D.; n=3) are from three independent experiments performed in triplicate. The difference in agonist-induced internalization at PAR1 WT and NA ECL2 at 5 min was significant (***, $p < 0.001$) by two-way ANOVA and Bonferroni post-tests.

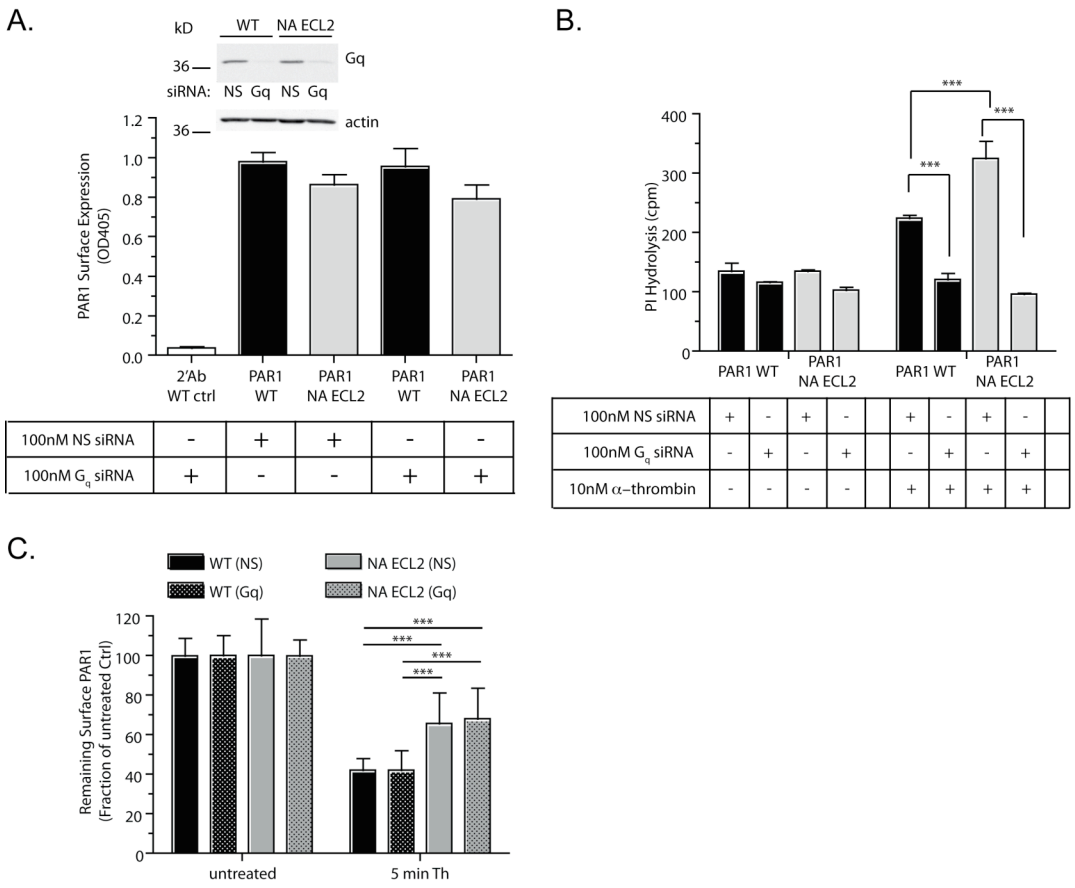

Figure 3.7: Internalization of PAR1 NA ECL2 is not affected by inhibition of G_q-mediated PI hydrolysis. (*A*) The amounts of PAR1 wild-type (WT) and NA ECL2 mutant expressed at the cell surface after 72 h siRNA knockdown was determined by ELISA. (*B*) HeLa cells stably expressing similar amounts of FLAG-tagged PAR1 WT or NA ECL2 mutant labeled with *myo*-[^{3}H]inositol were treated with non specific (NS) siRNA or siRNA against G_q at 37°C for 72 h, then were incubated with 10 nM α–thrombin (Th) for 60 min at 37°C in media containing LiCl. The data shown (mean ± S.D.; *n*=3) are expressed as counts per min and are from one experiment that is representative of three independent experiments performed in triplicate. The difference in agonist-stimulated signaling at PAR1 WT and NA was significant (***, $p < 0.001$) by two-way ANOVA and Bonferroni post-tests. (*C*) HeLa cells stable expressing similar amounts of FLAG-tagged PAR1 WT or NA ECL2 were treated with non specific (NS) siRNA or siRNA against G_q at 37°C for 72 h, then were incubated with 10 nM α–thrombin (Th) for 5 min at 37°C and remaining surface receptor was determined by ELISA. The data shown (mean ± S.D.; *n*=3) are from three independent experiments performed in triplicate. The difference in agonist-induced internalization at PAR1 WT and NA ECL2 at 5 min was significant (***, $p < 0.001$) by two-way ANOVA and Bonferroni post-tests.

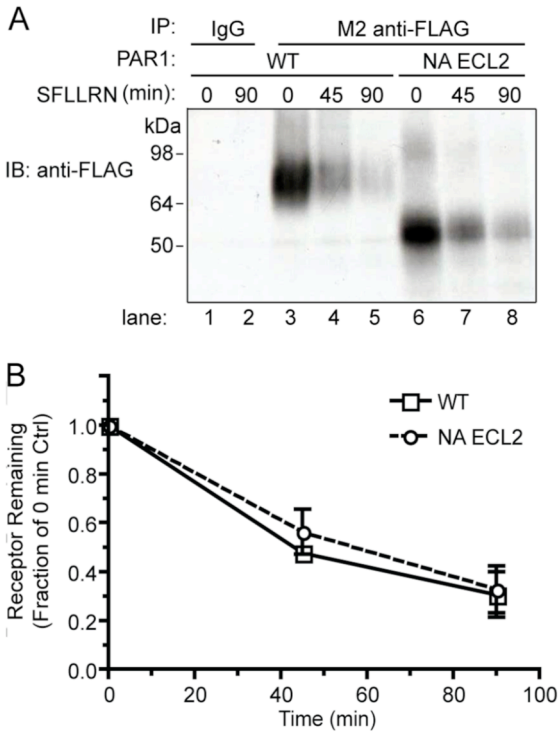

Figure 3.8: PAR1 wild-type and NA ECL2 mutant display similar rates of agonist-induced degradation. (*A*) HeLa cells stably expressing PAR1 wild-type (WT) or NA ECL2 mutant were incubated with 100 μM SFLLRN for various times at 37°C. Cells were lysed and PAR1 immunoprecipitated with M2 anti-FLAG antibody or IgG control. Immunoprecipitates were resolved by SDS-PAGE and transferred to membranes. PAR1 was detected by immunoblotting with rabbit polyclonal anti-FLAG antibody. Similar findings were observed in three independent experiments. (*B*) The amount of PAR1 remaining after agonist treatment detected in immunoblot analysis were quantified using ImageJ software and the data shown (mean ± S.D.; *n*=3) are expressed as the fraction of untreated control and are the averages of three separate experiments.

3.8 References

1. Vu, T. K., Hung, D. T., Wheaton, V. I., and Coughlin, S. R. (1991) Molecular cloning of a functional thrombin receptor reveals a novel proteolytic mechanism of receptor activation. *Cell* **64**, 1057-1068

2. Benka, M. L., Lee, M., Wang, G.R., Buckman, S., Burlacu, A., Cole, L., DePina, A., Dias, P., Granger, A., Grant, B., et al (1995) The thrombin receptor in human platelets is coupled to a GTP binding protein of the G alpha q family. *FEBS lett.* **363**, 49-52

3. Majumdar, M., Seasholtz, T. M., Buckmaster, C., Toksoz, D., and Brown, J. H. (1999) A rho exchange factor mediates thrombin and Galpha(12)-induced cytoskeletal responses. *J Biol Chem* **274**, 26815-26821

4. Baffy, G., Yang, L., Raj, S., Manning, D.R., and Williamson, J.R. (1994) G protein coupling to the thrombin receptor in Chinese hamster lung fibroblasts. *J Biol Chem.* **269**, 8483-8487

5. Offermanns, S., Toombs, C. F., Hu, Y. H., and Simon, M. I. (1997) Defective platelet activation in G alpha(q)-deficient mice. *Nature* **389**, 183-186

6. Lagerstrom, M. C., and Schioth, H. B. (2008) Structural diversity of G protein-coupled receptors and significance for drug discovery. *Nat Rev Drug Discov* **7**, 339-357

7. Rosenbaum, D. M., Rasmussen, S. G., and Kobilka, B. K. (2009) The structure and function of G-protein-coupled receptors. *Nature* **459**, 356-363

8. Parthier, C., Reedtz-Runge, S., Rudolph, R., and Stubbs, M. T. (2009) Passing the baton in class B GPCRs: peptide hormone activation via helix induction? *Trends Biochem Sci* **34**, 303-310

9. Ahn, K. H., Bertalovitz, A. C., Mierke, D. F., and Kendall, D. A. (2009) Dual role of the second extracellular loop of the cannabinoid receptor 1: ligand binding and receptor localization. *Mol Pharmacol* **76**, 833-842

10. Shi, L., and Javitch, J. A. (2004) The second extracellular loop of the dopamine D2 receptor lines the binding-site crevice. *Proc Natl Acad Sci U S A* **101**, 440-445

11. Datta, A., and Stone, M. J. (2003) Soluble mimics of a chemokine receptor: chemokine binding by receptor elements juxtaposed on a soluble scaffold. *Protein Sci* **12**, 2482-2491

12. Peeters, M. C., van Westen, G. J., Li, Q., and AP, I. J. (2011) Importance of the extracellular loops in G protein-coupled receptors for ligand recognition and receptor activation. *Trends in pharmacological sciences* **32**, 35-42

13. Peeters, M. C., Wisse, L. E., Dinaj, A., Vroling, B., Vriend, G., and Ijzerman, A. P. (2012) The role of the second and third extracellular loops of the adenosine A1 receptor in activation and allosteric modulation. *Biochemical pharmacology* **84**, 76-87

14. Seibt, B. F., Schiedel, A. C., Thimm, D., Hinz, S., Sherbiny, F. F., and Muller, C. E. (2013) The second extracellular loop of GPCRs determines subtype-selectivity and controls efficacy as evidenced by loop exchange study at A2 adenosine receptors. *Biochemical pharmacology* **85**, 1317-1329

15. Gerszten, R. E., Chen, J., Ishi, M., Ishi, K., Wang, L., Nanevicz, T., Turck, C.W., Vu, T.K.H., and Coughlin, S.R. (1994) Specificty of the thrombin receptor for agonist peptide is defined by its extracellular surface. *Nature* **368**, 648-651

16. Lerner, D. J., Chen, M., Tram, T., and Coughlin, S. R. (1996) Agonist recognition by proteinase-activated receptor 2 and thrombin receptor. Importance of extracellular loop interactions for receptor function. *J Biol Chem* **271**, 13943-13947

17. Zhang, C., Srinivasan, Y., Arlow, D. H., Fung, J. J., Palmer, D., Zheng, Y., Green, H. F., Pandey, A., Dror, R. O., Shaw, D. E., Weis, W. I., Coughlin, S. R., and Kobilka, B. K. (2012) High-resolution crystal structure of human protease-activated receptor 1. *Nature* **492**, 387-392

18. Paing, M. M., Stutts, A.B., Kohout, T.A., Lefkowitz, R.J., and Trejo, J. (2002) beta-arrestins regulate protease-activated receptor-1 desensitization but not internalization or down-regulation. *The Journal of Biological Chemistry* **277**, 1292-1300

19. Ishii, K., Hein, L., Kobilka, B., and Coughlin, S. R. (1993) Kinetics of thrombin receptor cleavage on intact cells. Relation to signaling. *J Biol Chem* **268**, 9780-9786

20. Trejo, J., Hammes, S.R., and Coughlin, S.R. (1998) Termination of signaling by protease-activated receptor-1 is linked to lysosomal sorting. *J Biol Chem* **95**, 13698-13702

21. Trejo, J., and Coughlin, S. R. (1999) The cytoplasmic tails of protease-activated receptor-1 and substance P receptor specify sorting to lysosomes versus recycling. *J Biol Chem* **274**, 2216-2224

22. Paing, M. M., Johnston, C. A., Siderovski, D. P., and Trejo, J. (2006) Clathrin adaptor AP2 regulates thrombin receptor constitutive internalization and endothelial cell resensitization. *Mol Cell Biol* **26**, 3231-3242

23. Chen, B., Dores, M. R., Grimsey, N., Canto, I., Barker, B. L., and Trejo, J. (2011) Adaptor protein complex-2 (AP-2) and epsin-1 mediate protease-activated receptor-1 internalization via phosphorylation- and ubiquitination-dependent sorting signals. *J Biol Chem* **286**, 40760-40770

24. Hein, L., Ishii, K., Coughlin, S. R., and Kobilka, B. K. (1994) Intracellular targeting and trafficking of thrombin receptors. A novel mechanism for resensitization of a G protein-coupled receptor. *J Biol Chem* **269**, 27719-27726

25. Shapiro, M. J., and Coughlin, S. R. (1998) Separate signals for agonist-independent and agonist-triggered trafficking of protease-activated receptor 1. *J Biol Chem* **273**, 29009-29014

26. Trejo, J., Altschuler, Y., Fu, H. W., Mostov, K. E., and Coughlin, S. R. (2000) Protease-activated receptor-1 down-regulation: a mutant HeLa cell line suggests novel requirements for PAR1 phosphorylation and recruitment to clathrin-coated pits. *J Biol Chem* **275**, 31255-31265

27. Soto, A. G., and Trejo, J. (2010) N-linked glycosylation of protease-activated receptor-1 second extracellular loop: a critical determinant for ligand-induced receptor activation and internalization. *J Biol Chem* **285**, 18781-18793

28. Booden, M. A., Eckert, L. B., Der, C. J., and Trejo, J. (2004) Persistent signaling by dysregulated thrombin receptor trafficking promotes breast carcinoma cell invasion. *Mol Cell Biol* **24**, 1990-1999

29. Wolfe, B. L., Marchese, A., and Trejo, J. (2007) Ubiquitination differentially regulates clathrin-dependent internalization of protease-activated receptor-1. *J Cell Biol* **177**, 905-916

30. Coughlin, S. R. (2000) Thrombin signalling and protease-activated receptors. *Nature* **407**, 258-264

31. Taylor, S. J., Chae, H. Z., Rhee, S. G., and Exton, J. H. (1991) Activation of the beta 1 isozyme of phospholipase C by alpha subunits of the Gq class of G proteins. *Nature* **350**, 516-518

32. Hains, M. D., Wing, M. R., Maddileti, S., Siderovski, D. P., and Harden, T. K. (2006) Galpha12/13- and rho-dependent activation of phospholipase C-epsilon

by lysophosphatidic acid and thrombin receptors. *Mol Pharmacol* **69**, 2068-2075

33. Marchese, A., Paing, M. M., Temple, B. R., and Trejo, J. (2008) G protein-coupled receptor sorting to endosomes and lysosomes. *Annual review of pharmacology and toxicology* **48**, 601-629

34. Jope, R. S., Song, L., and Powers, R. (1994) Agonist-induced, GTP-dependent phosphoinositide hydrolysis in postmortem human brain membranes. *Journal of neurochemistry* **62**, 180-186

35. Olianas, M. C., Dedoni, S., and Onali, P. (2007) Proteinase-activated receptors 1 and 2 in rat olfactory system: layer-specific regulation of multiple signaling pathways in the main olfactory bulb and induction of neurite retraction in olfactory sensory neurons. *Neuroscience* **146**, 1289-1301

36. Pioszak, A. A., Parker, N. R., Suino-Powell, K., and Xu, H. E. (2008) Molecular recognition of corticotropin-releasing factor by its G-protein-coupled receptor CRFR1. *J Biol Chem* **283**, 32900-32912

37. Hoare, S. R. (2005) Mechanisms of peptide and nonpeptide ligand binding to Class B G-protein-coupled receptors. *Drug Discov Today* **10**, 417-427

38. Bokoch, M. P., Zou, Y., Rasmussen, S. G., Liu, C. W., Nygaard, R., Rosenbaum, D. M., Fung, J. J., Choi, H. J., Thian, F. S., Kobilka, T. S., Puglisi, J. D., Weis, W. I., Pardo, L., Prosser, R. S., Mueller, L., and Kobilka, B. K. Ligand-specific regulation of the extracellular surface of a G-protein-coupled receptor. *Nature* **463**, 108-112

39. Arora, P., Ricks, T. K., and Trejo, J. (2007) Protease-activated receptor signalling, endocytic sorting and dysregulation in cancer. *J Cell Sci* **120**, 921-928

40. Arora, P., Cuevas, B. D., Russo, A., Johnson, G. L., and Trejo, J. (2008) Persistent transactivation of EGFR and ErbB2/HER2 by protease-activated receptor-1 promotes breast carcinoma cell invasion. *Oncogene* **27**, 4434-4445

Chapter 4:

An N-linked glycosylation switch for GPCR-G protein coupling specificity

4.1 Abstract

PAR1 is capable of coupling to multiple distinct G-protein subtypes within the same cell including G_q, G_i, and $G_{12/13}$. The mechanisms that contribute to PAR1's ability to signal through different G-protein subtypes are not known. Thus, we examined whether N-linked glycosylation of PAR1 affects receptor-G protein coupling specificity. In these studies we focused on the function of N-linked glycosylation at the PAR1 second extracellular loop (ECL2), which is important for ligand docking interactions and assessed G protein coupling by co-immunoprecipitation and bioluminescence resonance energy transfer (BRET) assays. We also examined the consequences of PAR1 differential coupling by examining G_q-stimulated phosphoinositide hydrolysis and $G_{12/13}$-induced RhoA activation and stress fiber formation. Here, we report for the first time that N-linked glycosylation influences PAR1-G protein coupling specificity. We show that PAR1 wild-type preferentially couples to $G_{12/13}$ compared to G_q, whereas a PAR1 mutant lacking N-linked glycosylation at ECL2 preferentially couples G_q versus $G_{12/13}$. Intriguingly, however, both PAR1 wild-type and NA ECL2 mutant deficient in N-linked glycosylation coupled to G_i comparably. Taken together these findings suggest that N-linked glycosylation of PAR1 is a critical determinant for GPCR-G protein coupling specificity.

4.2 Introduction

Many activated GPCRs can couple to multiple distinct heterotrimeric G protein subtypes that lead to diverse downstream cellular responses (1, 2). In addition to G

proteins, activated GPCRs are able to interact directly with non-G protein signaling effectors. The studies from Lefkowitz and colleagues, using the angiotensin II receptor as a prototype, showed that GPCRs could signal through β-arrestins independently of G proteins (3, 4). This revelation led to the search and discovery of "biased ligands" or ligands that selectively activate only one of the GPCR promoted signaling pathways and not others (5, 6). The ability to pharmacologically and selectively modulate which GPCR signaling pathway is activated opened new possibilities for drug design. It made it possible to determine which signaling pathways were important for therapeutic benefits versus unwanted side effects. Thus, a drug can be better tailored for specific treatments. This idea was recently supported by work done with the angiotensin II type 1 receptor in rats with the β-arrestin bias agonist TRV120027 (7). It was shown that TRV120027, similar to unbiased antagonists losartan and telmisartan, was able to reduce mean arterial pressure. Unlike the unbiased antagonist, which decreased cardiac performance, TRV120027 actually increased cardiac performance and preserved cardiac stroke volume (7). The concept of bias signaling strongly supports the idea that GPCRs are able to adopt multiple distinct active conformations that facilitate interaction with their downstream signaling and trafficking components in a unique manner. However, whether GPCR posttranslational modifications or other factors influence the stability of different GPCR active conformations has not been previously examined.

PAR1 has been shown to display biased signaling as described in studies examining thrombin versus APC signaling in endothelial cells. Thrombin cleaves at arginine 41, which reveals the SFLLRN tethered ligand and promotes RhoA activation

and endothelial barrier disruption (8). Protein C is a zymogen that circulates in plasma and is activated by thrombin bound to thrombomodulin when Protein C is associated with the endothelial protein C receptor on the surface of endothelial cells (9, 10). APC is a serine protease and mediates anticoagulant activities by cleaving and inactivating Factors V and VIII, upstream coagulant proteases important for thrombin generation (11). In addition, APC can cleave PAR1 at arginine 46 resulting in the generation of a distinct tethered ligand which activates a Rac1 signaling pathway important for endothelial barrier stability (12, 13). Recent work from our lab revealed that the APC-induced Rac1 signaling pathway important for cytoprotection is mediated by β-arrestin recruitment and activation of the dishevelled-2 scaffold and appears to occur preferentially in caveolar microdomains (14, 15).

GPCR biased signaling has been best described for G protein versus β-arrestin signaling, however it can also pertain to how GPCRs are able to couple to different G proteins within the same cell. In most cases bias signaling is dictated by different ligands, with each ligand able to promote the stability of a unique active conformation. However, there are also examples of the same ligand promoting different signaling even in the same cells. An example of PAR1 G_o protein bias was recently reported in work done with mice examining neuronal plasticity and fear (16). The study showed mice that underwent fear conditioning shifted PAR1-G protein subtype coupling to favor G_o compared to G_q. The shift in G protein subtype coupling to preference G_o resulted in inhibition of neuronal excitability, activity, and synaptic plasticity (16). These studies involved cells from the amygdala, but such switches in G protein

preference are likely to occur in other cell types as well. However, the mechanisms that allow for the dynamic switch in G protein preference are not known.

In the present work, we examined for the first time the function of N-linked glycosylation in mediating GPCRs biased coupling to specific G protein subtypes. The PAR1 NA ECL2 mutant deficient in N-linked glycosylation at ECL2 showed preferentially coupling to G_q versus $G_{12/13}$ signaling, whereas wild-type receptor exhibited an opposite phenotype. In contrast, both PAR1 wild-type and NA ECL2 mutant coupled similarly to G_i protein as assessed by coimmunoprecipitation and BRET. These findings suggest that glycosylation of a GPCR can influence G protein subtype coupling.

4.3 Materials and methods

Reagents and Antibodies- Human α-thrombin was obtained from Enzyme Research Laboratories (South Bend, IN). The PAR1-activating peptide, SFLLRN, was synthesized as the carboxyl amide and purified by reverse phase high-pressure chromatography at Tufts University Core Facility (Boston, MA). Rabbit polyclonal anti-FLAG antibody, mouse monoclonal M2 anti- FLAG antibody, TRITC-conjugated phalloidin, and mouse anti-β-actin antibody were purchased from Sigma- Aldrich. The anti-PAR1 WEDE mouse antibody was purchased from Beckman Coulter (Fullerton, CA). Anti-PAR1 rabbit polyclonal antibody (C5433) was previously described (17). RhoA, $G\alpha q_{11}$, $G\alpha q_{12}$, and $G\alpha q_{13}$ antibodies were from Santa Cruz Biotechnology. The mouse Renilla Luciferase antibody was purchased from Millipore. Horse-radish peroxidase (HRP)-conjugated goat anti-mouse and goat anti-rabbit antibodies were

purchased from Bio-Rad Laboratories (Richmond, CA). Glutathione-Sepharose 4B beads and protein A-Sepharose CL-4B beads were from GE Healthcare.

cDNAs and Cell lines- A cDNA encoding human PAR1 with an N-terminal FLAG epitope sequence cloned into pBJ vector was previously described (18) and used for transient transfections. Mutations were introduced into FLAG-tagged PAR1 by site-directed mutagenesis using the QuikChange Mutagenesis kit (Stratagene) and confirmed by dideoxy sequencing (Moores Cancer Center Core Facility, La Jolla, CA). HeLa cells stably expressing FLAG-tagged PAR1 wildtype and mutants were generated and maintained as previously described (18). HA-$G\alpha_q$ was from Dr. Philip Wedegaertner (Thomas Jefferson University, Philadelphia, PA). $G\alpha_{12}$-EE and $G\alpha_{13}$-EE constructs were a gift from Dr. John R. Hepler (Emory University, Atlanta, GA). $G\alpha_i$-Rluc, $G\alpha_{12}$-Rluc, $G\alpha_{13}$-Rluc, and PAR1-YFP was generously provided by Dr. Jean-Philippe Pin (Montpellier University, Montpellier, France). Mutations were introduced into PAR1-YFP by site-directed mutagenesis using the QuikChange Mutagenesis kit (Stratagene) and confirmed by dideoxy sequencing (Moores Cancer Center Core Facility, La Jolla, CA). COS-7 and HeLa cells were grown in DMEM containing 10% (v/v) fetal bovine serum.

Cell Transfections- Cells were transiently transfected with various cDNA plasmids using 6 μl 1mg/ml Polyethylenimie (Polysciences Inc.) per μg plasmid. COS-7 cells

were transfected with plasmids using FuGENE 6 (Roche Applied Science) as recommended by the manufacturer for bioluminescence resonance energy transfer (BRET) assays.

$G\alpha_{12/13}$ siRNA knockdown- HeLa cells stably expressing FLAG-tagged PAR1 wild-type or mutant were plated in a 12-well culture dish or fibronectin coated 24-well culture dish and grown overnight. Cells were then transfected with 50 nM nonspecific (NS) or specific $G\alpha_{12}$ and $G\alpha_{13}$ siRNAs using Oligofectamine according to the manufacturer's instructions (Invitrogen) and knockdown allowed to proceed for 72 h before assaying cell surface ELISA or RhoA activation. The nonspecific siRNA 5'-CUACGUCCAGGAGCGCACC-3' was synthesized by Dharmacon (Lafayette, CO). The $G\alpha_{12}$ siRNA 5'-GGAUCGGCCAGCUGAAUUATT-3' and $G\alpha_{13}$ siRNA 5'-CGACUGCUUACCAAAUUAATT-3' were synthesized by Qiagen.

PAR1 Immunoprecipitation and Immunoblotting- COS-7 cells or HeLa cells stably expressing FLAG-tagged PAR1 wild-type or mutants were plated in 6-well culture dishes and grown overnight at 37°C. The next day cells were transiently transfected with plasmid and allowed to express for 48 hrs prior to immunoprecipitation. To assess PAR1 coupling to G protein subtypes, cells were serum starved and then incubated with or without agonists in serum-free media at 37°C. Cells were washed, solubilized with Triton X-100 lysis buffer (50 mM Tris-HCl pH 7.4, 100 mM NaCl, 5

mM EDTA, 50 mM NaF, 10 mM NaPP, 1% Triton X-100) containing freshly added protease inhibitors. Cell lysates were solubilized for 1.5 h at 4°C and clarified by centrifugation at 14,000 rpm for 20 min at 4°C. The total amount of protein in cell lysates was quantified using a Bicinchoninic acid (BCA) Protein Assay Reagent (Thermo Scientific) and equivalent amounts of lysates were used for immunoprecipitation with anti-PAR1 WEDE mouse antibody, M2 anti-FLAG antibody, or IgG control. Beads were washed with lysis buffer and proteins eluted with 2x SDS-sample buffer [125 mM Tris-HCl (pH 6.8), 20% (v/v) glycerol, 5% (wt/v) SDS, 200 mM DTT, 0.01% (wt/v) bromophenol blue]. Samples were analyzed by SDS- PAGE, transferred to membranes and G protein subtype association with PAR1 was detected by immunoblotting with G protein specific antibodies or mouse anti-Renilla Luciferase antibody for $G\alpha_i$-Rluc. Membranes were stripped and PAR1 was detected by immunoblotting with anti-PAR1 antibody. Immunoblots were developed with Enhanced Chemiluminescence, imaged by autoradiography and quantitated with ImageJ software (National Institutes of Health).

Cell Surface ELISA- COS-7 cells or HeLa cells stably expressing FLAG-tagged PAR1 wild-type or mutant were plated in a fibronectin coated 24-well culture dish and grown overnight at 37°C. Cells were transfected with various plasmids or they were transfected with various siRNAs prior to assay. After transfections, cells were placed on ice, washed with PBS and then fixed with 4% paraformaldehyde (PFA) for 5 min at 4°C. Cells were washed, and then incubated with polyclonal anti-FLAG antibody

diluted 1:1000 or rabbit polyclonal anti- PAR1 C5433 diluted 1:500 in DMEM/BSA/HEPES for 1 h at room temperature. Cells were washed and then incubated with secondary HRP-conjugated goat anti-rabbit antibody for 1 h at room temperature and washed extensively. The amount of secondary antibody bound was determined by incubation with 1-Step ABTS (2,2′-azinobis-3-ethylbenz-thiazoline-6-sulfonic acid) (Thermo Scientific) substrate for 10–20 min at 25 °C. An aliquot was removed, and the optical density (OD) determined at 405 nm using a Molecular Devices SpectraMax Plus microplate reader.

Phosphoinositide Hydrolysis- COS-7 cells transiently expressing FLAG-tagged PAR1 wild-type or mutant were plated in a fibronectin coated 24-well culture dish and grown at 37°C. Cells were labeled with 1 μCi/ml of *myo*-[^{3}H]inositol (American Radiolabeled Chemicals, St. Louis, MO) diluted in serum- and inositol-free DMEM containing 1 mg/ml BSA overnight. Cells were washed, treated with or without agonists in DMEM media containing 20 mM lithium chloride (LiCl) for 30 min at 37°C and accumulated [^{3}H]inositol phosphates (IPs) were measured as described (19).

BRET assays- COS-7 cells were transfected for 48 h, detached with Cellstripper^{TM} (Mediatech), washed with PBS, and resuspended in PBS containing 0.5 mM $MgCl_2$ abd 0.1% glucose at a density of 5 X 10^5 cells/ml. An aliquot (80 μl) of cells was added to a 96-well microplate in triplicate, and 10 μl of coelentrazine h substrate was

added at a final concentration of 5 μM. After an 8 min delay, signals were determined with a TriStar LB 941 plate reader (Berthold Biotechnologies) using two filter settings (480 nm for Rluc and 530 nm for YFP). The BRET ratio was calculated as emission at 530 nm/emission at 480 nm, and net BRET was determined by subtracting the background BRET ratio (BRET ratio from cells expressing the Rluc construct only) using MicroWIN 2000 software (Berthold Technologies). The YFP signal was determined by excitation at 485 nm, and emission was detected at 535 nm. Total luminescence was measured by integrating the signal for 1 s/well without filter selection.

RhoA Activity Assay- GST-rhotekin Rho-binding domain fusion proteins were transformed into BL21 (DE3) *Escherichia coli*; fusion proteins were induced and purified using standard techniques, and assays were conducted as previously described (15). Briefly, HeLa cells were grown in 6-well or 12-well culture plates. Cells were starved overnight and were then treated with agonist or left untreated for various times, or for 1 min with various concentrations of agonist at 37°C. Cells were lysed in buffer containing 50 mM Tris-HCl (pH 7.4), 100 mM sodium chloride, 2 mM $MgCl_2$, 1% (v/v) triton X-100, 10% (v/v) glycerol, and freshly added protease inhibitors. Equivalent amounts of lysates were used in pull-down assays with GST ctrl and GST Rhotekin-RBD bound to glutathione-Sepharose beads for 45 min at 4 °C. Beads were washed with lysis buffer, and GTP bound RhoA was eluted in 2x SDS samples buffer. Samples were resolved by SDS/PAGE, transferred to PVDF membranes, and

immunoblotted with an anti RhoA antibody. Immunoblots were developed with enhanced chemiluminescence and analyzed with ImageJ software.

Immunofluorescence Microscopy- HeLa cells stably expressing FLAG-PAR1 wild-type and mutant were plated on fibronectin coated glass coverslips in 12-well dishes. Cells were serum starved overnight and then treated with or without agonist. Cells were then placed on ice and washed with ice cold PBS, then fixed with ice cold 4% PFA for 30 min. Cells were washed with PBS then permeabilized with 0.5% (v/v) Triton X-100 in PBS for 5 min. Cells were washed then non-specific binding was blocked using 7% (v/v) fetal bovine serum in PBS for 30 min. After blocking cells were washed with PBS and stress fibers stained with Phalloidin-TRITC diluted 1:1,000 in 7% (v/v) fetal bovine serum in PBS for 1 h. Cells were washed multiple times and then mounted and processed for confocal microscopy as described (18). Images were collected using an Olympus DSU spinning disk confocal microscope configured with a PlanApo 60x oil objective and a Hamamatsu ORCA-ER digital camera. Fluorescent images of X-Y sections at 0.28 μm were collected using Intelligent Imaging Innovations Slidebook 4.2 software and composite configured using Adobe Photoshop CS3. For each of three experiments four fields of cells for each condition were imaged and a mask created and mean fluorescence obtained using Slidebook 4.2 software.

Data Analysis- Data were analyzed using Prism software, and statistical analysis was determined using the Prism data analysis tool as noted. Statistical analysis was determined by performing student t-test, one-way ANOVA and Dunnett multiple comparison test, or two-way ANOVA and Bonferroni post-tests.

4.4 Results

4.4.1 PAR1 NA ECL2 mutant associates with more $G\alpha_q$ under basal conditions compared to wild-type

We previously showed that a mutant of PAR1 incapable of being modified by N-linked glycosylation at the second extracellular loop (NA ECL2) displays enhanced PI hydrolysis (**see Fig. 2.8 and Fig. 3.1)**. The PI hydrolysis is PLC and $G\alpha_q$-dependent (**see Fig. 3.6 and 3.7**) and the enhanced signaling by mutant receptor is not due to differences in thrombin cleavage, desensitization, or constitutive activation (**see Fig. 2.7, Fig. 3.2, and Fig. 3.3 respectively**). To further explore $G\alpha_q$ interaction with PAR1 wild-type and NA ECL2 mutant we examined the capacity of the receptor to form a complex with $G\alpha_q$. HeLa cells stably expressing similar amounts of PAR1 wild-type and NA ECL2 mutant at the cell surface were co-transfected with varying amounts of HA-tagged $G\alpha_q$ and association was examined by co-immunoprecipitation. Cell surface ELISA indicates that expression levels of PAR1 wild-type and NA ECL2 mutant were unaltered by overexpression of $G\alpha_q$ (**Fig. 4.1A**). We did detect an increase in the amount of $G\alpha_q$ associated with receptor over

increasing HA-Gα_q amounts transfected, for both the wild-type and NA ECL2 mutant. Surprisingly, at 3.0 μg HA-Gα_q transfected there was a significantly larger signal for Gα_q association with the NA ECL2 mutant compared to wild-type (**Fig. 4.1B, C**).

We next determined whether there were any differences in Gα_q association after thrombin stimulation. HeLa cells were co-transfected with 3.0 μg HA-Gα_q and the amount of Gα_q associated with receptor after 1 min thrombin stimulation was determined by co-immunoprecipitation. We were able to replicate the unstimulated results seen previously as NA ECL2 mutant gave a larger signal compared to wild-type. Interestingly, the wild-type PAR1 displayed a higher signal upon thrombin stimulation, while there was no change in the NA ECL2 mutant (**Fig. 4.1D, E)**. These results suggest a difference in PAR1 wild-type versus NA ECL2 mutant interaction with Gα_q protein.

4.4.2 PAR1 NA ECL2 enhanced PI hydrolysis and basal Gα_q association are not cell type specific

To ensure that PAR1 NA ECL2 mutant enhanced Gα_q coupling and Gα_q associated PI hydrolysis signaling was not a cell type specific phenomena we performed additional experiments in COS-7 cells. We first determined whether PAR1 was glycosylated in COS-7 similar to HeLa and Endothelial cells (**see Fig. 2.2 and 2.6**). COS-7 cells transiently transfected with FLAG-tagged PAR1 wild-type were lysed and a similar protocol as we used for HeLa cells was performed to confirm

PAR1 glycosylation (**Fig. 4.2A**). Next, we assayed for PI hydrolysis in cells transiently transfected to express similar surface levels of either FLAG-tagged PAR1 wild-type or NA ECL2 mutant (**Fig. 4.2B**). COS-7 cells were labeled with *myo*-[^{3}H]inositol and incubated with thrombin for 30 min at 37ºC and the accumulation of total [^{3}H]inositol phosphates (IPs) were measured. After 30 min of thrombin stimulation, an ~3-fold increase in PI hydrolysis was detected in cells expressing wild-type PAR1, whereas a significantly greater ~4.5-fold increase in signaling was observed in cells expressing the PAR1 NA ECL2 mutant (**Fig. 4.2C**). Consistent with a marked increase in PI hydrolysis, PAR1 NA ECL2 also displayed a greater capacity to assemble with $G\alpha_q$ compared to wild-type receptor in COS-7 cells (**Fig. 4.2D,E**). These data suggest that PAR1 lacking N-linked glycosylation at ECL2 stabilizes a receptor conformation that preferentially preassembles with $G\alpha_q$ and exhibits a greater efficiency to couple to $G\alpha_q$ signaling effectors following activation.

4.4.3 PAR1 wild-type and NA ECL2 mutant associate with $G\alpha_i$ in a similar manner

PAR1 is promiscuous and couples to multiple heterotrimeric G protein subtypes including G_q, G_i and $G_{12/13}$ even in the same cell (2, 8). To examine whether N-linked glycosylation of PAR1 at ECL2 functions globally to affect PAR1 coupling to other heterotrimeric G protein subtypes, we examined association with $G\alpha_i$ using bioluminescence resonance energy transfer (BRET) in living cells. To assess PAR1

association with $G\alpha_i$ by BRET a PAR1 wildtype and NA ECL2 mutant fused to YFP at the C-terminus and a $G\alpha_i$ construct containing Rluc inserted within the helical domain were utilized. PAR1 wild-type and NA ECL2 mutant fused to YFP are expressed similarly, assessed by cell surface ELISA (**Fig. 4.3A**) and western blot (**Fig. 4.3B**) and PAR1-YFP signals normally (20). We initially examined the capacity of PAR1 wild-type and NA ECL2 mutant to specifically associate with $G\alpha_i$ using a BRET saturation assay. COS-7 cells were transfected with a constant amount of $G\alpha_i$-Rluc and increasing amounts of wild-type or NA ECL2 PAR1-YFP and the net BRET signal was determined. As expected, increasing amounts of PAR1-YFP with a fixed amount of $G\alpha_i$-Rluc resulted in a corresponding increase in the net BRET signal that reached a plateau (**Fig. 4.3C**), indicating that $G\alpha_i$-Rluc and PAR1-YFP interaction is specific. Intriguingly, increased expression of PAR1 NA ECL2-YFP with a constant amount of $G\alpha_i$-Rluc also yielded a hyperbolic increase in the net BRET signal (**Fig. 4.3C**). In addition, PAR1-YFP and NA ECL2-YFP coexpressed with $G\alpha_i$-Rluc yielded similar maximal BRET responses and $BRET_{50}$ values (**Fig. 4.3D**), suggesting that $G\alpha_i$ interacts with PAR1 wild-type and NA ECL2 in a similar manner. Thus, in contrast to $G\alpha_q$, N-linked glycosylation does not affect PAR1 basal association with $G\alpha_i$ protein.

4.4.4 $G\alpha_i$ association and recruitment after thrombin stimulation is similar in PAR1 wild-type and NA ECL2 mutant

We next examined whether N-linked glycosylation affected the kinetics of PAR1-Gα_i protein interaction after thrombin stimulation using BRET. COS-7 cells expressing comparable amounts of PAR1-YFP or NA ECL2-YFP and Gα_i-Rluc (**Fig. 4.4A, *inset***) were treated with or without 10 nM thrombin for various times at 37ºC and the net BRET signal was determined. In cells expressing PAR1-YFP and Gα_i-Rluc, thrombin caused a rapid and transient increase in net BRET that peaked at approximately 1 min and returned to basal levels after several minutes of agonist stimulation (**Fig. 4.4A**). These findings indicate that agonist induces a change in PAR1-Gα_i coupling that is efficiently uncoupled within minutes of activation as reported previously (20). Interestingly, thrombin-activation of PAR1 NA ECL2-YFP resulted in a similar rapid and transient increase in the net BRET response that nearly overlapped with wild-type PAR1-YFP (**Fig. 4.4A**), suggesting that activated PAR1-Gα_i coupling is not regulated by N-linked glycosylation. To determine whether the change in net BRET induced by thrombin correlates with recruitment of Gα_i we examined PAR1 association with Gα_i by co-immunoprecipitation using the same constructs and conditions. To ensure that overexpression of Gα_i-Rluc didn't affect surface expression an ELISA was run in parallel with the co-immunoprecipitation experiments (**Fig. 4.4C, *inset***). In the absence of agonist, both PAR1-YFP and NA ECL2-YFP mutant displayed a modest association with Gα_i-Rluc compared to control cells (**Fig. 4.4B, C**). Whereas incubation with thrombin caused a significant ~4-fold increase in Gα_i-Rluc association with both activated PAR1 wild-type and NA ECL2 mutant (**Fig. 4.4B, C**). At face value, these data suggest that activated PAR1 coupling

to $G\alpha_i$ is insensitive to the glycosylation status of the receptor and is likely regulated by distinct molecular determinants compared to PAR1-$G\alpha_q$ coupling.

4.4.5 PAR1 NA ECL2 associates with $G\alpha_{12}$ to a lesser degree than PAR1 wild-type

To determine whether N-linked glycosylation preferentially regulates PAR1 coupling to $G\alpha_q$ signaling only, we examined PAR1 association with $G\alpha_{12/13}$ family proteins by BRET and co-immunoprecipitation experiments. PAR1 is known to signal through $G\alpha_{12/13}$ to stimulate RhoA signaling in multiple cell types (2, 8, 21). We first examined wild-type PAR1-YFP and NA-ECL2-YFP association with $G\alpha_{12}$-Rluc in COS-7 cells expressing equivalent amounts of receptor together with $G\alpha_{12}$-Rluc. Unlike $G\alpha_i$ and PAR1-YFP which resulted in a basal net BRET value of ~0.12, co-transfection of PAR1-YFP constructs and $G\alpha_{12}$-Rluc resulted in a significantly lower basal net BRET of ~0.007 (**Fig. 4.5A**), the lower $G\alpha_{12}$-Rluc versus $G\alpha_i$-Rluc basal net BRET is consistent with previously published results (22). However, upon activation of wild-type PAR1 by thrombin there was a moderate increase net BRET signal. While there was no statistical difference in the BRET data generated for the $G\alpha_{12}$-Rluc construct there was clearly a trend for wild-type PAR1 induced BRET values to be larger after thrombin treatment compared to buffer only controls, which was not observed with the PAR1 NA ECL2 mutant. These results suggest that the wild-type PAR1 may interact with $G\alpha_{12}$-Rluc differently than the glycosylation-deficient NA ECL2 mutant.

To further explore $G\alpha_{12}$ interaction with PAR1 wild-type and NA ECL2 mutant we examined receptor association with $G\alpha_{12}$ by co-immunoprecipitation. HeLa cells stably expressing similar amounts of FLAG-tagged PAR1 wild-type and NA ECL2 mutant at the cell surface were co-transfected with varying amounts of EE-tagged $G\alpha_{12}$ and association was examined by co-immunoprecipitation. Cell surface ELISA indicates that PAR1 wild-type and NA ECL2 mutant expression is comparable in $G\alpha_{12}$ expressing cells (**Fig. 4.5B**). We observed an increase in the amount of $G\alpha_{12}$ associated with receptor as the amounts of $G\alpha_{12}$ were increased for both the PAR1 wild-type and NA ECL2 mutant. However, at 0.2 μg transfected there was a smaller signal for $G\alpha_{12}$ association with the PAR1 NA ECL2 mutant compared to wild-type receptor (**Fig. 4.1C, D**). In addition, there was a difference in the apparent amount of $G\alpha_{12}$ associated with PAR1 wild-type versus NA ECL2 mutant after thrombin treatment. These findings support the idea that PAR1 NA ECL2 mutant may exhibit a distinct conformation compared to wild-type receptor that interacts differently with distinct heterotrimeric G protein subtypes.

4.4.6 PAR1 NA ECL2 associates with $G\alpha_{13}$ to a lesser degree than PAR1 wild-type

To next assessed whether $G\alpha_{13}$ also differentially associates with PAR1 wild-type versus NA ECL2 mutant. The basal net BRET was significantly lower than that of the $G\alpha_i$ experiments. Moreover, activation of PAR1 wild-type elicited no

significant change in net BRET detected between PAR1-YFP-$G\alpha_{13}$-Rluc consistent with previously published data (22), whereas activation of PAR1 NA ECL2-YFP resulted in a modest but significant increase in the net BRET signal after prolonged agonist stimulation (**Fig. 4.6A**). These results could be indicative of the NA ECL2 mutant interacting with $G\alpha_{13}$ in a different manner than wild-type receptor. To confirm that $G\alpha_{13}$ association with NA ECL2 mutant is different compared to wild-type we performed co-immunoprecipitation experiments. We ensured that surface levels of PAR1 wild-type and NA ECL2 were similar in cells overexpressing of EE-tagged $G\alpha_{13}$ protein (**Fig. 4.6B**). Interesting, we found that PAR1 NA ECL2 mutant displayed lower signal for association with $G\alpha_{13}$ compared to wild-type receptor (**Fig. 4.6C,D**). Similar to $G\alpha_q$, N-linked glycosylation appears to modulate PAR1 association with $G\alpha_{12/13}$ proteins.

4.4.7 $G\alpha_{12/13}$ associated RhoA activation is diminished in the PAR1 NA ECL2 mutant compared to wild-type receptor

To determine whether N-linked glycosylation functions to regulate PAR1-promoted $G\alpha_{12/13}$ effector signaling, we examined activation of endogenous RhoA in HeLa cells. HeLa cells expressing similar amounts of FLAG-tagged PAR1 wild-type or NA ECL2 on the cell surface (**Fig. 4.7A, *inset*)** were incubated with thrombin for various times at 37°C and activation of RhoA was determined using GST-Rhotekin pull-down assays as we described (14, 15). In cells expressing PAR1 wild-type,

thrombin-induced a rapid and robust increase in RhoA signaling at 2.5 min, which substantially declined after 15 min of agonist stimulation. In striking contrast, activation of PAR1 NA ECL2 with thrombin resulted in a significantly weaker RhoA signaling response compared to wild-type receptor examined over a similar time course (**Fig. 4.7A**). To assess whether there were any differences in signaling through $G\alpha_{12}$ versus $G\alpha_{13}$ for wild-type and NA ECL2 mutant we employed siRNAs to specifically knockdown either $G\alpha_{12}$ or $G\alpha_{13}$ proteins. We found that RhoA activation in $G\alpha_{12}$, $G\alpha_{13}$, or $G\alpha_{12/13}$ knockdown cells was completely abolished for both wild-type (**Fig. 4.7C**) and NA ECL2 mutant (**Fig. 4.7D**), indicating that both $G\alpha_{12}$ and $G\alpha_{13}$, contribute to activated PAR1 stimulated RhoA activation. Thus, thrombin-stimulated RhoA activation requires $G\alpha_{12}$ and $G\alpha_{13}$, however, PAR1 NA ECL2 mutant is less able to elicit a full $G\alpha_{12/13}$ response compared to wild-type receptor.

4.4.8 PAR1 NA ECL2 diminished RhoA activation is not due to kinetics of activation, generation of ligand, clonal or cell type differences

To further evaluate $G\alpha_{12/13}$ mediated RhoA activation by PAR1 wild-type and NA ECL2 mutant we assayed earlier times of activation, activation by the peptide agonist SFLLRN, in a different HeLa PAR1 NA ECL2 clone and COS-7 cells. Thrombin induced RhoA activation by PAR1 wild-type and NA ECL2 mutant at earlier times yielded similar results as that examined at later times, suggesting that differences in RhoA activation are not due to changes in the kinetics of effector

activation by the PAR1 wild-type versus mutant receptor (**Fig. 4.8A**). To ensure that differences observed with PAR1 wild-type and NA ECL2 mutant RhoA signaling are not due to defects in generation of the N-terminal tethered ligand, cells were stimulated with the synthetic peptide agonist SFLLRN which represents the naturally occurring tethered ligand sequence of PAR1. SFLLRN-induced a significantly greater increase of RhoA activation in cells expressing PAR1 wild-type compared to NA ECL2 mutant (**Fig. 4.8B**), whereas untransfected cells failed to elicit a response, indicating that SFLLRN-stimulated RhoA signaling is PAR1 dependent. We next assessed whether the differences in RhoA activation could be due to a clonal or cell specific phenomena. To this end we tested a different PAR1 NA ECL2 clone in HeLa cells with comparable cell surface expression to wild-type receptor (**Fig. 4.8C, *inset***) and obtained comparable results (**Fig. 4.8C**). Furthermore, PAR1 wild-type and NA ECL2 mutant expressing similar surface levels in COS-7 cells (**Fig. 4.8D, *inset***) also exhibited significant differences in RhoA activation (**Fig. 4.8D**). These results further support that idea that activated PAR1 NA ECL2 exhibits a distinct active conformation compared to wild-type receptor that facilitates differences in G protein coupling specificity.

4.4.9 EC_{50} for RhoA activation is similar in PAR1 wild-type and NA ECL2 expressing cells

We next examined whether the initial coupling of activated PAR1 wild-type

and NA ECL2 mutant to $G\alpha_{12/13}$-stimulated RhoA activation was affected. The concentration effect curves for thrombin at PAR1 wild-type and the mutant lacking N-linked glycosylation at ECL2 were determined by incubating cells with varying concentrations of thrombin for 1 min at 37°C. Interestingly, the effective concentration of thrombin to stimulate half-maximal response after agonist stimulation was similar for both PAR1 wild-type and NA ECL2 mutant (**Fig. 4.9**). However, activation of PAR1 wild-type resulted in a significantly greater increase in RhoA activation compared to NA ECL2 mutant (**Fig. 4.9**). These data suggest that N-linked glycosylation stabilizes an active PAR1 conformation that favors $G\alpha_{12/13}$ coupling and effector signaling, but is markedly less favorable and efficacious at coupling to $G\alpha_q$ signaling. Together our findings indicate that N-linked glycosylation stabilizes a unique active GPCR conformation that displays preferential signaling to distinct heterotrimeric G protein subtypes.

4.4.10 Stress fiber formation in PAR1 NA ECL2 mutant expressing cells is altered compared to PAR1 wild-type expressing cells

We next examined whether the difference in PAR1 wild-type versus NA ECL2 mutant ability to couple to $G\alpha_{12/13}$ signaling was sufficient to affect a cellular response such as stress fiber formation which is modulated by RhoA signaling (23, 24). HeLa cells stably expressing similar levels of FLAG-tagged PAR1 wild-type or NA ECL2 mutant were serum starved overnight. Cells were left untreated or were treated with 10

nM thrombin for 5 min at 37°C. After agonist stimulation cells were fixed, permeabalized, blocked and then stained for stress fibers with Phalloidin-TRITC. Unstimulated cells showed some background staining for both wild-type and NA ECL2 mutant expressing cells, however, upon stimulation with thrombin Phalloidin staining significantly increased for both receptors (**Fig. 4.10A, B**). Intriguingly, the fluorescence intensity of F-actin staining observed in thrombin treated PAR1 wild-type expressing cells was significantly different compared to thrombin treated PAR1 NA ECL2 mutant expressing cells, which suggest that differences observed between PAR1 wild-type and NA ECL2 mutant are sufficient to affect important cellular responses.

4.5 Discussion

Many GPCRs signal through multiple different G protein subtypes and non-G protein signaling pathways (5, 25, 26). The precise mechanism(s) by which a receptor is able to dictate which signaling effector it couples to and signals through remains poorly understood. One contributing factor is the nature of the activating ligand. Each ligand can interact with its receptor in a unique manner and stabilize a distinct active conformation of the receptor and promote distinct downstream signaling responses. Our knowledge of the mechanisms that control GPCR activation has evolved greatly. From the idea of simply being “on” or “off” state, to having agonist, partial agonist, and antagonist, to finally what it is now with the discovery of “biased ligands” and the ability of ligands to elicit distinct signaling profiles. The discovery of biased ligands

further supports the concept that is now generally accepted of GPCRs existing in multiple different conformations. In addition, with the first GPCR structure solved in 2000 (27) followed by the first high-resolution crystal structures of a GPCR published in 2007 (28), and additional structures in the years that followed we have learned a great deal of GPCR activation mechanisms (29, 30). Of note, is the finding that while the transmembrane domains of various GPCRs are closely related and seem to have very distinct structure, the extracellular and intracellular portions are dynamic. Thus, the dynamic portions of the GPCRs are more likely to contribute to a receptors ability to couple to multiple signaling and trafficking proteins.

In addition to being more dynamic, phosphorylation, ubiquitination, plamitoylation, glycosylation, and others modify the extracellular and intracellular domains of GPCRs. These various modifications could play a role in G protein subtype coupling and signal regulation. In one review on β_2AR ERK activation, the author comes to the conclusion that phosphorylation might regulate GPCR coupling to different G proteins (31). PAR1 phosphorylation and its affects on subtype specific coupling of G proteins have not been thoroughly studied. A recent paper on PAR1 implicated that palmitoylation may play a role in $G\alpha_q$ but not $G\alpha_{12}$ signaling through the use of an allosteric modulator (32). More studies will be required on GPCR modifications to determine their specific involvement with G protein subtype bias. We report here that N-linked glycosylation of PAR1 extracellular loop 2 affects G protein subtype coupling through the use of co-immunoprecipitation experiments, as well as, the live cell assay BRET. These results suggest that PAR1 unable to undergo N-linked

glycosylation at extracellular loop 2 may adopt a different conformation with a distinct G protein coupling profile.

To date only a handful of GPCRs have been crystallized, recently a high-resolution structure for PAR1 bound to the antagonist, vorapaxar, was published (33). The results revealed highly structured transmembrane domains with more dynamic extracellular portions. The PAR1 crystal structure and previous publications using mutagenesis and chimeras strongly suggests that the extracellular loop 2 plays an important role in ligand interactions (34-36). Interestingly, we found that a PAR1 mutant unable to undergo glycosylation at ECL2 (NA ECL2) displayed enhanced PI hydrolysis signaling after either peptide mimetic or thrombin activation (37). In addition, we report here that the PAR1 NA ECL2 mutant has a diminished ability to activate $G\alpha_{12/13}$ dependent RhoA activation (**Fig. 4.7, 4.8, and 4.9**) that leads to a difference in stress fiber formation (**Fig. 4.10**).

Our studies reveal for the first time a function for extracellular loop two N-linked glycosylation in regulation of G protein subtype coupling and signaling. We speculate that N-linked glycosylation of PAR1 influences the active conformation of the receptor following tethered ligand binding that results in less efficient coupling to G_q signaling while promoting $G\alpha_{12/13}$ signaling. Interestingly, we also observed a difference at basal G protein association, which could help explain the differences in signaling. Taken together the results found with the PAR1 NA ECL2 mutant suggests that N-linked glycosylation can influence active conformation of a GPCR and ultimately G protein biased signaling. Intriguingly, it has been shown that N-linked glycosylation of proteins can be different in various cell and tissue types (38-42),

suggesting the possibility that N-linked glycosylation may be utilized by cells to bias signaling in specific cell types. Whether this could play an important role in general signaling and GPCR biology has not been studied. Altered glycosylation status is commonly seen in cancers (43, 44) and may also be playing a role in signal regulation. Whether GPCR glycosylation in cancers influences differential signaling in metastatic versus benign tumors is an area of research that remains unexplored.

4.6 Acknowledgements

This work was supported by National Institutes of Health grant HL073328 (J. Trejo) and an American Heart Association Established Investigator Award (J. trejo). A. G. Soto was supported by a T32 NIGMS Pharmocological Sciences Training Grant. The authors have no conflict of interest to declare.

The contents of Chapter 4, in full, is in preparation: **Soto, A.G.,** Smith, T.H., and Trejo, J. (2013) An N-linked Glycosylation Switch for GPCR-G Protein Coupling Specificity. *Journal TBD*. The dissertation author was the primary investigator and author of this paper. All co-authors have given written permission for its use and the reproduction of all associated data in this dissertation.

4.7 Figures

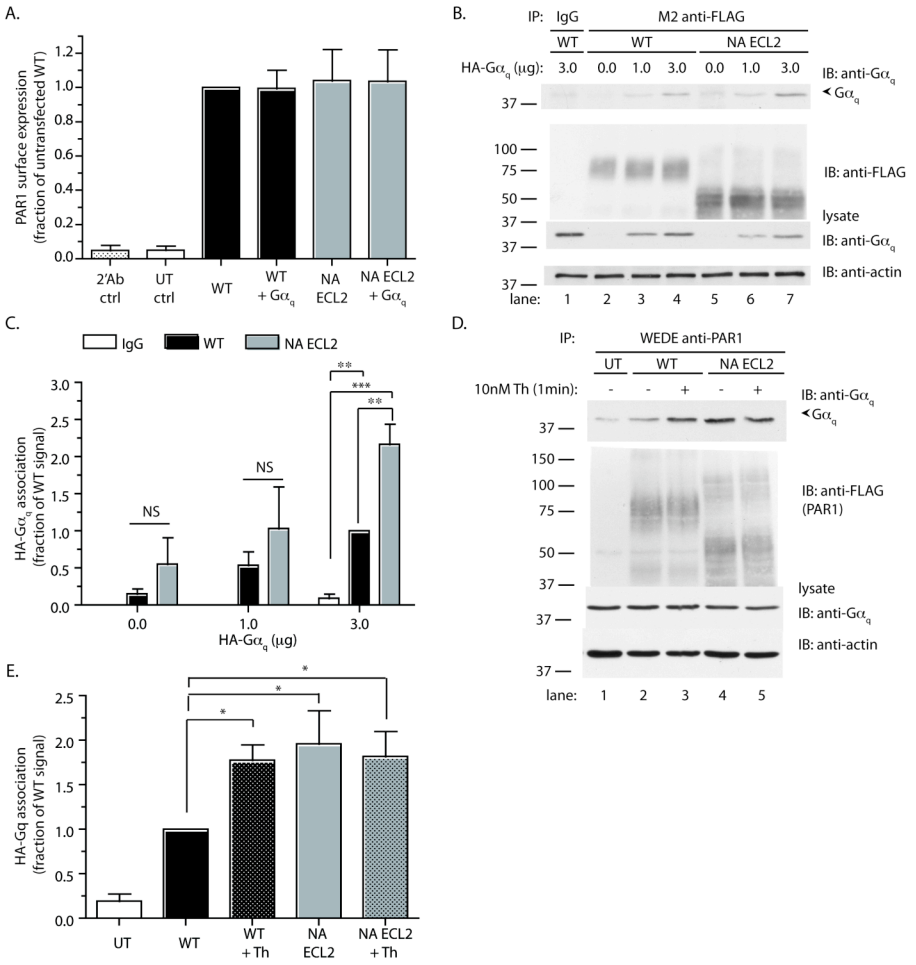

Figure 4.1: PAR1 NA ECL2 mutant associates with more Gα$_q$ under basal conditions compared to PAR1 wild-type. (*A*) HeLa cells expressing equivalent amounts of FLAG-tagged PAR1 wild-type (WT) or NA ECL2 mutant were transiently transfected with HA-tagged Gα$_q$ (HA-Gα$_q$) and surface levels determined by ELISA. The data shown (mean± S.D.; *n*=3) are expressed as the fraction of untransfected WT signal measured as the absorbance at 405 nm and are the averages from three independent experiments performed in triplicate. (*B-E)* HeLa cells stably expressing equivalent amounts of FLAG-tagged PAR1 WT or NA ECL2 mutant were transiently transfected with increasing amounts of HA-Gα$_q$ (*B,C*) or a fixed amount of HA-Gα$_q$ (*D,E*). Cells were either left untreated (*B, D lanes 1,2,and 4*) or were treated with 10 nM thrombin for 1 min (*D lanes 3 and 5*), lysed, processed and PAR1 immunoprecipitated. Immunoprecipitates were resolved by SDS-PAGE and Gα$_q$ was detected by immunoblotting with rabbit polyclonal anti-Gα$_q$ antibody. (*C*) The data shown (mean± S.D.; *n*=3) are expressed as the fraction of 3 μg HA-Gα$_q$ transfected WT signal and are from three independent experiments. The difference in Gα$_q$ association was significant (**, $p < 0.01$) by two-way ANOVA and Bonferroni post-tests. (*D*) The data shown (mean± S.E.M; *n*=4) are expressed as the fraction of 3 μg HA-Gα$_q$ transfected WT signal and are from four independent experiments (UT values from 3 experiments). The difference in Gα$_q$ association was significant (*, $p < 0.05$) by two-way ANOVA and Bonferroni post-tests.

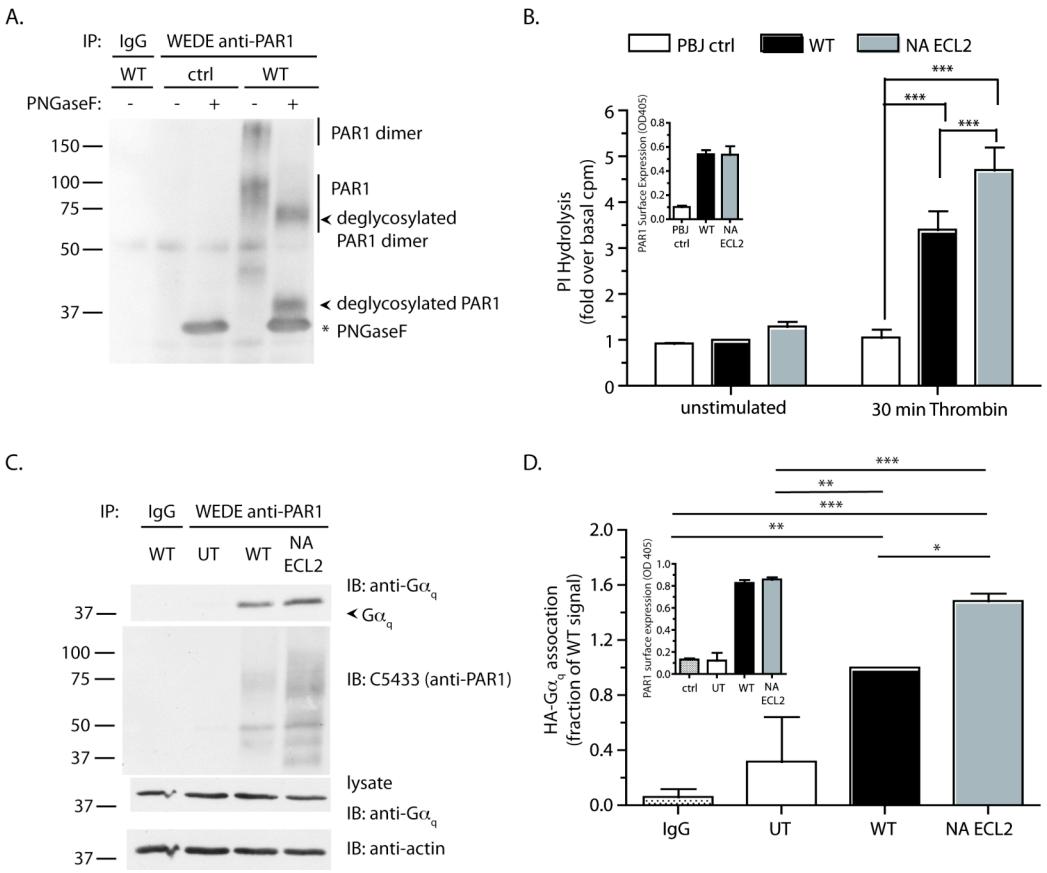

Figure 4.2: Enhanced PI hydrolysis and basal $G\alpha_q$ association of PAR1 NA ECL2 is not cell type specific. (*A*) COS-7 cells were transiently transfected with FLAG-tagged PAR1 wild-type or pCDNA (ctrl). After 48 hours cells were lysed, processed and PAR1 immunoprecipitated. Immunoprecipitates were treated with PNGaseF overnight (16 h) at 37°C. Samples were resolved by SDS-PAGE and PAR1 detected by immunoblotting with polyclonal anti-PAR1 antibody (C5433). Similar findings were observed in multiple independent experiments. (*B*) COS-7 cells transiently transfected with FLAG-tagged PAR1 WT or NA ECL2 mutant, with comparable surface expression (*B, inset*), labeled with *myo*-[^{3}H]inositol were incubated with media containing LiCl alone (unstimulated) or media containing LiCl and 10 nM thrombin for 30 min at 37°C. The amounts of accumulated [^{3}H]IPs were then measured. The data shown (mean ± S.D.; n=3) are expressed as the fold increase in [^{3}H]IPs accumulation over basal amounts and are the averages from three independent experiments performed in triplicate. The difference in agonist-induced signaling at PAR1 WT and NA ECL2 mutant was significant (***, $p < 0.001$) by two-way ANOVA and Bonferroni post-tests. (*C,D*) COS-7 cells transiently transfected with FLAG-tagged PAR1 WT or NA ECL2 mutant and HA-$G\alpha_q$, with comparable surface expression (*D, inset*), were lysed, processed and PAR1 immunoprecipitated. Immunoprecipitates were resolved by SDS-PAGE and $G\alpha_q$ was detected by immunoblotting with rabbit polyclonal anti-$G\alpha_q$ antibody. The data shown (mean± S.D.; n=3) are expressed as the fraction of WT signal and are from three independent experiments. The difference in $G\alpha_q$ association was significant (*, $p < 0.05$; **, $p < 0.01$; ***, $p < 0.001$) by one-way ANOVA and Tukey's multiple comparison post-tests.

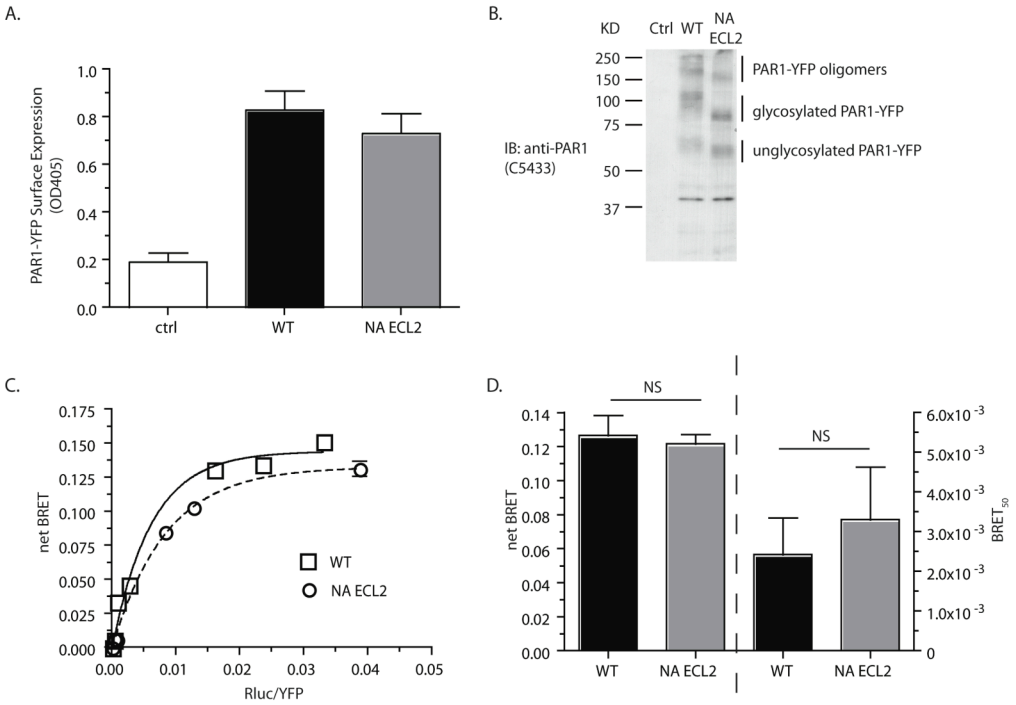

Figure 4.3: PAR1 wild-type and NA ECL2 mutant associate with Gα_i in a similar manner. (*A, B)* COS-7 cells were transiently transfected with PAR1 YFP-tagged wild-type (WT) or NA ECL2 mutant and surface expression measured by ELISA (*A*) or total protein detected by immunoblot (*B*). (*C*) Net BRET data were determined from COS-7 cells transiently transfected with a constant amount of PAR1 YFP-tagged wild-type (WT) or NA ECL2 and an increasing amount of Gα_i-Rluc protein measured in triplicate at 37°C. These data are representative of at least three independent experiments. (*D*) $BRET_{max}$ (left bars) and $BRET_{50}$ (right bars) are shown (mean ± S.D.; *n*=3) and are from three independent experiments measured in triplicate.

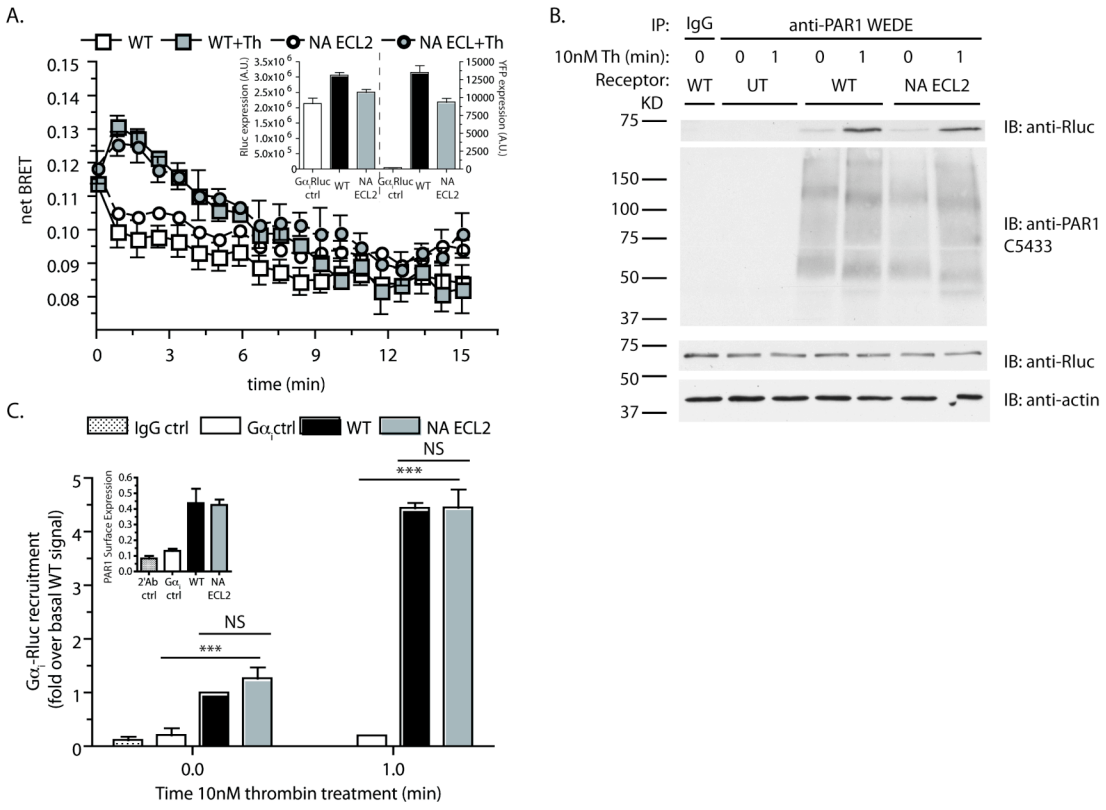

Figure 4.4: Gα$_i$ association and recruitment after thrombin stimulation are similar in PAR1 wild-type and NA ECL2 mutant. (*A*) COS-7 cells transiently transfected with similar amounts of PAR1 YFP-tagged wild-type (WT) or NA ECL2 mutant and Gα$_i$-Rluc (*A, inset*) were processed for BRET, treated with thrombin and net BRET measured in triplicate. The data shown (mean ± S.D.; *n*=3) are graphed as net BRET over time and is representative of three independent experiments. (*B, C*) COS-7 cells were transfected similar to experiments in *A* and surface expression measured by ELISA (*C, inset*) or basal and 1-minute thrombin stimulated Gα$_i$-Rluc association measured by co-immunprecipitation and immunblotting (*B, C*). Data shown (mean ± S.D.; *n*=3) are expressed as fold over basal WT signal and are from three independent experiments. The difference in Gα$_i$-Rluc association with PAR1 WT-YFP and NA ECL2-YFP mutant was significant (***, $p < 0.001$) by two-way ANOVA and Bonferroni post-tests.

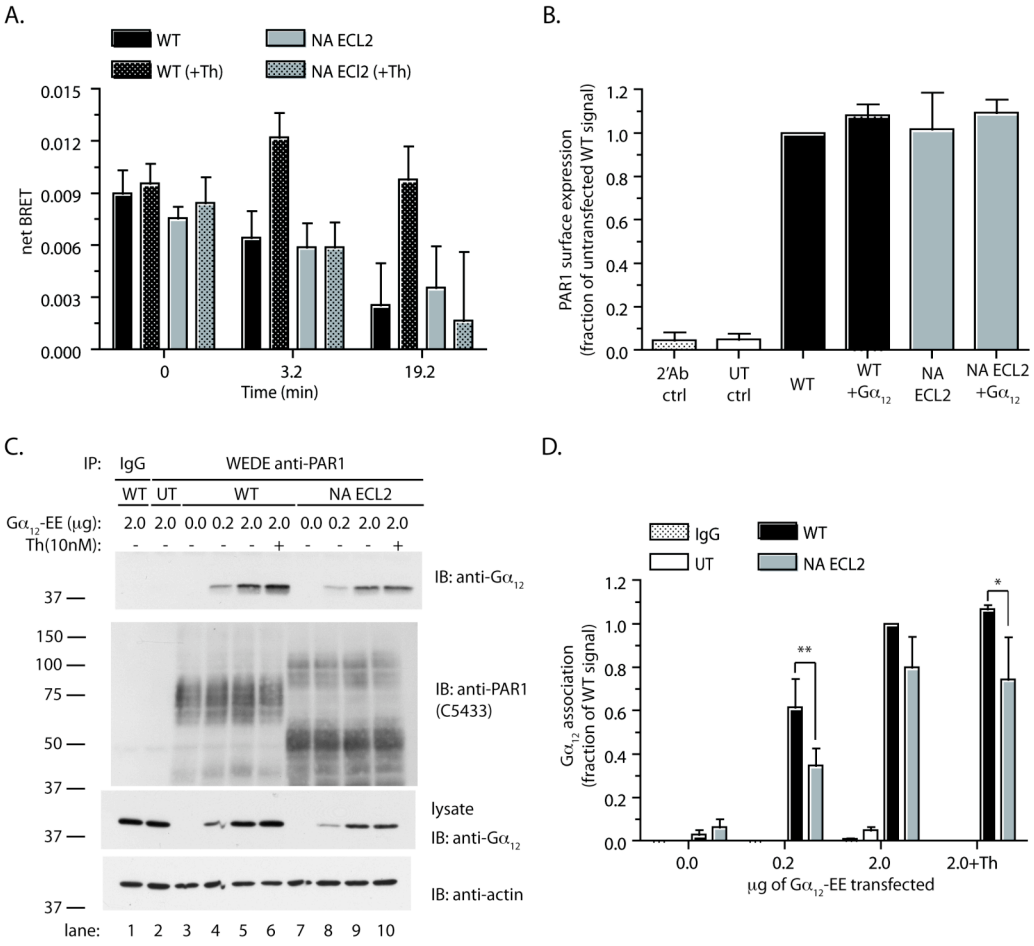

Figure 4.5: PAR1 NA ECL2 associates with Gα$_{12}$ to a lesser degree than PAR1 wild-type. (*A*) COS-7 cells transiently transfected with similar amounts of PAR1 YFP-tagged wild-type (WT) or NA ECL2 mutant and Gα$_{12}$-Rluc were processed for BRET, treated with thrombin and net BRET measured in triplicate. The data shown (mean ± S.D.; *n*=3) are graphed as net BRET and are the averages from three independent experiments performed in triplicate. (*B*) HeLa cells expressing similar amounts of FLAG-tagged PAR1 wild-type (WT) or NA ECL2 mutant were transiently transfected with Gα$_{12}$-EE and surface levels determined by ELISA. The data shown (mean± S.D.; *n*=3) are expressed as the fraction of untransfected WT signal measured as the absorbance at 405 nm and are the averages from three independent experiments performed in triplicate. (*C, D*) HeLa cells stably expressing similar amounts of FLAG-tagged PAR1 WT or NA ECL2 mutant were transiently transfected with increasing amounts of Gα$_{12}$-EE. Cells were either left untreated (*C lanes 1-5,and 7-9*) or were treated with 10 nM thrombin for 1 min (*C lanes 6 and 10*), lysed, processed and PAR1 immunoprecipitated. Immunoprecipitates were resolved by SDS-PAGE and Gα$_{12}$ was detected by immunoblotting with rabbit polyclonal anti-Gα$_{12}$ antibody. (*D*) The data shown (mean± S.D.; *n*=3) are expressed as the fraction of 2 μg Gα$_{12}$-EE transfected WT signal and are from three independent experiments. The difference in Gα$_{12}$ association was significant (*, $p < 0.05$; **, $p < 0.01$) by two-way ANOVA and Bonferroni post-tests.

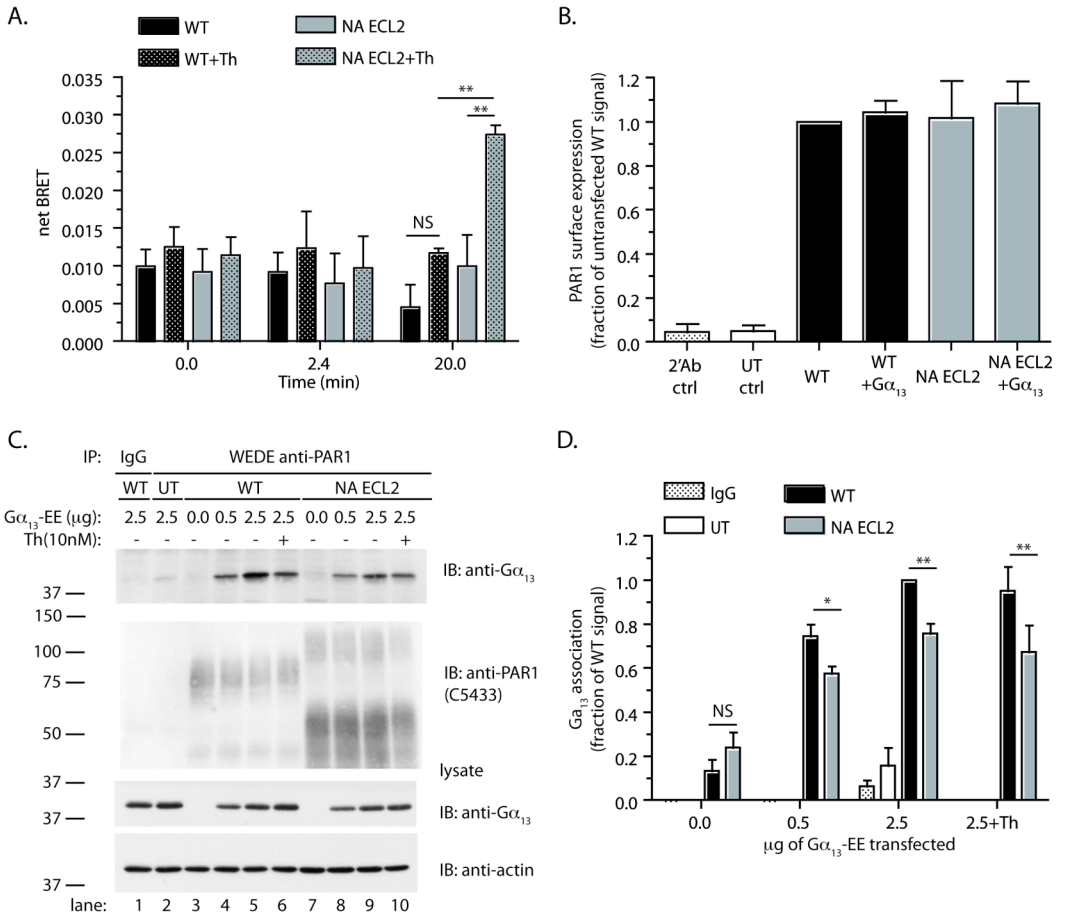

Figure 4.6: PAR1 NA ECL2 associates with Gα$_{13}$ to a lesser degree than PAR1 wild-type. (*A*) COS-7 cells transiently transfected with similar amounts of PAR1 YFP-tagged wild-type (WT) or NA ECL2 mutant and Gα$_{13}$-Rluc were processed for BRET, treated with thrombin and net BRET measured in triplicate. The data shown (mean ± S.D.; *n*=3) are graphed as net BRET and are the averages from three independent experiments performed in triplicate. The difference in Gα$_{13}$ net BRET was significant (**, $p < 0.01$) by two-way ANOVA and Bonferroni post-tests. (*B*) HeLa cells expressing similar amounts of FLAG-tagged PAR1 wild-type (WT) or NA ECL2 mutant were transiently transfected with Gα$_{13}$-EE and surface levels determined by ELISA. The data shown (mean± S.D.; *n*=3) are expressed as the fraction of untransfected WT signal measured as the absorbance at 405 nm and are the averages from three independent experiments performed in triplicate. (*C, D*) HeLa cells stably expressing similar amounts of FLAG-tagged PAR1 WT or NA ECL2 mutant were transiently transfected with increasing amounts of Gα$_{13}$-EE. Cells were either left untreated (*C lanes 1-5,and 7-9*) or were treated with 10 nM thrombin for 1 min (*C lanes 6 and 10*), lysed, processed and PAR1 immunoprecipitated. Immunoprecipitates were resolved by SDS-PAGE and Gα$_{13}$ was detected by immunoblotting with rabbit polyclonal anti-Gα$_{13}$ antibody. (*D*) The data shown (mean± S.D.; *n*=3) are expressed as the fraction of 2.5 μg Gα$_{13}$-EE transfected WT signal and are from three independent experiments. The difference in Gα$_{13}$ association was significant (*, $p < 0.05$; **, $p < 0.01$) by two-way ANOVA and Bonferroni post-tests.

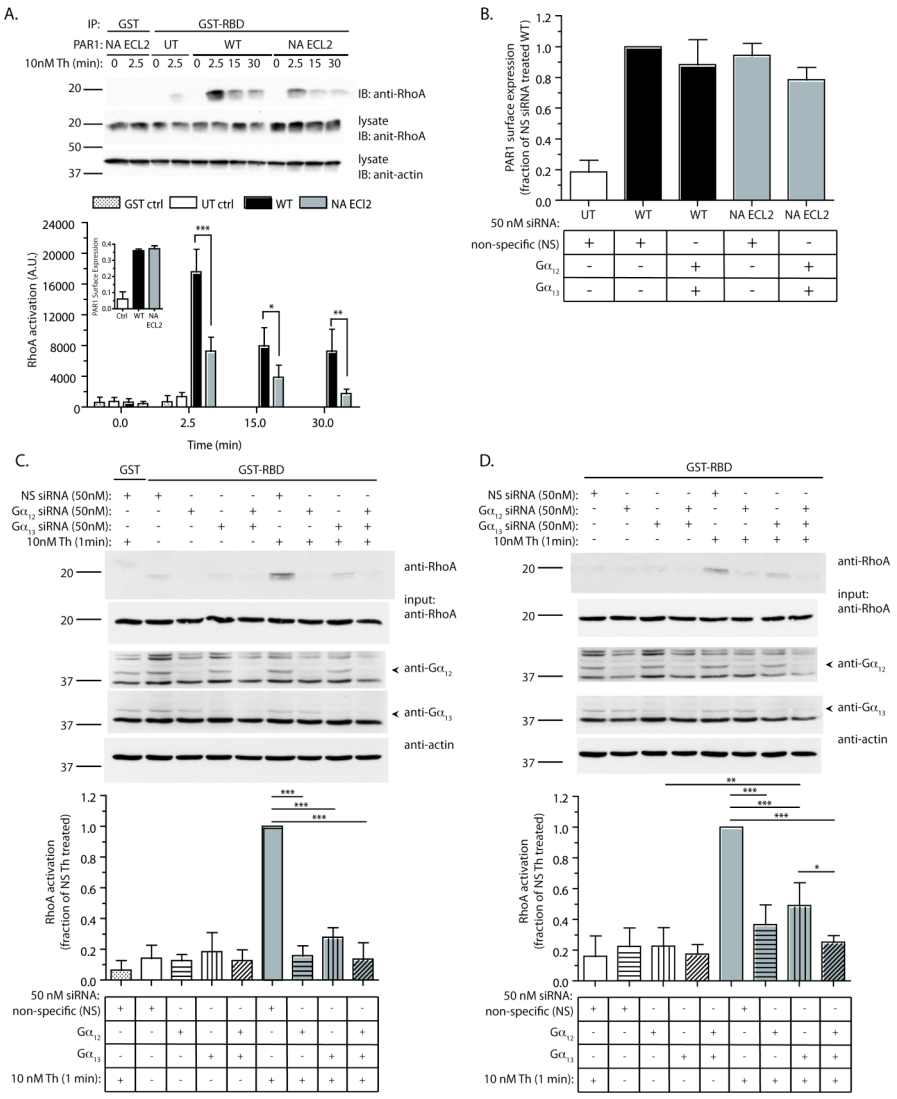

Figure 4.7: Gα$_{12/13}$ associated RhoA activation is diminished in the PAR1 NA ECL2 mutant compared to wild-type. (*A*) HeLa cells expressing similar amounts of FLAG-tagged PAR1 wild-type (WT) or NA ECL2 mutant (*A,inset*) were treated with 10 nM thrombin for various times, lysed and processed for GST-RBD pulldown. Samples were resolved by SDS-PAGE and activated RhoA was detected by immunoblotting with mouse monoclonal anti-RhoA antibody. The data shown (mean± S.D.; *n*=3) are expressed raw ImageJ signal and are from three independent experiments. The difference in RhoA activation was significant (*, p <0.05; **, $p < 0.01$; ***, $p < 0.001$) by two-way ANOVA and Bonferroni post-tests. (*B-D*) HeLa cells expressing similar amounts of FLAG-tagged PAR1 wildtype (*C*) or NA ECL2 mutant (*D*) were treated with indicated siRNA for 72 h, lysed and processed for GST-RBD pulldown. Samples were resolved by SDS-PAGE and activated RhoA was detected by immunoblotting with mouse monoclonal anti-RhoA antibody. The data shown (mean± S.D.; *n*=3) are expressed as the fraction of 1 min Thrombin (Th) treated WT signal and are from three independent experiments. The difference in RhoA activation was significant (*, p <0.05; **, $p < 0.01$; ***, $p < 0.001$) by one-way ANOVA and Tukey's multiple comparison post-tests.

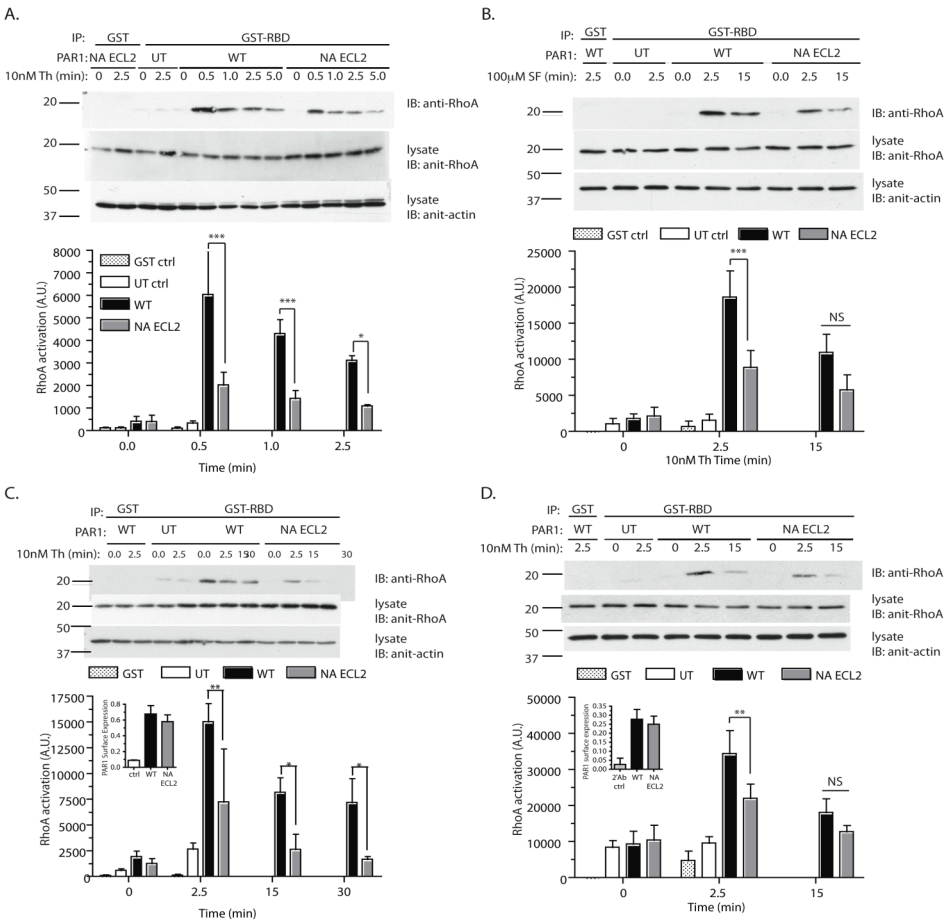

Figure 4.8: The diminished RhoA activation of PAR1 NA ECL2 is not due to kinetics of activation, generation of ligand, clonal or cell type differences. (*A, B*) HeLa cells expressing similar amounts of FLAG-tagged PAR1 wild-type (WT) or NA ECL2 mutant were treated with 10 nM thrombin (*A*) or 100 μM SFLLRN (*B*) for various times, lysed and processed for GST-RBD pulldown. Samples were resolved by SDS-PAGE and activated RhoA was detected by immunoblotting with mouse monoclonal anti-RhoA antibody. The data shown (mean± S.D.; *n*=3) are expressed as raw ImageJ signal and are from three independent experiments. The difference in RhoA activation was significant (*, $p < 0.05$; ***, $p < 0.001$) by two-way ANOVA and Bonferroni post-tests. (*C*) A different NA ECL2 clone expressing similar surface levels of receptor (*C, inset*) was used to perform similar experiments as in *A*. The data shown (mean± S.D.; *n*=3) are expressed as raw ImageJ signal and are from three independent experiments. The difference in RhoA activation was significant (*, $p < 0.05$; **, $p < 0.01$) by two-way ANOVA and Bonferroni post-tests. (*D*) COS-7 cells transiently transfected with FLAG-tagged PAR1 WT or NA ECL2 mutant, with comparable surface expression (*D, inset*), were treated with 10 nM thrombin for various times, lysed and processed for GST-RBD pulldown. Samples were resolved by SDS-PAGE and activated RhoA was detected by immunoblotting with mouse monoclonal anti-RhoA antibody. The data shown (mean± S.D.; *n*=3) are expressed as raw ImageJ signal and are from three independent experiments. The difference in RhoA activation was significant (**, $p < 0.01$) by two-way ANOVA and Bonferroni post-tests.

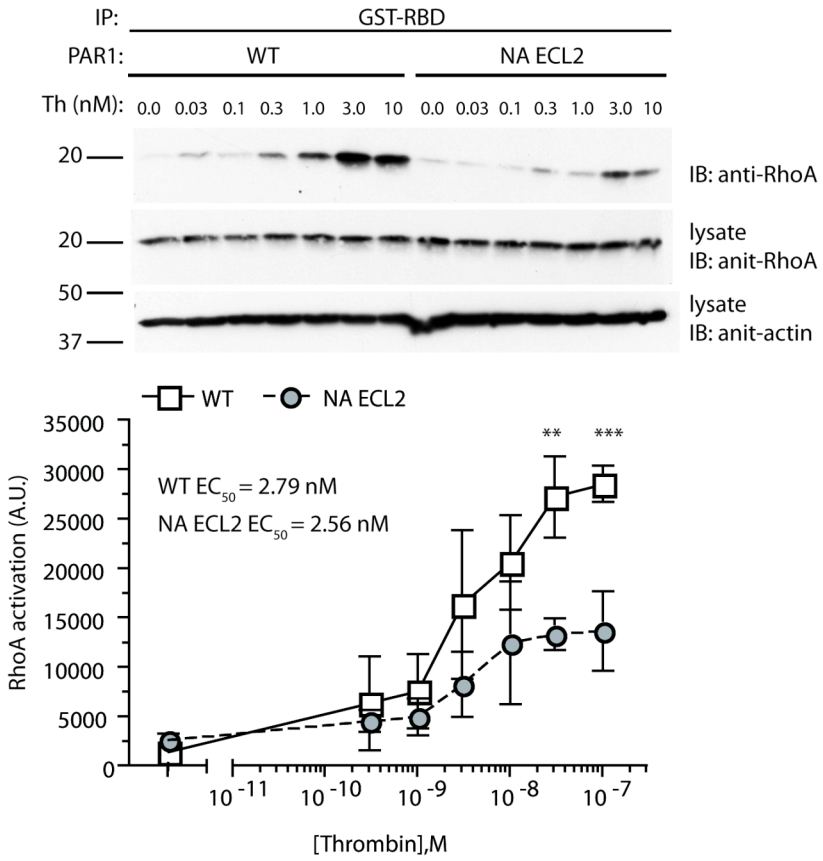

Figure 4.9: EC_{50} for RhoA activation is similar in PAR1 wild-type and NA ECL2 expressing cells. HeLa cells expressing similar amounts of FLAG-tagged PAR1 wild-type (WT) or NA ECL2 mutant were treated with increasing concentrations of thrombin for 1 min, lysed and processed for GST-RBD pulldown. Samples were resolved by SDS-PAGE and activated RhoA was detected by immunoblotting with mouse monoclonal anti-RhoA antibody. The data shown (mean± S.D.; n=3) are expressed as raw ImageJ signal and are from three independent experiments. The difference in RhoA activation was significant (**, p <0.05; ***, p < 0.001) by two-way ANOVA and Bonferroni post-tests.

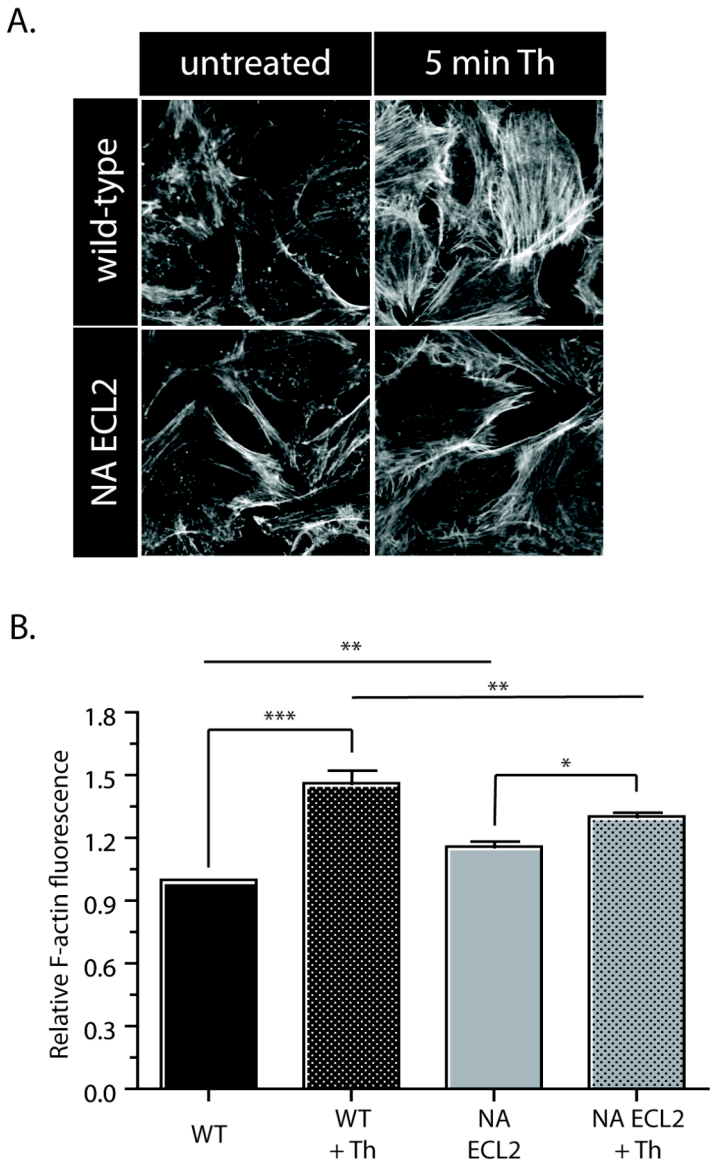

Figure 4.10: Stress fiber formation in PAR1 NA ECL2 mutant expressing cells is altered compared to PAR1 wild-type expressing cells. (*A*) HeLa cells expressing similar amounts of FLAG-tagged PAR1 wild-type (WT) or NA ECL2 mutant were left untreated or were treated with 10 nM thrombin for 5 minutes, fixed, permeabilized, stained with Phalloidin-TRITC and processed for immunofluorescence. Samples were imaged using Slidebook 4.2 and masks created and applied consistent through each slide and experiment. Shown are representative images from one experiment of multiple different experiments. (*B*) The data shown (mean± S.D.; n=3) are expressed as relative F-actin fluorescence and are the averages from 4 slides per experiment and 3 different experiments. The difference in stress fiber staining was significant (*, $p < 0.05$; **, $p < 0.01$; ***, $p < 0.001$) by two-way ANOVA and Bonferroni post-tests.

4.8 References

1. Rosenbaum, D. M., Rasmussen, S. G., and Kobilka, B. K. (2009) The structure and function of G-protein-coupled receptors. *Nature* **459**, 356-363

2. Coughlin, S. R. (2000) Thrombin signalling and protease-activated receptors. *Nature* **407**, 258-264

3. Lefkowitz, R. J., and Shenoy, S. K. (2005) Transduction of receptor signals by beta-arrestins. *Science* **308**, 512-517

4. Wei, H., Ahn, S., Shenoy, S. K., Karnik, S. S., Hunyady, L., Luttrell, L. M., and Lefkowitz, R. J. (2003) Independent beta-arrestin 2 and G protein-mediated pathways for angiotensin II activation of extracellular signal-regulated kinases 1 and 2. *Proc Natl Acad Sci U S A* **100**, 10782-10787

5. Violin, J. D., and Lefkowitz, R. J. (2007) Beta-arrestin-biased ligands at seven-transmembrane receptors. *Trends Pharmacol Sci* **28**, 416-422

6. DeWire, S. M., and Violin, J. D. (2011) Biased ligands for better cardiovascular drugs: dissecting G-protein-coupled receptor pharmacology. *Circ Res* **109**, 205-216

7. Violin, J. D., DeWire, S. M., Yamashita, D., Rominger, D. H., Nguyen, L., Schiller, K., Whalen, E. J., Gowen, M., and Lark, M. W. (2010) Selectively engaging beta-arrestins at the angiotensin II type 1 receptor reduces blood pressure and increases cardiac performance. *J Pharmacol Exp Ther* **335**, 572-579

8. Coughlin, S. R. (2005) Protease-activated receptors in hemostasis, thrombosis and vascular biology. *J Thromb Haemost* **3**, 1800-1814

9. Stearns-Kurosawa, D. J., Kurosawa, S., Mollica, J. S., Ferrell, G. L., and Esmon, C. T. (1996) The endothelial cell protein C receptor augments protein C activation by the thrombin-thrombomodulin complex. *Proc Natl Acad Sci U S A* **93**, 10212-10216

10. Taylor, F. B., Jr., Peer, G. T., Lockhart, M. S., Ferrell, G., and Esmon, C. T. (2001) Endothelial cell protein C receptor plays an important role in protein C activation in vivo. *Blood* **97**, 1685-1688

11. Griffin, J. H., Zlokovic, B. V., and Mosnier, L. O. (2012) Protein C anticoagulant and cytoprotective pathways. *Int J Hematol* **95**, 333-345

12. Schuepbach, R. A., Madon, J., Ender, M., Galli, P., and Riewald, M. (2012) Protease-activated receptor-1 cleaved at R46 mediates cytoprotective effects. *J Thromb Haemost* **10**, 1675-1684

13. Niessen, F., Furlan-Freguia, C., Fernandez, J. A., Mosnier, L. O., Castellino, F. J., Weiler, H., Rosen, H., Griffin, J. H., and Ruf, W. (2009) Endogenous EPCR/aPC-PAR1 signaling prevents inflammation-induced vascular leakage and lethality. *Blood* **113**, 2859-2866

14. Soh, U. J., and Trejo, J. (2011) Activated protein C promotes protease-activated receptor-1 cytoprotective signaling through beta-arrestin and dishevelled-2 scaffolds. *Proc Natl Acad Sci U S A* **108**, E1372-1380

15. Russo, A., Soh, U. J., Paing, M. M., Arora, P., and Trejo, J. (2009) Caveolae are required for protease-selective signaling by protease-activated receptor-1. *Proc Natl Acad Sci U S A* **106**, 6393-6397

16. Bourgognon, J. M., Schiavon, E., Salah-Uddin, H., Skrzypiec, A. E., Attwood, B. K., Shah, R. S., Patel, S. G., Mucha, M., John Challiss, R. A., Forsythe, I. D., and Pawlak, R. (2012) Regulation of neuronal plasticity and fear by a dynamic change in PAR1-G protein coupling in the amygdala. *Mol Psychiatry*

17. Paing, M. M., Johnston, C. A., Siderovski, D. P., and Trejo, J. (2006) Clathrin adaptor AP2 regulates thrombin receptor constitutive internalization and endothelial cell resensitization. *Mol Cell Biol* **26**, 3231-3242

18. Trejo, J., Altschuler, Y., Fu, H. W., Mostov, K. E., and Coughlin, S. R. (2000) Protease-activated receptor-1 down-regulation: a mutant HeLa cell line suggests novel requirements for PAR1 phosphorylation and recruitment to clathrin-coated pits. *J Biol Chem* **275**, 31255-31265

19. Paing, M. M., Stutts, A.B., Kohout, T.A., Lefkowitz, R.J., and Trejo, J. (2002) beta-arrestins regulate protease-activated receptor-1 desensitization but not internalization or down-regulation. *The Journal of Biological Chemistry* **277**, 1292-1300

20. Ayoub, M. A., Maurel, D., Binet, V., Fink, M., Prezeau, L., Ansanay, H., and Pin, J. P. (2007) Real-time analysis of agonist-induced activation of protease-activated receptor 1/Galphai1 protein complex measured by bioluminescence resonance energy transfer in living cells. *Mol Pharmacol* **71**, 1329-1340

21. Martin, C. B., Mahon, G. M., Klinger, M. B., Kay, R. J., Symons, M., Der, C. J., and Whitehead, I. P. (2001) The thrombin receptor, PAR-1, causes transformation by activation of Rho-mediated signaling pathways. *Oncogene* **20**, 1953-1963

22. Ayoub, M. A., Trinquet, E., Pfleger, K. D., and Pin, J. P. (2010) Differential association modes of the thrombin receptor PAR1 with Galphai1, Galpha12, and beta-arrestin 1. *FASEB J* **24**, 3522-3535

23. Macfarlane, S. R., Seatter, M. J., Kanke, T., Hunter, G. D., and Plevin, R. (2001) Proteinase-activated receptors. *Pharmacol Rev* **53**, 245-282

24. Ruiz-Loredo, A. Y., Lopez, E., and Lopez-Colome, A. M. (2011) Thrombin promotes actin stress fiber formation in RPE through Rho/ROCK-mediated MLC phosphorylation. *J Cell Physiol* **226**, 414-423

25. Luttrell, L. M., and Kenakin, T. P. (2011) Refining efficacy: allosterism and bias in G protein-coupled receptor signaling. *Methods Mol Biol* **756**, 3-35

26. Maudsley, S., Patel, S. A., Park, S. S., Luttrell, L. M., and Martin, B. (2012) Functional signaling biases in G protein-coupled receptors: Game Theory and receptor dynamics. *Mini Rev Med Chem* **12**, 831-840

27. Palczewski, K., Kumasaka, T., Hori, T., Behnke, C. A., Motoshima, H., Fox, B. A., Le Trong, I., Teller, D. C., Okada, T., Stenkamp, R. E., Yamamoto, M., and Miyano, M. (2000) Crystal structure of rhodopsin: A G protein-coupled receptor. *Science* **289**, 739-745

28. Cherezov, V., Rosenbaum, D. M., Hanson, M. A., Rasmussen, S. G., Thian, F. S., Kobilka, T. S., Choi, H. J., Kuhn, P., Weis, W. I., Kobilka, B. K., and Stevens, R. C. (2007) High-resolution crystal structure of an engineered human beta2-adrenergic G protein-coupled receptor. *Science* **318**, 1258-1265

29. Jacobson, K. A., and Costanzi, S. (2012) New insights for drug design from the X-ray crystallographic structures of G-protein-coupled receptors. *Mol Pharmacol* **82**, 361-371

30. Zhao, Q., and Wu, B. L. (2012) Ice breaking in GPCR structural biology. *Acta Pharmacol Sin* **33**, 324-334

31. Lefkowitz, R. J., Pierce, K. L., and Luttrell, L. M. (2002) Dancing with different partners: protein kinase a phosphorylation of seven membrane-spanning receptors regulates their G protein-coupling specificity. *Mol Pharmacol* **62**, 971-974

32. Swift, S., Leger, A. J., Talavera, J., Zhang, L., Bohm, A., and Kuliopulos, A. (2006) Role of the PAR1 receptor 8th helix in signaling: the 7-8-1 receptor activation mechanism. *J Biol Chem* **281**, 4109-4116

33. Zhang, C., Srinivasan, Y., Arlow, D. H., Fung, J. J., Palmer, D., Zheng, Y., Green, H. F., Pandey, A., Dror, R. O., Shaw, D. E., Weis, W. I., Coughlin, S. R., and Kobilka, B. K. (2012) High-resolution crystal structure of human protease-activated receptor 1. *Nature* **492**, 387-392

34. Gerszten, R. E., Chen, J., Ishi, M., Ishi, K., Wang, L., Nanevicz, T., Turck, C.W., Vu, T.K.H., and Coughlin, S.R. (1994) Specificty of the thrombin receptor for agonist peptide is defined by its extracellular surface. *Nature* **368**, 648-651

35. Lerner, D. J., Chen, M., Tram, T., and Coughlin, S. R. (1996) Agonist recognition by proteinase-activated receptor 2 and thrombin receptor. Importance of extracellular loop interactions for receptor function. *J Biol Chem* **271**, 13943-13947

36. Nanevicz, T., Ishii, M., Wang, L., Chen, M., Chen, J., Turck, C. W., Cohen, F. E., and Coughlin, S. R. (1995) Mechanisms of thrombin receptor agonist specificity. Chimeric receptors and complementary mutations identify an agonist recognition site. *J Biol Chem* **270**, 21619-21625

37. Soto, A. G., and Trejo, J. (2010) N-linked glycosylation of protease-activated receptor-1 second extracellular loop: a critical determinant for ligand-induced receptor activation and internalization. *J Biol Chem* **285**, 18781-18793

38. West, M. B., Segu, Z. M., Feasley, C. L., Kang, P., Klouckova, I., Li, C., Novotny, M. V., West, C. M., Mechref, Y., and Hanigan, M. H. (2010) Analysis of site-specific glycosylation of renal and hepatic gamma-glutamyl transpeptidase from normal human tissue. *J Biol Chem* **285**, 29511-29524

39. Serrano, R., Barrenetxe, J., Orbe, J., Rodriguez, J. A., Gallardo, N., Martinez, C., Andres, A., and Paramo, J. A. (2009) Tissue-specific PAI-1 gene expression and glycosylation pattern in insulin-resistant old rats. *Am J Physiol Regul Integr Comp Physiol* **297**, R1563-1569

40. Henkel, W., Rauterberg, J., and Stirtz, T. (1976) Isolation of a crosslinked cyanogen-bromide peptide from insoluble rabbit collagen. Tissue differences in hydroxylation and glycosylation of the crosslink. *Eur J Biochem* **69**, 223-231

41. Rougon, G., Deagostini-Bazin, H., Hirn, M., and Goridis, C. (1982) Tissue- and developmental stage-specific forms of a neural cell surface antigen linked to differences in glycosylation of a common polypeptide. *EMBO J* **1**, 1239-1244

42. Davies, L. R., and Varki, A. (2013) Why Is N-Glycolylneuraminic Acid Rare in the Vertebrate Brain? *Top Curr Chem*

43. Alley, W. R., Jr., Vasseur, J. A., Goetz, J. A., Svoboda, M., Mann, B. F., Matei, D. E., Menning, N., Hussein, A., Mechref, Y., and Novotny, M. V. (2012) N-linked glycan structures and their expressions change in the blood sera of ovarian cancer patients. *J Proteome Res* **11**, 2282-2300

44. Xiao, Y. P., Morice, A. H., Compton, S. J., and Sadofsky, L. (2011) N-linked glycosylation regulates human proteinase-activated receptor-1 cell surface expression and disarming via neutrophil proteinases and thermolysin. *J Biol Chem* **286**, 22991-23002

Chapter 5:

Conclusions and Discussion

Protease-Activated Receptor 1 (PAR1) was discovered nearly 20 years ago in a search for cell surface receptors that confer thrombin signaling on human platelets (1). PAR1 is a G-protein coupled receptor (GPCR) that has a unique mode of activation, functions in many aspects of vascular biology and is an important drug target (2, 3). Previous studies revealed that the second extracellular loop of PAR1 is a critical determinant for receptor-specific and species-specific ligand recognition as well as receptor activation (4-6). Additional studies on other GPCRs have confirmed the importance of the second extracellular loop in ligand interactions and receptor activation (7, 8). An interesting feature of the second extracellular loop of PAR1 is the inclusion of two consensus sites for N-linked glycosylation. Prior to the studies presented in this dissertation, the function of PAR1 N-linked glycosylation was largely unknown. Given the existence of N-linked glycosylation sites in the second extracellular loop of PAR1, we sought to examine the hypothesis that distinct PAR1 N-linked glycosylation regulates receptor signaling. I first conducted work to characterize PAR1 N-linked glycosylation by determining which sites were modified. Next, I utilized a PAR1 mutant which has the two critical asparagine residues (N) mutated to alanine (A) in the two extracellular loop two N-linked glycosylation consensus sites (NA ECL2). I used this mutant to examine the role of PAR1 N-linked glycosylation in signaling and trafficking. The conclusions and discussion of the work performed are briefly discussed in the following sections.

5.1 PAR1 is modified by N-linked glycosylation at both its N-terminus and second extracellular loop with complex glycans

Previous to this dissertation, the only experiments that had been performed on PAR1 N-linked glycosylation demonstrated that the receptor was modified by N-linked glycans (9) and that global disruption of N-linked glycosylation with tunicamycin caused a drastic reduction in surface expression (10). There were no detailed studies using mutagenesis to determine which of the five consensus sites contributed to the glycosylation status of PAR1. Thus, I generated PAR1 mutants lacking each of the N-linked glycosylation sites and determined that the main sites of receptor glycosylation were within the second extracellular loop (**Fig. 2.4**). Through the course of my thesis work I was able to confirm that the PAR1 NA ECL2 mutant consistently displayed a significant shift in apparent weight by immunoblot in multiple cell lines, including HeLa, COS-7, HEK293, and mouse knockout lung fibroblasts. Further characterization of PAR1 glycosylation was performed using different glycosidases to determine the nature of the glycosylation (**Fig. 2.6**). The results support the conclusion that PAR1 wild-type receptor, NA ECL2 mutant, and a mutant with the three N-terminus sites mutated (NA NTer) are modified with complex N-linked glycans.

It was interesting that the glycosidase experiment did not result in a detectable shift after treatment with sialidase. Most vertebrate N-linked glycans are modified with terminal sialic acids (11) and methods that are more sensitive should be used to follow up these experiments. The work presented here was a limited study on the nature of PAR1 N-linked glycans. It would be interesting to further pursue the glycan structures through the use of mass spectrometry, a newer method to research N-linked glycan composition (12). How the glycan structures differ at the PAR1 N-terminus

versus the extracellular loop two, how glycosylation of PAR1 differs in various cell lines, and how glycosylation of PAR1 differs in highly invasive versus non-invasive breast carcinoma are important questions that remain to be answered.

5.2 N-linked glycosylation of the N-terminus is important for proper PAR1 processing and export to the cell surface

A review of transmembrane receptors reported that approximately 90% of GPCRs contain at least one N-linked glycosylation consensus site within the N-terminus (13). Of the ~90% only one third of these contained additional sites within the extracellular domains. Thus, many GPCRs utilize this modification, but whether it serves a function is not known for the majority of GPCRs. Numerous studies have reported that GPCR N-linked glycosylation is important in proper processing and expression (14-16). Through the use of cell surface ELISAs (**Fig. 2.5A**) and immunofluorescence microscopy (**Fig. 2.5B**), I showed that the N-terminal N-linked glycosylation sites are critical for PAR1 processing and expression at the cell surface. I observed a decrease in PAR1 NA Nter surface expression compared to wild-type PAR1, and extensive co-localization of PAR1 NA NTer mutant the with golgi marker TGN230, suggesting that the PAR1 NA NTer mutant is retained in the biosynthetic pathway. Additional IMF studies examining co-localization with an endoplasmic reticulum marker, or perhaps calnexin and calreticulin could be used to further confirm our conclusion that glycosylation of the PAR1 N-terminus is critical in receptor processing within the biosynthetic pathway.

5.3 PAR1 ECL2 N-linked glycosylation affects agonist-induced internalization

Due to the unique mode of activation, whereby a protease cleaves the N-terminus of PAR1 revealing a tethered ligand, internalization and lysosomal degradation are critical for signal termination. A previously activated PAR1 mutant that aberrantly recycles is capable of signaling persistently even in the absence of thrombin (17, 18). Thus, I examined agonist-induced internalization, constitutive internalization, and degradation of the PAR1 NA ECL2 mutant. We observed by cell surface ELISA (**Fig. 3.4B and C**) and IMF (**Fig. 3.5**) that the PAR1 NA ECL2 mutant undergoes agonist-induced internalization, but with a modest defect. Compared to wild-type PAR1, there was less PAR1 NA ECL2 internalized after initial agonist treatment, however, following a longer stimulation, there were comparable amounts of receptor internalized. Interestingly, PAR1 NA ECL2 constitutive internalization (**Fig. 3.4A**) and degradation (**Fig. 3.8**) remained intact. In addition, co-localization of PAR1 NA ECL2 with the clathrin adaptors AP-2 and epsin-1 was delayed compared to wild-type receptor, suggesting that glycosylation of PAR1 is required for rapid recruitment of endocytic machinery. However, these studies confirmed that the mutant receptor is capable of associating with the endocytic components required for agonist-induced PAR1 internalization.

The finding that PAR1 NA ECL2 mutant is still able to associate with AP-2 and epsin-1 albeit less efficiently compared to wild-type receptor suggest that the PAR1 NA ECL2 mutant may adopt a different conformation less able to recruit the endocytic machinery. Additional experiments examining the defect in agonist-induced PAR1 NA ECL2 internalization should be considered using sophisticated live cell

imaging capable of assessing the dynamics of receptor recruitment to clathrin-coated pits. The use of live cell TIRF microscopy would allow for data collection and analysis of the dynamics of receptor recruitment from the addition of agonist to recruitment of adaptors and ultimately internalization from the plasma membrane.

5.4 PAR1 ECL2 N-linked glycosylation plays a role in G protein subtype coupling and signaling

PAR1 is a promiscuous GPCR with the ability to couple and signal through multiple heterotrimeric G protein subtypes (3, 19). The mechanisms responsible for dictating GPCR-G protein coupling specificity remain poorly understood. The studies in this dissertation are the first to show that N-linked glycosylation of a GPCR can contribute to biasing receptor coupling to distinct G protein subtypes. Co-immuneprecipitation studies performed with the PAR1 NA ECL2 mutant displayed a statistically significant difference in $G\alpha_q$ association compared to wild-type receptor (**Fig. 4.1 and 4.2**). In addition, $G\alpha_q$ (**Fig. 3.7B)** and PLC dependent (**Fig. 3.6B)** PI hydrolysis was enhanced in the PAR1 NA ECL2 mutant (**Fig. 2.8 and Fig. 3.1**). These results raised the question of whether coupling and signaling of other G proteins was altered in the PAR1 NA ECL2 mutant. To this end additional experiments were performed and revealed that in addition to $G\alpha_q$ that $G\alpha_{12/13}$ coupling (**Fig. 4.5 and 4.6**) and signaling (**Fig. 4.7, 4.8, and 4.9**) was also affected. Surprisingly, while the PAR1 NA ECL2 mutant displayed enhanced $G\alpha_q$ coupling and signaling the opposite response was observed for $G\alpha_{12/13}$. These data suggest a role for N-linked glycosylation in GPCR-G protein coupling bias and we conclude that PAR1 N-linked

glycosylation at ECL2 plays an important role in G protein subtype coupling and signaling.

It is important to note that we performed many of our experiments using ectopic expression of PAR1 and signaling proteins. To the best of our ability we examined cells that exhibited PAR1 expression that were deemed comparable, as assess by cell surface ELISA. However, future experiments are important to validate the findings within this dissertation by examining endogenous proteins, as well as cell lines in which PAR1 plays important physiological roles. Experiments with knockdown-rescue constructs of the PAR1 NA ECL2 mutant in endothelial cell lines would be of particular interest, since RhoA signaling is known to cause disruption of the endothelial barrier (19-21). In addition, experiments examining whether N-linked glycosylation of PAR1 impacts signaling by other proteases, such as APC which is important for endothelial barrier stability, would be an important pursuit (22, 23).

5.5 Concluding Remarks

All together the data presented in this thesis suggest that modification of PAR1 with glycosylation at its second extracellular loop regulates distinct active conformation states of the receptor. Consequently, activated PAR1 differentially interacts with signaling and trafficking proteins that result in distinct cellular responses. In contrast to wild-type PAR1, PAR1 NA ECL2 mutant couples preferentially through $G\alpha_q$ rather than $G\alpha_{12/13}$, indicating the N-linked glycosylation controls GPCR-G protein coupling specificity. However, it remains to be determined whether other factors also influence the capacity of the PAR1 mutant deficient in N-

linked glycosylation at ECL2 to switch G protein coupling specificity. As an example, is has not been determined if N-linked glycosylation of PAR1 affects homodimerization or heterodimerization with other PARs or GPCRs. In pilot studies using BRET, I found that PAR1 NA ECL2 mutant displayed a lower affinity to homodimerize compared to wild-type PAR1. In future experiments it will be important to confirm these findings using multiple approaches. The apparent differences in PAR1 NA ECL2 homodimerization suggest that there may also be differences in PAR1 heterodimerization. We recently showed that PAR1 and PAR2 form heterodimers constitutively and is important for thrombin-induced β-arrestin recruitment (24). It is possible that heterodimerization with other GPCRs and the NA ECL2 mutant is altered and further studies should be considered.

In addition to N-linked glycosylation, PAR1 is phosphorylated, ubiquitinated and palmitoylated (25-28). It is clear that PAR1 function is tightly controlled by these posttranslational modifications. Thus it is important to also determine whether the PAR1 NA ECL2 mutant has defects in phosphorylation, ubiquitination and/or palmitoylation. Based on the observation that the NA ECL2 mutant and the wild-type receptor having distinct rates of desensitization I predict that there is a difference in receptor phoshporylation. It is possible that the different conformation of the receptor due to lacking glycosylation not only affects how trafficking and signaling proteins interact with the receptor, but other proteins as well. This could also lead to differences in other post-translational modifications.

Finally, the work described within this thesis provides a basis to investigate other GPCRs that contain extracellular loop N-linked glycosylation consensus sites. It

is possible that glycosylation may regulate the G-protein specificity of other GPCRs, by regulating ligand binding and receptor conformational change. To start, GPCRs with similar functions and number of N-linked glycosylation sites as PAR1 should be taken into consideration. N-linked glycosylation is a highly heterogeneous modification that controls cell surface expression and, with my study, is critical for modulating the ability of GPCRs to signal to different intracellular pathways.

5.6 References

1. Vu, T. K., Hung, D. T., Wheaton, V. I., and Coughlin, S. R. (1991) Molecular cloning of a functional thrombin receptor reveals a novel proteolytic mechanism of receptor activation. *Cell* **64**, 1057-1068

2. Coughlin, S. R. (2000) Thrombin signalling and protease-activated receptors. *Nature* **407**, 258-264

3. Coughlin, S. R. (2005) Protease-activated receptors in hemostasis, thrombosis and vascular biology. *J Thromb Haemost* **3**, 1800-1814

4. Gerszten, R. E., Chen, J., Ishi, M., Ishi, K., Wang, L., Nanevicz, T., Turck, C.W., Vu, T.K.H., and Coughlin, S.R. (1994) Specificty of the thrombin receptor for agonist peptide is defined by its extracellular surface. *Nature* **368**, 648-651

5. Lerner, D. J., Chen, M., Tram, T., and Coughlin, S. R. (1996) Agonist recognition by proteinase-activated receptor 2 and thrombin receptor. Importance of extracellular loop interactions for receptor function. *J Biol Chem* **271**, 13943-13947

6. Nanevicz, T., Ishii, M., Wang, L., Chen, M., Chen, J., Turck, C. W., Cohen, F. E., and Coughlin, S. R. (1995) Mechanisms of thrombin receptor agonist specificity. Chimeric receptors and complementary mutations identify an agonist recognition site. *J Biol Chem* **270**, 21619-21625

7. Shi, L., and Javitch, J. A. (2004) The second extracellular loop of the dopamine D2 receptor lines the binding-site crevice. *Proc Natl Acad Sci U S A* **101**, 440-445

8. Peeters, M. C., van Westen, G. J., Li, Q., and AP, I. J. (2011) Importance of the extracellular loops in G protein-coupled receptors for ligand recognition and receptor activation. *Trends Pharmacol Sci* **32**, 35-42

9. Vouret-Craviari, V., Grall, D., Chambard, J. C., Rasmussen, U. B., Pouyssegur, J., and Van Obberghen-Schilling, E. (1995) Post-translational and activation-dependent modifications of the G protein-coupled thrombin receptor. *J Biol Chem* **270**, 8367-8372

10. Tordai, A., Brass, L. F., and Gelfand, E. W. (1995) Tunicamycin inhibits the expression of functional thrombin receptors on human T-lymphoblastoid cells. *Biochem Biophys Res Commun* **206**, 857-862

11. Davies, L. R., and Varki, A. (2013) Why Is N-Glycolylneuraminic Acid Rare in the Vertebrate Brain? *Top Curr Chem*

12. North, S. J., Hitchen, P. G., Haslam, S. M., and Dell, A. (2009) Mass spectrometry in the analysis of N-linked and O-linked glycans. *Curr Opin Struct Biol* **19**, 498-506

13. Landolt-Marticorena, C., and Reithmeier, R. A. (1994) Asparagine-linked oligosaccharides are localized to single extracytosolic segments in multi-span membrane glycoproteins. *Biochem J* **302 (Pt 1)**, 253-260

14. Roy, S., Perron, B., and Gallo-Payet, N. (2010) Role of asparagine-linked glycosylation in cell surface expression and function of the human adrenocorticotropin receptor (melanocortin 2 receptor) in 293/FRT cells. *Endocrinology* **151**, 660-670

15. Lanctot, P. M., Leclerc, P. C., Escher, E., Leduc, R., and Guillemette, G. (1999) Role of N-glycosylation in the expression and functional properties of human AT1 receptor. *Biochemistry* **38**, 8621-8627

16. Whitaker, G. M., Lynn, F. C., McIntosh, C. H., and Accili, E. A. (2012) Regulation of GIP and GLP1 receptor cell surface expression by N-glycosylation and receptor heteromerization. *PLoS One* **7**, e32675

17. Arora, P., Cuevas, B. D., Russo, A., Johnson, G. L., and Trejo, J. (2008) Persistent transactivation of EGFR and ErbB2/HER2 by protease-activated receptor-1 promotes breast carcinoma cell invasion. *Oncogene* **27**, 4434-4445

18. Arora, P., Ricks, T. K., and Trejo, J. (2007) Protease-activated receptor signalling, endocytic sorting and dysregulation in cancer. *J Cell Sci* **120**, 921-928

19. Adams, M. N., Ramachandran, R., Yau, M. K., Suen, J. Y., Fairlie, D. P., Hollenberg, M. D., and Hooper, J. D. (2011) Structure, function and pathophysiology of protease activated receptors. *Pharmacol Ther* **130**, 248-282

20. Russo, A., Soh, U. J., Paing, M. M., Arora, P., and Trejo, J. (2009) Caveolae are required for protease-selective signaling by protease-activated receptor-1. *Proc Natl Acad Sci U S A* **106**, 6393-6397

21. Soh, U. J., and Trejo, J. (2011) Activated protein C promotes protease-activated receptor-1 cytoprotective signaling through beta-arrestin and dishevelled-2 scaffolds. *Proc Natl Acad Sci U S A* **108**, E1372-1380

22. Griffin, J. H., Zlokovic, B. V., and Mosnier, L. O. (2012) Protein C anticoagulant and cytoprotective pathways. *Int J Hematol* **95**, 333-345

23. Mosnier, L. O., Zlokovic, B. V., and Griffin, J. H. (2007) The cytoprotective protein C pathway. *Blood* **109**, 3161-3172

24. Lin, H., and Trejo, J. (2013) Transactivation of the PAR1-PAR2 Heterodimer by Thrombin Elicits beta-Arrestin-mediated Endosomal Signaling. *J Biol Chem* **288**, 11203-11215

25. Macfarlane, S. R., Seatter, M. J., Kanke, T., Hunter, G. D., and Plevin, R. (2001) Proteinase-activated receptors. *Pharmacol Rev* **53**, 245-282

26. Chen, B., Dores, M. R., Grimsey, N., Canto, I., Barker, B. L., and Trejo, J. (2011) Adaptor protein complex-2 (AP-2) and epsin-1 mediate protease-activated receptor-1 internalization via phosphorylation- and ubiquitination-dependent sorting signals. *J Biol Chem* **286**, 40760-40770

27. Wolfe, B. L., Marchese, A., and Trejo, J. (2007) Ubiquitination differentially regulates clathrin-dependent internalization of protease-activated receptor-1. *J Cell Biol* **177**, 905-916

28. Canto, I., and Trejo, J. (2013) Palmitoylation of protease-activated receptor-1 regulates adaptor protein complex-2 and -3 interaction with tyrosine-based motifs and endocytic sorting. *J Biol Chem*